

ABSTRACT

SHU, YU. Biomechanical Analysis of Eccentric and Concentric Lifting Exertions. (Under the direction of Dr. Gary A. Mirka.)

Electromyographic (EMG) -assisted biomechanical models have been used to predict spinal reactions forces and evaluate risk of low back disorders (LBDs). One of the challenges facing previous EMG-assisted biomechanical models is that they rely heavily on the active muscle force component. In certain kinds of exertions (eccentric exertions and exertions at or near the full flexion trunk postures) the passive components of the extensor mechanism play a significant role in the net extensor moment, and these are not captured in the traditional EMG-assisted modeling technique.

This study introduces a new EMG assisted biomechanical model that includes passive components. Empirical experiments were conducted to evaluate the improvements in model predictions when these passive tissue components were considered. Eighteen subjects participated in two groups of experiments. In experiment one, subjects performed repetitive, eccentric and concentric lifting motions in a controlled dynamometer task environment. In experiment two, subjects performed a repetitive, free dynamic lifting and lowering exertions. In both experiments, the subjects were asked to reach their full trunk flexion posture during the lifting motion. As they performed these tasks, the EMG activity of the major trunk muscles was collected. The passive tissue forces were estimated through the use of a finite element model of the lumbar region. Estimates of the net internal moment from two different EMG-assisted models (with and without passive components) were compared with the measured net external moment to provide insight into the utility of the inclusion of these passive tissue forces.

The results indicated the necessity of involving passive components in the EMG-assisted biomechanical model when studying the trunk flexion/extension exertions at full trunk flexion postures. The mean absolute error between the measured moment and model predicted moment was significantly smaller for the model with passive components as compared to the model without passive components (19.6 Nm vs. 25.5 Nm in experiment one, and 19.4 Nm vs. 54.9 Nm in experiment two, respectively). The R squared value of the measured and predicted load demonstrated great improvements by involving passive components (37% to 66% in experiment one, 12% to 75% in experiment two, respectively).

In a second phase of this research, this new EMG-assisted model was used to study the differences in the biomechanical response between lowering (eccentric) and lifting (concentric) exertions. Eccentric exertions induced significantly ($p < 0.05$) higher mean maximum spine compression forces in both experiments as compared to concentric exertions (3680N vs. 3114N in experiment one, and 2516N vs. 1870N in experiment two, respectively). The variability of the spinal load in these two types of exertions was also compared in terms of the average absolute deviation from the median (AADM) of the compression values (where the median refers to the median values of the multiple repetitions of the same task). This AADM of the maximum compression force was 281N for concentric versus 472N for eccentric exertions in experiment one, and 134N for concentric versus 207N for eccentric exertions in experiment two. These differences were shown to be affected by the lifting/lowering velocity, knee posture and load levels. This result has significant meaning when considering the relative risk of lifting and lowering exertions in the workplace.

This study demonstrated an innovative method to quantitatively include the effects of the passive components of the spine into the EMG-assisted biomechanical model and showed

the importance of involving these passive components in the estimation of the spinal load at the full flexed posture and eccentric exertions. The results of this study have also provided some insight into the relative risk of eccentric vs. concentric exertions by understanding the trade-offs between the active and passive tissues of the spine during eccentric exertions.

Biomechanical Analysis of
Eccentric and Concentric
Lifting Exertions

by
Yu Shu

A dissertation submitted to the Graduate Faculty of
North Carolina State University
in partial fulfillment of the requirements for
the Degree of Doctor of Philosophy

Industrial and Systems Engineering

Raleigh, NC

2007

APPROVED BY:

Simon M. Hsiang

David B. Kaber

Gregory D. Buckner

Gary A. Mirka
(Chair of Advisory Committee)

DEDICATION

献给我的家人
To my family.

BIOGRAPHY

Yu Shu was born in Sichuan province, China. After graduating from Tsinghua University in Beijing with a Bachelor's degree in Industrial Engineering, he joined the Ergonomics Laboratory in the Edward P. Fitts Department of Industrial and Systems Engineering in North Carolina State University. He worked as a research assistant under the direction of Dr. Gary A. Mirka. He received his Master's degree in 2005 and continued to pursue his PhD degree in NCSU. His research areas included spine biomechanics, electromyography, biomechanical modeling, and ergonomic intervention effectiveness research.

ACKNOWLEDGEMENTS

I would like to thank Dr. Gary Mirka, my advisor and mentor, for his invaluable counsel and advice for the last five years, and my committee members: Dr. David Kaber, Dr. Simon Hsiang and Dr. Gregory Buckner for their academic support and counsel.

I would like to acknowledge many graduate students during my Master and Doctoral degrees for their assistance and support. I would like to thank the subjects who voluntarily participated in my studies. I would like to thank my friends who shared their life and joy with me in Raleigh.

TABLE OF CONTENTS

List of Figures.....	ix
List of Tables	xiv
1 A brief introduction.....	1
1.1 Ergonomics	1
1.2 Epidemiology of low back disorders	1
1.3 Low back disorder risk factors.....	2
1.4 Spinal biomechanical models	3
1.5 Improving biomechanical models with passive components.....	4
1.6 Passive components in eccentric muscle contractions.....	5
1.7 The purpose of this research	7
2 Literature review	8
2.1 Biomechanics of the low back	8
2.1.1 Basic anatomy of the low back	8
2.1.2 Failure and injury of the low back	9
2.2 Muscle contractions: eccentric versus concentric.....	11
2.2.1 Differences in force generation capacity	12
2.2.2 Differences in EMG activities and training	13
2.2.3 Differences in nervous control strategy	14
2.2.4 Differences in force-velocity relationship	16
2.2.5 Differences in variability	17
2.3 Biomechanical models of the spine	18

2.3.1	Early physical models	19
2.3.2	Optimization models	21
2.3.3	EMG driven biomechanical models.....	22
2.3.4	Models with eccentric motions	30
2.3.5	Models with passive components	33
3	Pilot work.....	41
3.1	Subjects	41
3.2	Apparatus	42
3.3	Independent variables	42
3.4	Dependent variables.....	43
3.5	Experimental procedures	43
3.6	Data processing.....	45
3.7	Data analysis	45
3.8	Results.....	46
4	Model development	50
4.1	Input data	51
4.2	External moment calculation	52
4.3	Internal moment calculation	54
4.3.1	Calculating the moment from the passive components	55
4.3.2	Calculating the moment from the active muscles.....	57
5	Experimental method	67
5.1	Summary of literature review	67
5.2	Experiment one: dynamometer study	68

5.2.1	Subjects	68
5.2.2	Equipment	69
5.2.3	Experimental design.....	70
5.2.4	Procedure	71
5.2.5	Data processing.....	73
5.2.6	Model evaluation	75
5.2.7	Statistical analysis.....	76
5.3	Experiment two: free lifting/lowering study.....	77
5.3.1	Subjects.....	78
5.3.2	Equipment.....	78
5.3.3	Experimental design.....	80
5.3.4	Procedure	81
5.3.5	Data Processing.....	83
5.3.6	Model evaluation	84
5.3.7	Statistical analysis.....	85
6	Results.....	87
6.1	Experiment one: dynamometer study	87
6.1.1	Model Evaluation.....	87
6.1.2	Comparison of eccentric versus concentric exertions.....	93
6.2	Experiment two: free lifting/lowering study.....	102
6.2.1	Model evaluation	102
6.2.2	Comparison of eccentric versus concentric exertions.....	104
7	Discussion.....	113

7.1	Assessment of the model	113
7.2	Comparison of eccentric and concentric exertions	123
7.3	Limitations of this study	129
8	Conclusion	131
	References.....	133
	Appendix.....	142
	Appendix A: Matlab code.....	143
	Appendix B: Adequacy of the statistical model	150

LIST OF FIGURES

Figure 1. Lines of action of major trunk muscles (from Marras and Granata, 1995).....	29
Figure 2. Empirical length-strength and force-velocity modulations from Davis (1998)	30
Figure 3. Nonlinear stress-strain curves of spinal ligaments (from Shin, 2005)	38
Figure 4. Measured muscle force verses model predicted muscle force in different tasks (from Shin, 2005).....	39
Figure 5. Normalized EMG of lumbar extensors vs. knee angle and trunk angle (50% MVC)	47
Figure 6. Normalized EMG of erector spinae muscle vs. flexibility and trunk angle (50% MVC condition) (group 1 : high-flexible, group 2 : mid-flexible, group 3 : low-flexible)	47
Figure 7. Normalized EMG of lumbar extensors vs. knee angle, trunk angle, and flexibility (50% MVC condition)	48
Figure 8. Model predicted L5/S1 joint compression force and torque from muscles vs. flexibility.....	49
Figure 9. Inputs and flow of the model.....	51
Figure 10. Illustration of the 3D surface of passive moment vs. load and lumbar flexion angle	56
Figure 11. Illustration of the range of trunk motion in previous models and current study ...	67
Figure 12. Controlled flexion/extension exertions in ARF.....	72
Figure 13. Motion sensors placed on the back of the subject	79
Figure 14. A dynamic lifting exertion at full flexion posture	83
Figure 15. Mean and standard deviation of the maximum muscle stress value versus trunk flexion angle.....	88

Figure 16. Measured and model predicted moment at 45° trunk flexion angle in controlled static exertion.....	89
Figure 17. Measured and model predicted moment at medium trunk flexion angle in controlled static exertion.....	90
Figure 18. Measured and model predicted moment at full trunk flexion angle in controlled static exertion.....	90
Figure 19. External and internal moment in controlled dynamic exertion on dynamometer.	92
Figure 20. Maximum spinal compression force vs. Load, Velocity and Direction.....	95
Figure 21. Interaction between Load and Velocity on maximum compression force.....	95
Figure 22. Maximum spinal compression force in dynamic controlled trials.....	96
Figure 23. Maximum spinal shear force vs. Load, Velocity and Direction.....	96
Figure 24. Interaction between Load and Velocity on maximum spinal shear force.....	97
Figure 25. Maximum spinal shear force in dynamic controlled trials.....	97
Figure 26. Median deviation of the maximum compression force in controlled dynamic exertions.....	99
Figure 27. Median deviation of the maximum compression force.....	99
Figure 28. Interaction between Load and speed on median deviation of the maximum compression force.....	100
Figure 29. Median deviation of the maximum shear force in controlled dynamic exertions.....	100
Figure 30. Maximum spinal shear force vs. Load, Velocity and Direction.....	101
Figure 31. Interaction between Load and Velocity on the median deviation of the maximum shear force.....	101

Figure 32. Interaction between Load and Direction on the median deviation of the maximum shear force.....	102
Figure 33. Measured external moment and model predicted internal moment in free lifting/lowering exertions.....	103
Figure 34. Maximum spinal compression force in free lifting/lowering exertions.	105
Figure 35. Maximum compression force vs. Posture, Load and Direction.	106
Figure 36. Interaction between Posture and Direction on maximum compression force.	106
Figure 37. Maximum spinal shear force in free lifting/lowering exertions.	107
Figure 38. Maximum spinal shear force vs. Posture, Load and Direction.....	107
Figure 39. Interaction between Posture and Direction on the maximum shear force.....	108
Figure 40. Median deviation of maximum compression force in free lifting/lowering exertions.....	109
Figure 41. Median deviation of maximum compression force vs. Posture, Load and Direction.	109
Figure 42. Interaction between Load and Direction on the maximum compression force...	110
Figure 43. Median deviation of maximum shear force in free lifting/lowering exertions....	111
Figure 44. Median deviation of maximum shear force vs. Posture, Load and Direction.	111
Figure 45. Interaction of Load and Direction on median deviation of the maximum shear force.	112
Figure 46. Normal probability plot of the residuals of the original maximum shear force ..	150
Figure 47. Normal probability plot of the residuals of the log transformed maximum shear force	151
Figure 48. Residuals vs. predicted values of the original maximum shear force data.....	151

Figure 49. Residuals vs. predicted values of log transformed maximum shear force data...	152
Figure 50. Normal probability plot of the residuals of the maximum compression force....	153
Figure 51. Residuals vs. predicted values of the maximum compression force	153
Figure 52. Normal probability plot of the residuals of the median deviation of the peak compression force	154
Figure 53. Residuals vs. predicted values of the median deviation of the maximum compression force	154
Figure 54. Normal probability plot of the residuals of the median deviation of the peak shear force	155
Figure 55. Residuals vs. predicted values of the median deviation of the maximum shear force	155
Figure 56. Normal probability plot of the residuals of the maximum flexion/extension velocity.....	156
Figure 57. Residuals vs. predicted values of the maximum flexion/extension velocity.....	156
Figure 58. Normal probability plot of the residuals of the maximum compression force....	157
Figure 59. Residuals vs. predicted values of the maximum compression force	157
Figure 60. Normal probability plot of the residuals of the maximum shear force.....	158
Figure 61. Residuals vs. predicted values of the maximum shear force.....	158
Figure 62. Normal probability plot of the residuals of the median deviation of the peak compression force	159
Figure 63. Residuals vs. predicted values of the median deviation of the maximum compression force	159

Figure 64. Normal probability plot of the residuals of the median deviation of the maximum shear force.....	160
Figure 65. Residuals vs. predicted values of the median deviation of the maximum shear force	160

LIST OF TABLES

Table 1. List of important EMG-assisted biomechanical models.....	40
Table 2. Coefficients of muscle coordinates and cross-sectional areas (Marras and Granata, 1995).....	60
Table 3. Range of maximum muscle stress values (gain) found in the literature.....	66
Table 4. Anthropometric data of the subjects in experiment one.....	69
Table 5. Anthropometric data of the subjects in experiment two.....	78
Table 6. MANOVA and ANOVA results of the maximum spine reaction forces in the dynamic exertions.....	94
Table 7. MANOVA and ANOVA results of the median deviation values.....	98
Table 8. Comparison of mean absolute error and R^2 values in free lifting/lowering exertions.....	104
Table 9. MANOVA and ANOVA test results of the maximum values in free lifting/lowering exertions.....	104
Table 10. MANOVA and ANOVA test results of the median deviation of the maximum values.....	108

1 A BRIEF INTRODUCTION

1.1 Ergonomics

Ergonomics is the scientific discipline concerned with understanding the interactions between human beings and other elements in a system in order to optimize the overall system performance and protect the human users. The goal of ergonomics is to “design the job to fit people” using the knowledge of human anatomical, physiological and psychological capabilities and limitations. There are three broad domains of specialization within the discipline of ergonomics: physical ergonomics, cognitive ergonomics and organizational ergonomics. The focus of the current work is in the area of physical ergonomics. Physical ergonomics includes the consideration of human anatomical, anthropometric, physiological and biomechanical characteristics in the design of occupational activities of human beings. Within physical ergonomics, the study of spine biomechanics is a specialized field that focuses on reducing the risk of low back disorders (LBDs).

1.2 Epidemiology of low back disorders

LBDs are a world-wide health problem and the most common and costly musculoskeletal disorder in the workplace (Marras 2000; Lahiri, Markkanen et al. 2005). The prevalence of LBDs is estimated to be between 10% and 80%, depending on the population (Verhaak, Kerssens et al. 1998; Gilgil, Kacar et al. 2005). Older people are not the only ones that suffer from LBDs, a relatively large percentage of young adults (14.3%) are affected as well (Mallen, Peat et al. 2005). According to the annual report of the Bureau of Labor

Statistics (BLS 2004), more workers complained of pain in the lower back region than in any other part of the body.

LBDs generate a great economic cost to society. Workers suffer loss of income and medical costs in addition to the physical pain and stress of LBDs. In addition, industry also spends significant resources on direct and indirect costs related to LBDs. The direct costs include the worker's compensation and medical treatment costs. Indirect costs include the extra cost for hiring temporary workers and the other costs associated with lost work days are examples of indirect costs. The total cost for LBDs has exceeded \$100 billion in the United States (Katz 2006). As a result, preventing LBDs has become a major research topic in ergonomics.

1.3 Low back disorder risk factors

It is generally believed that LBDs occur when the applied load exceeds the failure tolerance of one or more of the low back tissues (McGill 1997). Six specific occupational risk factors have been identified as being associated with LBDs: lifting and forceful movements, static work postures, physically heavy work, frequent bending and twisting, repetitive work, and vibration (Marras, Lavender et al. 1993). Lifting (and lowering) has been shown as one of the most dangerous occupational activities in terms of inducing LBDs (Bernard 1997; McGill 1997). Lifting is defined as moving or bringing something from a lower level to a higher one and vice versa for lowering. During lifting/lowering, the posterior erector spinae muscles generate the torque to support and extend the trunk. The spine, acting as the fulcrum of this mechanical system, must withstand not only the forces from gravity acting on the load and the body segments, but also more significantly, the muscle forces being generated to counter these external loads. The load on the spine increases as the trunk

flexion angle increases during lowering with the maximum moment occurring near the fully flexed posture. The full flexed posture is often seen in industries such as agriculture and construction, and this is generally considered as a risk factor that can cause LBDs (McGill, 1997). Many tasks in the agriculture and construction industries require this posture when farmers and construction workers manipulate objects at ground level. These industries are noted for their high levels of low back injury/illness, e.g. vegetable farming in agricultural production (Incidence Rate (IR) of back injury or illness = 36.2 cases per 10,000 full-time workers), and construction field (IR = 40.2). These jobs require substantial time spent in full or near full flexed postures and report higher incidence rates of LBDs compared to average industry (IR of private industry of back injury or illness = 27.1) (BLS 2006).

1.4 Spinal biomechanical models

Over the years, a number of spinal biomechanical models have been developed to quantitatively study the loading on the spine caused by various lifting activities. The purpose of using a spinal biomechanical model is to provide a representation of the spine that can be quantitatively analyzed and understood. For example, the compression force between two vertebrae of spine is hard to measure in a living human body, but it can be estimated with the help of the spinal biomechanical models. Recent biomechanical spinal models utilize a three-dimensional multi-vector system where the major trunk muscles are modeled as single force vectors. These force vectors counter the external moments to satisfy the static equilibrium during isometric holding exertions and the dynamic equilibrium during dynamic lifting motions (e.g. Marras and Granata 1995; Davis and Mirka 2000).

Accurate estimates of muscle forces are important in biomechanical models. However, since it is almost impossible to measure muscle force directly from the living body, indirect

assessment is necessary. Electromyography (EMG) has been established as the most widely used bioinstrumentation method for estimating muscular forces (DeLuca 1997). The theoretical foundation is the EMG-force relationship, which has been investigated and validated in the literature (Perry-Rana, Housh et al. 2003). Briefly, during muscle contraction a motor unit action potential is created as the motor neuron initiates the muscle contraction and ions flow into and out of a muscle cell. Surface electrodes can be placed on the skin over the muscle to measure this electrical activity. As more force is generated by the muscle more electrical activity can be measured. Using information with regard to the cross-sectional area of the muscle, the maximum muscle stress (force-generating capacity per unit cross-sectional area), and the muscle activation level measured using EMG technology *in vivo*, the magnitude of the force for a specific muscle in living body can be estimated and used in the spinal biomechanical models.

1.5 Improving biomechanical models with passive components

The EMG based biomechanical models depend heavily on the measured EMG activities of trunk muscles. However, previous research has shown that the posterior trunk muscles show near zero activity when one bends to full flexed posture. (Colloca and Hinrichs 2005) This is called the “flexion-relaxation phenomenon” (FRP). During the FRP, the myoelectrical silence of muscles makes it difficult to use EMG based biomechanical models.

Consequently, the effects of the passive components including the elastic proportions of the muscles, ligaments and disc should be considered in generating the restorative moments in a full trunk flexion posture. McGill and Kippers (1994) confirmed that the spinal ligaments generated the majority of the restorative moment during the FRP. It is reasonable to argue that the restorative moment from passive components will decrease as the trunk

flexion angle decreases, while the restorative moment from active muscles will increase and finally take the role of supporting the trunk. However, this interplay between the passive and active components of the trunk has not been fully explored in the literature.

1.6 Passive components in eccentric muscle contractions

The passive component of the restorative moment is important during eccentric contractions. Eccentric contractions are defined as contractions wherein a muscle lengthens as it is generating muscle force, as would be seen in the biceps brachii muscle when a person is lowering the load. For multiple muscles system such as trunk muscles, the eccentric contractions are often described as exhibiting a negative correlation between the joint torque and joint velocity. On the other hand, concentric contractions are contractions where the muscle is shortening as it is generating force, as would be seen in the biceps brachii muscle when that same person is lifting a load by flexing the elbow. They can also be defined as the positive correlation between the joint torque and joint velocity. Research has shown that the mechanical properties of a muscle during eccentric contractions are different from the mechanical properties of a muscle during concentric contractions. One major difference is that muscles are able to generate greater force during eccentric contractions than during concentric contractions (Huang and Thorstensson 2000; Fang, Siemionow et al. 2004). It has been hypothesized that the passive components in muscles may provide the extra tension force during eccentric contractions (Proske and Morgan 2001). Similarly, eccentric contractions generate more force as compared to concentric contractions at the same EMG activation level (Huang and Thorstensson 2000). In other words, to provide the same amount of force, a muscle generates less EMG activity in an eccentric contraction than in a concentric contraction (Aagaard, Simonsen et al. 2000; Fang, Siemionow et al. 2001;

Grabiner and Owings 2002). When using the EMG signals as inputs for a spinal biomechanical model, this important difference between the eccentric and concentric contractions must be considered (Davis, Marras et al. 1998).

Eccentric contractions have also been found to be more variable than concentric contractions (Fang, Siemionow et al. 2001; Christou and Carlton 2002). Christou and Carlton (2002) found that when the subjects were asked to reach the same knee-extension torque in both eccentric and concentric exertions, the standard deviation of the forces generated in the eccentric contractions was larger than those in the concentric contractions. In another study, Fang, Siemionow et al (2001) found that controlled eccentric motions were more difficult to perform because of higher force fluctuations as compared to controlled concentric motions (Fang, Siemionow et al. 2001).

From the injury prevention standpoint, eccentric contractions have been found to be more likely to cause injury than concentric contractions. For a given level of force production, eccentric contractions cause more damage to the myotendinous tissues, as compared to concentric movements, because muscle fibers are forced to elongate when contracting (Friden, Sjostrom et al. 1983; Newham, Mills et al. 1983; Newham 1988; Shellock, Fukunaga et al. 1991; Proske and Morgan 2001). Clinical reports suggest that hamstring injuries occur most often as a result eccentric contractions (Sallay, Friedman et al. 1996). It is important to note that most of the biomechanical models that have been developed to quantify risk of injury during strenuous manual materials handling tasks have focused on concentric contractions (i.e. lifting activities), while there are many lowering tasks (i.e. eccentric contractions) performed every day by material handlers (McGill and Norman 1986; Marras and Sommerich 1991; Marras and Granata 1997). Lortie and Baril-Gingras (1998)

reported that lowering exertions represented 15% of all kinds of exertions (lifting, lowering, pushing, pivoting and turning, etc.) performed by 31 handlers in a warehouse. When only considering the exertions that require vertical displacement of the load (lifting and lowering), then 37% of these exertions were actually eccentric contractions. Understanding the risks posed by these eccentric contractions is the focus of this study.

1.7 The purpose of this research

The focus of this research is to develop an EMG-assisted biomechanical model that can accurately predict the spinal load from active muscles and passive components. This model will allow for a demonstration of the transfer of the trunk support mechanism between active muscles and passive components during the lifting/lowering trunk exertions throughout a full range of trunk flexion, including near full flexion angle.

After that, this model will be used to explore the difference in the magnitude and variability of the L5/S1 joint reaction forces between the eccentric (lowering) and concentric (lifting) motions in the full range (stand straight to full flexion) of lifting and lowering exertions. Several occupational lifting factors are considered in this study: lifting direction (concentric vs. eccentric exertions), load weight, and lifting posture (bent or straight knee). The results of this study will generate quantitative information about the biomechanical loading during dynamic trunk eccentric and concentric motions and will provide additional insight into the mechanism of low back injury.

2 LITERATURE REVIEW

2.1 Biomechanics of the low back

2.1.1 Basic anatomy of the low back

The spine consists of seven cervical vertebrae, twelve thoracic vertebrae, five lumbar vertebrae, five fused sacral vertebrae, and three to four fused coccygeal segments. The focus of this study is the lumbar spine. A lumbar vertebra consists of an anterior block of bone, the vertebral body, and a posterior bony ring, known as the neural arch, containing articular, transverse and spinous processes. Between the vertebral bodies are intervertebral discs that withstand compression loads and limit intervertebral motion. Around the vertebra and between the posterior processes are ligaments that provide additional tensile resistance to intervertebral motion. The relative movements of the vertebral bones are well-defined and limited by these passive structures. In terms of their relative contribution to the extensor moment during lifting, these passive tissues contribute very little in typical lifting motions (McGill and Norman 1986) but do contribute to a greater degree in full trunk flexion conditions (McGill and Kippers 1994).

Under normal lifting conditions, the forces generated by the trunk extensor musculature contribute the majority of the trunk extension moment. The major muscles that contribute to the extension of the spine are the erector spinae muscles (iliocostalis, longissimus and spinalis) and the latissimus dorsi. The major muscles that contribute to the flexion of the spine are the rectus abdominis, external oblique and internal oblique. When the extensor muscles contract they use the spine as the fulcrum and extend the torso. During

lifting activities the activation of the flexor muscles is often seen and is believed to provide stability to the biomechanical system. These five pairs of muscles (left and right erector spinae, latissimus dorsi, rectus abdominis, external and internal obliques) are included in the majority of the spinal biomechanical models.

Under specific lifting conditions, such as picking out an item from a deep container at ground level, the near full trunk flexion posture is often used. In this posture, the elastic force from elongated muscles can generate a large amount of the moment to maintain the spine. The passive components of the spine, such as ligaments and disc also function as the prime contributors to support the spine. Sometimes, the moment from elastic muscle forces and passive components is large enough that it is unnecessary for the nervous system to activate muscles. In this case, myoelectric silence can be observed in the erector spinae muscles, which is called “flexion-relaxation phenomenon”.

2.1.2 Failure and injury of the low back

Low back injury can take place in any of the tissues listed above and the degree to which these tissues are able to heal will determine whether the damage creates an acute or chronic injury. The majority of low back pain comes from injury to the muscles and ligaments. The cause could be the repetitive tissue micro-trauma or a single acute trauma and inflammation, edema and pain are the result. Fortunately, these tissues are able to heal relatively quickly. In muscle tissue, tears are called muscle strains, while in the ligaments, tears are called ligament sprains.

Injury to the intervertebral discs is much more problematic in that the healing capabilities of these tissues are quite limited. Damage to the intervertebral disc can lead to chronic pain and suffering and high workers compensation costs. For this reason many

biomechanical models concentrate on quantifying the loading of these structures. The L5/S1 joint of the spine (and intervertebral disc) is the focus of the majority of biomechanical models for lifting, holding and other industrial tasks because it is at the site of the greatest force concentration—the base of the spine. There are three kinds of loads that occur on this joint: compression, torsion, and shear.

Understanding the ultimate strength limits of the intervertebral discs can be an important component to establishing safe lifting limits and is an area of considerable research. It is impractical and unsafe to measure the maximum strength limits within a living human subject. Most researchers in this area gather measurements in vitro on cadavers. Jager and Luttmann (1989) reported that the mean of the compression strength limit for the spine components was 4.36kN with a standard deviation of 1.88kN. For its updated 1991 lifting equation, NIOSH concluded that a maximum safe compressive strength limit of 3.4kN is appropriate for the L5/S1 intervertebral disc (Waters, Putz-Anderson et al. 1993). The maximum torsion and shear strength for the thoracic and lumbar spine were reported to be 150N and 1800N, respectively (White and Panjabi 1990 p.9). Berkson et al. (1979) illustrated the importance of the support of the posterior elements and ligamentous structure of the spine in addressing the shear loads on the spine. The most significant finding was that with a constant 400N compressive and 145N shear load applied separately toward anterior, posterior and lateral directions, the lumbar disc displacements were approximately 50 percent larger (0.085cm vs. 0.121cm) during posterior shear than during anterior shear with the posterior elements intact. However, the lumbar disc displacements were approximately the same (0.124cm vs. 0.142cm) for anterior and posterior shear load when the posterior elements were destroyed. Berkson et al. results indicated the spinal shear forces are resisted

primarily by the posterior elements (facet joints in the lumbar spine). It is important to note that the results from in vitro studies should be used with caution because the mechanical properties of the intervertebral disc in vivo may be significantly different from those in vitro. For instance, Keller et al. (1990) found significant differences between the in vivo mechanical creep behaviors of animals' lumbar vertebrae compared to those seen in vitro.

2.2 Muscle contractions: eccentric versus concentric

According to the cross-bridge theory of muscle contraction, force is generated by the interaction of actin and myosin filaments in the muscle fibers (cells). In concentric contraction motion, these filaments interact and slide so that the degree of overlap of the filaments increases, which causes the entire muscle to shorten and creates the movement. During eccentric contractions force is generated in the same way (cyclical interaction between the cross bridges), but the force generated is not sufficient to overcome the external force and therefore the muscle lengthens as it is exerting force. Because the bonds between these filaments are disrupted by the mechanical movement of the fibers as the muscle lengthens, damage is more likely to occur in eccentric motions (Proske and Morgan 2001). The abnormalities in the muscle fibers that have been observed after eccentric motion include sarcolemmal disruption, distortion of myofibrillar components, lesions of the plasma membranes, etc (Friden, Sjostrom et al. 1983; Friden and Lieber 1992; Enoka 1996). It is also hypothesized that the dead fibers which decompose in the hours after excessive eccentric exercise leave one feeling stiff and sore (Proske and Morgan 2001). In addition to the difference in movement direction, there are many other differences between eccentric and concentric motions such as the force generating capacity, electromyographic response, force-

velocity relationship, control strategy employed by the central nervous system and variability in performance.

2.2.1 Differences in force generation capacity

Research has consistently shown that maximum eccentric motions produce more force than maximum concentric motions. Fang et al. (2004) found that the force exerted by the elbow flexor muscles of the subjects during eccentric maximum voluntary contraction exertions (210.63N) was significantly higher than the force during concentric exertions (184.06N). In a study of trunk muscle strength in eccentric and concentric lateral flexion, Huang and Thorstensson (2000) found that the lateral flexion torque was always higher in eccentric than in concentric actions (211 to 218Nm vs. 66 to 140Nm). Similar results were found by Westing et al. (1990) in the study of electrical stimulation on eccentric and concentric torque-velocity relationships during knee extensions. Nine subjects performed maximal voluntary, electrically evoked and superimposed eccentric and concentric knee extensions at velocities of 60, 180 and 360°/s. The torque outputs measured at 60° for the three eccentric contraction conditions (about 220 to 350Nm) were significantly higher than those in concentric conditions (about 150 to 190Nm). Another important finding in this study was that the superimposed eccentric torque was on average 21-24% greater, and electrically evoked eccentric torques were 11-12% greater than the corresponding maximal voluntary torques. This indicated that eccentric knee extension torque in maximal voluntary conditions does not represent the maximal torque producing capacity. The authors proposed a neural inhibitory mechanism to explain this finding: the neural system prevents real maximum tension during the maximum voluntary eccentric contractions because of the risk of damage from extreme muscle tensions.

2.2.2 Differences in EMG activities and training

Using EMG technology, researchers have found significant difference between eccentric and concentric motions in terms of EMG activities. Generally, if the output force generated by the muscles is the same, then eccentric motions have less EMG activity as compared to concentric motions (Tesch, Dudley et al. 1990; Huang and Thorstensson 2000). Aagaard et al. (2000) did a study in which the EMG activities of three knee extensor muscles were measured before and after 14 weeks of heavy resistance training. Two levels of speed (30 and 40°/s) were tested for eccentric and concentric motions. The EMG activities for these pre-training muscles were 17-36% lower in eccentric motions than concentric motions. After the heavy resistance training, the eccentric strength increased 15%-17% while the concentric strength increased 8%-15%. The EMG activities for after-training muscles in eccentric motions were still lower (16%-22% less) than those in concentric motions. Similar results were found by Tesch et al. (1990). They studied the force and EMG signal patterns in concentric and eccentric actions of knee extensor muscles. Fourteen subjects performed unilateral, maximal voluntary concentric or eccentric quadriceps muscles actions on separate days. The results showed that the torque in eccentric actions were greater than in concentric actions (about 175Nm to 225Nm vs. 75Nm to 150Nm). The eccentric torque did not decline throughout the experiment time, while concentric torque markedly decreased with time. Though the torque was larger in eccentric actions, the integrated EMG signal was smaller as compared to concentric actions. Thus, the ratio of integrated EMG/torque was twofold greater at the beginning, and fivefold greater at the end for concentric than eccentric muscle actions. These results indicated that additional force during eccentric actions must be generated by mechanisms other than the recruitment of the active component of the muscles.

The authors noted that the elastic components of the muscle tissue contributed to the additional force production during the eccentric contractions.

2.2.3 Differences in nervous control strategy

It has been suggested that the nervous control system (NCS) uses a simple, consistent strategy to control muscle force: the NCS grades the external force and controls the muscle to generate greater, equal or less force as compared to the external force to induce concentric, isometric, or eccentric motions separately. However, this idea has been challenged by the evidence found in experiments that study maximum voluntary contractions (MVC) and the initial EMG right before both type of contractions. Fang et al. (2001; 2004) reported that the NCS signals for eccentric actions differ from those for concentric actions. In 2001, Fang et al. measured the electroencephalography-derived movement-related cortical potential (MRCP) and EMG signals when eight subjects performed eccentric and concentric actions of the elbow extensor muscles. The same amount of load (10% of the subject body weight) was applied to the left hand of the subject during these two types of contractions. It was found that the negative potential values of the MRCP, which are related to cortical activities for movement preparation and execution, were greater during eccentric than concentric tasks. The positive potential values of the MRCP, which are associated with the processing of the feedback signals, were also greater during eccentric than concentric actions. These results indicated that the brain plans for eccentric movements differently that it does for concentric movements. In 2004, Fang et al. did a similar study in which the subjects performed maximum voluntary eccentric and concentric contractions of elbow flexor muscles. Two-dimensional mapping of MRCP was measured to examine the spatial and temporal distribution of cortical activities during the two types of muscle activities. Several major

differences occurred in both temporal and spatial distributions, which suggest that “cortical activation patterns between the controlling processes of eccentric and concentric movements are not the same” (p.206). The number of activation areas determined by number of electroencephalogram electrodes passing a threshold was larger at all time points in eccentric muscle activities than in concentric ones. The patterns of activation areas in eccentric contractions were almost completely different from those in concentric contractions.

There is other evidence to support the different control strategies between eccentric and concentric contractions. Grabiner and Owings (2002) did some experiments studying the EMG of the knee extensor muscles. In one experiment, when the subject performed a normal sub maximal eccentric contraction, the EMG during the eccentric contraction averaged 84% of the value for the concentric contraction at the same force level. However, when the subject performed an unexpected sub maximal eccentric contraction - the subject expected to perform a concentric contraction while the device actually forced an eccentric contraction - the magnitude of the initial EMG for the unexpected eccentric contraction averaged 104% of the concentric contraction. In another experiment reported in the same article, the EMG activities of knee extensor muscles during isometric periods preceding both concentric and eccentric exertions were evaluated. The results of this study showed that the EMG of these muscles preceding eccentric contractions was 13% to 25% lower in the eccentric contractions as compared to those preceding concentric contractions, again indicating a differential “preparation” between the two types of exertions. This empirical evidence revealed that the NCS uses different strategies to control muscles in eccentric and concentric contractions.

2.2.4 Differences in force-velocity relationship

Just as the mechanism and control strategy are different for eccentric and concentric contractions, other basic characteristics of muscle function vary between eccentric and concentric exertions. The most obvious difference is in the force-velocity relationship. Early research showed that as velocity of shortening (concentric contractions) increased, the force producing capability decreased rapidly (Wilkie 1949; Bigland and Lippold 1954). Other studies have shown that changes in lengthening velocity (eccentric contractions) have a much smaller impact on the force producing capability of the muscle. Huang and Thorstensson (2000) investigated the position and velocity dependency of the torque output of lateral flexor muscles of the trunk. The subjects in this study performed lateral eccentric and lateral concentric isokinetic movements in the frontal plane at different lateral bending velocities (range from $-60^{\circ}/s$ to $60^{\circ}/s$) were tested. The lateral trunk flexor torque in eccentric movements was not affected by velocity, but in concentric movements, the lateral trunk flexor torque decrease as velocity increased. Similar results were found for trunk flexion in the sagittal plane, the trunk flexor torque decreased as the sagittal extension speed increased (Raschke and Chaffin 1996). Sutarno and McGill (1995) did a thorough investigation of the behavior of the erector spinae muscles in iso-velocity motions. Ten subjects performed sagittally symmetric flexion and extension motions while the EMG of the erector spinae muscles and the kinematics of the trunk were measured. The lower erector spinae muscles (L3 level) followed the typical force-velocity relationship. During the eccentric exertions, the muscle force remained at approximately 1.3 times that of the maximum force under isometric conditions, while the muscle force decreased when the velocity of the concentric contractions increased.

2.2.5 Differences in variability

There have been a number of studies that have shown differences in measures of variability of biomechanical performance when comparing eccentric and concentric exertions. In a study of elbow flexor muscles, Fang et al. (2001) reported greater force fluctuations during controlled sub-maximal eccentric contractions as compared to concentric exertions. The same amount of load was applied to the forearm of the subject when the subject performed simple elbow flexion/extension activities. The actual dynamic force was measured by a transducer attached to the load. The results showed that the standard deviation of the force measured in eccentric contractions was significantly larger than that in concentric contractions. (1.14N vs. 0.76N). In their study of maximum voluntary elbow flexion exertions, Fang et al. (2004) considered the standard deviation of the mean force value for the first and last of three trials for both eccentric and concentric tasks. Eccentric tasks had significantly higher standard deviation than concentric tasks (34.15N vs. 21.80N). It was explained by the authors that this difference in variability may be related to periodic stretch reflex-reduced EMG bursts and elective recruitment of larger-size motor unit for eccentric contractions. In a study of knee extension exertions, Christou and Carlton (2002) found that motor unit output was more variable in eccentric contractions as compared with concentric contractions. Ten subjects performed concentric and eccentric knee extension tasks while the torque generated by the knee extensor muscles was measured by an isokinetic dynamometer. Five absolute target force levels were given (50, 100, 150, 200 and 250N) and the subjects were asked to reach the target force level when performing eccentric or concentric motions at an angular velocity of 50°/s. Concentric motions started from 90° and moved to 110° knee angle. Eccentric motions moved in the opposite direction in same range, from 110° to 90°

knee angle. The results showed that mean force value at each target level was not significantly different between eccentric and concentric motions, but the standard deviation and coefficient of variation of peak force were larger in the eccentric than concentric exertions. Furthermore, the variability of the time to reach peak force was also greater for eccentric motions. It is believed that these differences in variability reflect differences in control strategy/capability and this most likely due to differences in the relative contribution of the passive component of the muscle force found in the eccentric exertions. As introduced before, the difference in nervous control strategy may also contribute to the difference in the variability of force production between eccentric and concentric contractions.

2.3 Biomechanical models of the spine

As described in the Introduction, spinal biomechanical models can be used to quantitatively analyze the reaction forces and moments on the spine. The general steps of developing a spinal model are as follows:

- 1) Establish a boundary and identify the components in this model, i.e., muscles, ligaments, and bones, and coordinate the axes.
- 2) Consider the effects of gravity on the body parts and other external loads (i.e., objects in hands).
- 3) Add the internal load (force by ligaments and muscles, etc) into this model. The external and internal load must fit the static equilibrium ($\sum F = 0, \sum M = 0$) if this is a static condition (i.e., holding a load in hand or isometric lifting). If this is a dynamic condition (i.e. lifting or lowering), then the dynamic equilibrium ($\sum F = m \cdot a, \sum M = \mathbf{I} \cdot \boldsymbol{\alpha}$) should be used.

Regardless of the type of condition, the internal load is important because most of the compression force on the spine comes from the forces generated by the trunk musculature and passive tissues. The key point here is that the moment is the product of the force times the length of the moment arm (the distance from the force line of action to the L5/S1 joint). The erector spinae muscles have much shorter moment arms as compared to the external load. To generate the same amount of moment to balance the external load, the erector spinae muscles must exert much larger forces than the gravity force of the external load alone (McGill and Norman 1986; Mirka, Kelaher et al. 1997). With the activation of the antagonist abdominal muscles, the forces are even greater. All these forces are internal forces that must be resisted by the spine. Thus, with the help of the spinal biomechanical model, researchers can take an inside view of the “real” load on the spine and have a better understanding of the risk factors related to LBDs.

2.3.1 Early physical models

Early biomechanical modeling attempts for the lumbar spine were done by Morris, et al. (1961). The authors used a single vector of force in the sagittal plan to represent the erector spinae group of muscles forces. The moment arm of the back muscles related to the fulcrum (the lower lumbar part of the spine) was two inches. In their model the force generated by back muscles was calculated under the condition of static equilibrium. The total external moment from the weight of the body and the load was calculated first. The internal moment calculated as the back muscle force times the moment arm was set to be equal to the external moment. In this condition, the only unknown variable was the back muscle force, so it could be determined. After the force from the back muscles was calculated, the total load

on the spine could be determined (Morris, Lucas et al. 1961). This model demonstrated the logic of calculating the spinal load from external load and muscles forces.

Later, Chaffin and colleagues (Chaffin 1969; Chaffin and Baker 1970) introduced a static sagittal plane model that could be used to predict the capacity of hand lifting strength. The goal of the model was to use the body anthropometry data, posture data, and maximum voluntary articulation torques as input data to predict the lifting capacity in various postures. First, the whole human body was divided into segments and described as seven solid links: feet, lower legs, upper legs, trunk (with neck and head), upper arms, lower arms, and hands. Then, the anthropometric data of the body such as body weight, stature, center of gravity of the hand to wrist distance, and foot length, etc., were collected. The articulation angles of the seven body parts were recorded along with the maximum voluntary torque between each pair of connected body parts, e.g., maximum elbow flexion torque, shoulder flexion, hip extension, knee extension and ankle planter flexion. With all these inputs, the author was able to predict the maximum hand lifting torque at a specific position and tell which joint was the weak point or, in other words, when a specific joint reached the maximum voluntary torque. In addition to these predictions, the biomechanical model was also able to calculate the moments/forces acting about/on the individual joints in the kinematic chain. To calculate these forces in the low back, a single extensor equivalent muscle was introduced, which generated the required force to create the necessary extensor moment. This basic approach allowed the researcher to show how varying the lifting posture affected not only the lifting capacity, but also the stresses on the low back.

From that point, biomechanical models were improved in two major directions: 1) greater accuracy from considering more detailed aspects of the low back anatomy/physiology,

(i.e., examining multiple muscle models instead of using the single extensor equivalent; considering the origin, insertion and line of action of the trunk muscles; considering both the length-tension and force-velocity relationship of the trunk muscles) and 2) greater applicability by considering more kinds of motions of the body including flexion, lateral bending and twisting; moving from static posture to dynamic exertions; and considering stochastic features.

2.3.2 Optimization models

The major problem with the multi-muscle biomechanical models is that the number of muscles in the model is often larger than the number of equilibrium equations, which results in an indeterminate system. From a biomechanical point of view, there are numerous solutions for the activation patterns of the agonist and antagonist muscles to fit the force and moment equilibriums during lifting activities (Mirka and Marras 1993). When only one muscle was used to counter the external load, the calculation of the muscle force could be done using simple algebra. As additional muscles were added, the system became statically indeterminate and other approaches needed to be considered. One such approach was the use of optimization through linear programming. Schultz and Andersson (1982) used this approach to estimate the forces generated by five major bilateral trunk muscles. The objective function of the linear programming formulation was the minimization of the compression on the spine while the constraints were that the static equilibrium was maintained and that all of the predicted muscle forces were within their feasible range. The results of this study showed that the muscles with the greatest moment arm were activated up to their maximum capacity and then other muscles were recruited. The authors pointed out two major problems with the results and optimization procedure: 1) there was no muscle

force from the abdominal muscles (not what really happens during realistic lifting tasks) and 2) there was no synergistic muscle activation of the extensor muscles (not what really happens during realistic lifting tasks). While there have been a great number of optimization models developed to try to overcome these challenges, none have been effective at predicting the complex synergist/antagonist muscle coactivation patterns that are utilized in complex three-dimensional lifting tasks.

2.3.3 EMG driven biomechanical models

Another approach that researchers have taken to try and overcome this static indeterminacy problem is to use empirical data describing muscle co-activation patterns. Electromyography plays a central role in this approach and these are called EMG-driven or EMG-assisted biomechanical models.

The use of the electromyographic method to study spine muscles can be traced back to the 1960's. In early EMG studies like Morris et al. (1962), the EMG signals was only used to detect the activation pattern in certain trunk motions, muscle on/off patterns, and relative muscle activation levels. The limitation to this approach was that these EMG values could only be compared within each individual muscle; the forces between different muscles could not be compared. In addition, the spine load could not be estimated as no actual muscular force was calculated. Despite these limitations, these studies did provide insightful information about the working parameters that would affect muscle activation patterns.

More recent studies have made use of the EMG data to predict the force generated by the individual muscles. The basic principle used in this modeling approach is that the force exerted by a muscle can be calculated using a maximum muscle stress value (sometimes called gain factor), which is the force generation capacity per unit of muscle cross-sectional

area (e.g. $50\text{N}/\text{cm}^2$). The muscle activation level during a task can be expressed as a percentage of their capacity often called the normalized EMG value. The 100% value used in this normalization can be determined when the person performs a maximum voluntary contraction. When the same muscle performs a normal exertion, the EMG signals measured are normalized to the maximum EMG signal and the result is expressed in terms of a percentage value, which can also be viewed as the percentage of maximum force generated by that muscle. For example, if a given muscle the EMG value generated during a maximum voluntary exertion was 2.5 volts and the EMG value for that muscle during a sub-maximal task was 0.5 volts, then that muscle has a normalized EMG value of 20% ($0.5/2.5$). If from other sources we know that the maximum muscle stress value is $50\text{N}/\text{cm}^2$ and the cross-sectional area is 5 cm^2 for that muscle, then the maximum muscle force which is related to the 100% EMG activity or maximum EMG signal is determined and can be calculated as $50\text{N}/\text{cm}^2 \times 5\text{ cm}^2 = 250\text{N}$. The muscle force in the sub-maximal task for that muscle can then be calculated as $0.2 \times 250\text{N} = 50\text{N}$. There are a number of other factors that need to be considered that will be addressed later, however this is the basic technique to be followed in the EMG-driven modeling approach.

The maximum muscle stress value (also called gain factor) is an important factor in this equation. It can be calculated in several different ways. Some models suggest the maximum muscle stress value could be calculated from regression based on a subject's anthropometry, but these are not extremely highly correlated (e.g., $R^2=75\%$) due to "reasons not fully understood at this point" (Marras and Sommerich 1991). Some models (McGill and Norman 1986; Reilly and Marras 1989) allow the maximum muscle stress value to vary from trial to trial to allow the net internal moment to match the net external moment (thereby

satisfying the equilibrium requirement). Some models calculate the average of maximum muscle stress value by comparing the external and internal torques from a subject's empirical data during a subset of experimental trials and then use that mean maximum muscle stress value in all subsequent calculations for that specific subject (Marras and Sommerich 1991; Marras and Granata 1995).

The most effective EMG-assisted models can be categorized into two major groups: the McGill group and the Marras group. The first EMG-assisted model in McGill's group was developed by McGill and Norman in 1986. This model employed many physical components from previous spinal biomechanical models but added the empirical EMG inputs to drive the model. Many of the basic procedures used in this model are still used in more recent EMG-assisted biomechanical models including this study, so a close look at some of the details of this model is useful.

This model uses three input sources: the surface EMG for measuring EMG activities of the trunk muscles, the trunk postural marker recorded on film providing the orientation and motion of the trunk, and the BIOMECH model (McGill and Norman 1987) that provided the reactive L5-L5 moment and force generated by the gravity of the body and the load in subject's hand. Three subjects were recruited from which source data was collected. The subjects were asked to perform six lifting tasks at different load and lifting speed conditions. The lifts were sagittally symmetric. The results of this model were the three dimensional reaction forces and moments on the L4-L5 joint.

There are three major steps in the processing of this model. First, the net external moments about L4-L5 joint are calculated through the BIOMECH model based on the anthropometry data of the subject and the kinematics and kinetics of the subject's posture

(McGill and Norman 1987). It is a fully dynamic, linked-segment, total body model that included hands, forearms, upper arms, head-neck, thorax-abdomen, pelvis, thighs, legs and feet segments. The film coordinate data and the forces on the hands are used as inputs and the external L4-L5 moment and force time histories generated in lifting the loads are the outputs.

Second, the net external moment is distributed to the restorative components provided by the disc bending, ligaments strain and active muscle contraction. The component distributions to the discs and ligaments are determined first, because the moments generated by these components depended only on trunk flexion angle. For example, the restorative moment produced by the disc is calculated from an exponential regression equation with the L4 disc flexion angle as the only variable. The remaining moment is then allocated to the muscles. The value of the force generated by a particular muscle is calculated as the product of normalized EMG, maximum muscle force (P_o) and an error term or gain value (G), and adjusted by the coefficient of velocity (Ω) and coefficient of length (δ). The equation is:

$$\text{Muscle force} = \text{normalized EMG} \times P_o \times G \times \Omega \times \delta$$

In this equation, the maximum muscle force and an error term represent the maximum muscle stress value and the muscle cross area, as noted before. The calculated muscle force is also modified by the instantaneous velocity of shortening and length of the muscle. Generally, the greater the velocity of shortening (concentric), the smaller the force generation capacity for that muscle. But when the muscle is lengthening (eccentric), the force generation capacity is a larger constant regardless of the lengthening velocity. So the force generated by the muscle should be “discounted” at a higher shortening velocity, and “inflated” at any lengthening velocity. The coefficient of velocity is calculated as:

$$\Omega = \begin{cases} 0.25 \times (0.9 - v) / (0.9 + v) & v \geq 0.125 \\ 1 - 1.6v & -0.125 < v < 0.125 \\ 1.2 & v \leq -0.125 \end{cases}$$

where v is the shortening/lengthening velocity relative to the resting length of that muscle. Similar procedures were conducted to adjust the force by the length and geometric restrictions. The force generation capacity reaches maximum when the muscle is at resting length. The coefficient of the length is calculated as:

$$\delta = \sin[\pi \times (l - 0.05)]$$

where the l is the length relative to the resting length of that muscle. The calculated net force is applied to the three-dimensional line of action of this muscle resulting in a force vector for that muscle. The moment generated by this muscle is a three dimensional vector, calculated as the cross product of the force vector and the muscle origin vector. The sum of the moment from all muscles, together with the restorative moments from the disc and ligaments, is compared with the total external moment. To bring this system to equilibrium, a gain value is calculated. The same gain value is used for the force calculation of all muscles in this step. This gain value is considered as an “error” term and is adjusted at each time point so that the total net restoration moment is the same as the net external moment in the whole lifting procedure. It is possible for the gain value to vary as a function of time for the same subject.

Finally, the compression, shear and torsion forces are calculated as the sum of the three-dimensional force vector generated by the muscles, disc and ligaments as well as the external load. This model revealed that the muscular components were the dominant factors in producing restoration moments and generated approximately 99% of the moments. The disc and the ligaments counted for less than 1%. While this model has great advantages as compared to previous models, it also has several shortcomings: 1) the gain factor (the

maximum stress value) was adjusted in each trial and was not consistent for the same subject, which directly opposes the physiological indications that a muscle's force generating capacity is directly related to muscular cross sectional area and should be consistent for an individual (Granata and Marras 1993); 2) the subjects were asked to maintain the flat-backed posture, which "reduced the action of ligaments to provide joint motion constraints". The activation of the passive posterior ligamentous system may be significant in flexed spine (White and Panjabi 1990; Granata and Rogers 2007) or full flexion conditions (McGill and Kippers 1994). Another limitation was that only sagittal lifting exertions were studied in this model. But McGill et al. expanded this model to explore axial trunk twisting motions (McGill and Hoodless 1990) and lateral bending motions (McGill 1992).

In addition to the McGill-group models, Marras and colleagues developed another group of EMG-assisted biomechanical models. The first model for the Marras-group was the SIMULEFT by Reilly and Marras (1989). This was a deterministic simulation model which described the relative changes of the spinal load based on trunk muscle EMG activities during a sagittally symmetric trunk exertion. The obvious disadvantage of this model was the lack of maximum muscle stress value, thus no direct calculation of muscular forces was presented.

Later in 1991, Marras and Sommerich introduced an EMG-assisted biomechanical model which included the maximum muscle stress value. (Marras and Sommerich 1991a; Marras and Sommerich 1991b) The advantage of this model was the capability of estimating the real magnitude of the trunk loading. This model suffered the same limitation as the early McGill models in that the maximum muscle stress value was adjusted for the same subject across trials. Another weakness was that though this was a three-dimensional model, the

muscles lines of action and moment arms data were the simplified three dimensional vectors adapted from Schultz and Andersson (1981). As the authors pointed out, this model could be improved with more accurate estimates of the force vectors, the muscle cross-sectional areas and the locations relative to the spine.

Granata and Marras (1993) expanded this model and conducted a new method to calculate the maximum muscle stress value. Unlike previous EMG-assisted biomechanical models that allowed the maximum muscle stress value to vary at each time point. This model adjusted the maximum muscle stress value so that the average value of the measured external torque was within 5% range of the average value of the model predicted torque. Thus, the equilibrium of the net external and internal torques was not met at each time point but equilibrium was met for the overall net external and internal torques. Through this method, the authors found that the maximum muscle stress value for a given subject did not vary significantly between the experimental trials, a result which was consistent with the physiological conclusion that the maximum muscle stress value should be constant for the same person.

The fixed maximum muscle stress value in this model had a significant advantage over the McGill and the previous Marras models with varied values. Not only because it was consistent with the physiological expectations, but also because it provided a means of validating the models. In previous models with varied maximum muscle stress values, the errors in the model (inaccurate position and orientation of the muscles, inappropriate presentation of the disc and ligaments) did not affect the performance of the model since the predicted internal torque always matched the external torque. In this model with fixed maximum muscle stress value, the changes of the external torque in the time domain must be

explained by the changes in the muscles' EMG activities and the trunk kinematics. In other words, the predicted torque should match the external torque as much as possible. The R^2 values between the external torque and model predicted torque could be used as the index of the performance of the model. Using this method, a validation procedure was conducted by the authors to verify the accuracy of this model. It was found that the model was able to reliably predict trunk torque. It was capable of explaining more than 70% of the variability in trunk torque production in most trials (Marras and Sommerich, 1991b). However, this model still utilized sub-optimal muscle force vector data. This problem was addressed when Marras and Granata replaced the structure with a more accurate anatomical muscle structure when expanding this model to include trunk twisting exertions (Marras and Granata 1995). In this model, they presented a truly three-dimensional structure of the major trunk muscles (see Figure 1).

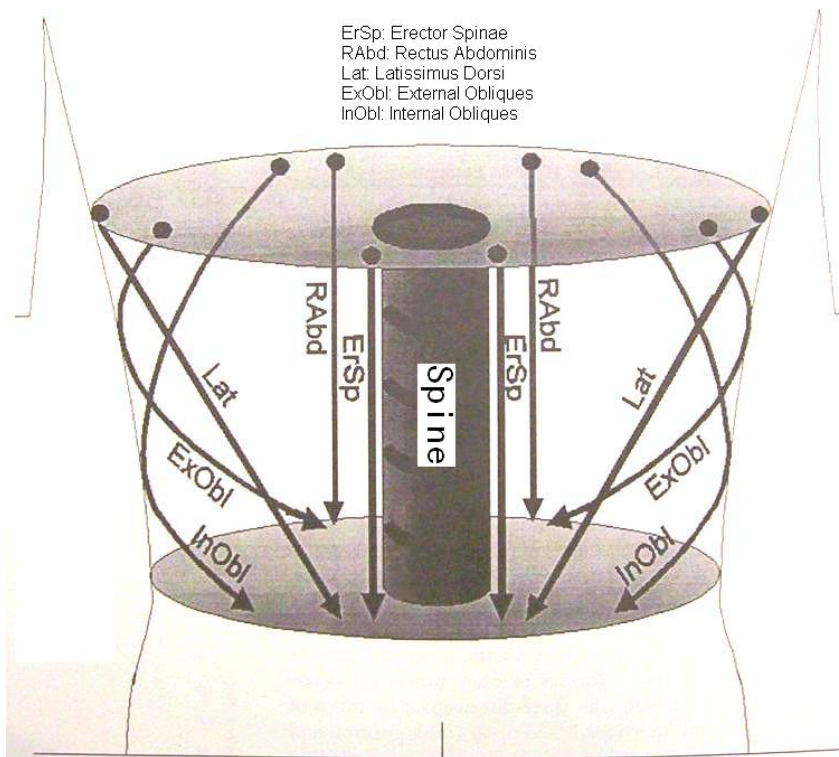


Figure 1. Lines of action of major trunk muscles (from Marras and Granata, 1995)

2.3.4 Models with eccentric motions

One limitation of these early models was that they were only validated in concentric motions (lifting). As described in the literature review, the force-velocity function in the eccentric phase has been shown to be significantly different from the one in the concentric phase. A recent expansion from the Marras group model was Davis et al. (1998) which included the eccentric phase. The advantage in this model was that the empirical relationships for length-strength and force-velocity under lowering conditions (eccentric contractions) were developed and incorporated into the model.

The length-strength and force-velocity relationships for both lifting and lowering were computed by minimizing the average variation in predicted muscle stress value as a function of muscle length and velocity, following the same method described in Granata and Marras (1995) and Raschke and Chaffin (1996). The length-strength relationship for lowering (eccentric) was found to be very similar to the one for lifting (concentric) exertions. It was described as a third-degree polynomial as determined by regression techniques. The force-velocity modulation for lowering was found to be a constant at 1.56 as best fit equations derived from regression methods (Figure 2)

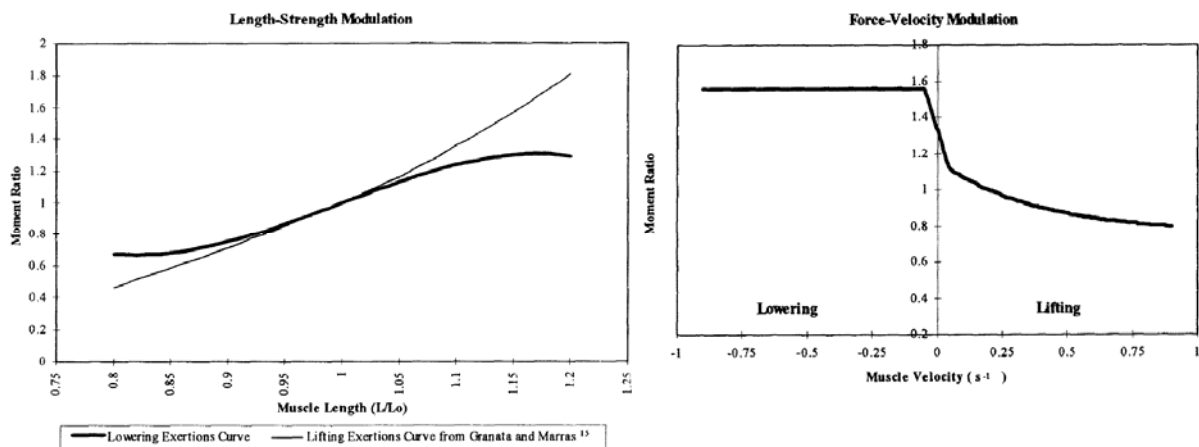


Figure 2. Empirical length-strength and force-velocity modulations from Davis (1998)

The new empirical length-strength and force-velocity relationships were then incorporated in the EMG-assisted model. The three-dimensional spinal loads were predicted by the vector summation of the forces of the ten major trunk muscles in this study. The estimation of muscle force was calculated by the following equation:

$$\text{Muscle force} = \text{cross - sectional area} \times \text{Muscle stress value} \times \text{NEMG} \\ \times f(\text{length - strength}) \times f(\text{force - velocity})$$

In this equation, the cross-sectional area is the physiological muscle cross-sectional area which was estimated from the anthropometry data of the subject (stature, weight, waist width and depth, etc.). The muscle stress value is an estimate of the force generation capacity of the muscle, which was set to minimize the sum of square errors of the predicted moment and the actual measured external moment. The NEMG is the EMG activity normalized to the peak EMG in maximum voluntary exertions. The factor of length-strength was determined from the trunk flexion angle which directly related to the length of the muscles. The factor of force-velocity was determined from the trunk flexion angular velocity.

Once the muscle force was calculated, the moment created by this force related to the L5/S1 joint was calculated as the cross product of the force vector and the vector of muscle origin. Then, the sum of all ten muscle forces and moments were calculated. With the forces and moments generated from the load in hand and body weight, the total reaction forces and moments on L5/S1 can be predicted by this model.

Using this model, Davis et al. studied the spine load at L5/S1 in both lifting and lowering tasks. Ten subjects lifted (40° of flexion to 0°) and lowered (0° of flexion to 40°) boxes while positioned in a structure that restrained the pelvis and hips. The tasks were performed under isokinetic trunk velocities of 5, 10, 20, 40 and 80°/s while holding a box

with weights of 9.1, 18.2 and 27.3kg. The lumbar motion monitor was used to measure the angular movements between the pelvis and the tenth thoracic vertebra, which was used as the trunk flexion angle in the model. The instantaneous trunk flexion velocity was measured and displayed on a computer display in front of the subject, allowing the subject to control their trunk flexion/extension velocity accurately. The subject was positioned into a pelvis support structure that was attached to a force plate. The position of the L5/S1 joint of the subject relative to the center of the force plate remained constant for the entire experiment. This setup permitted the trunk moment from the upper body and load in hand to be measured by the force plate accurately. EMG activity was measured through the use of bi-polar electrodes on the five pairs of major trunk muscles (left and right side) including erector spinae, latissimus dorsi, internal obliques, external obliques and rectus abdominis.

The trunk flexion angle, velocity and acceleration data were measured and recorded by the lumbar motion monitor. The EMG data were normalized with respect to the maximum muscle activity of each muscle with respect to length and velocity. The kinematic, kinetic and EMG data were used as inputs in the EMG-assisted spinal load model to calculate spinal forces and moments on the L5/S1 joint.

This study found that maximum compression force was significantly higher in lowering than in lifting (3269.1N vs. 2665.2N). Another important finding related to current work was that the standard deviation of the maximum compression force was also larger in lowering than in lifting (843.3 vs. 719.6). As the mean and standard deviation are larger in lowering, the spine load would more likely exceed its tolerance under lowering conditions than under lifting conditions.

Several limitations of this study must be addressed. First, there was no contribution of the passive components such as ligaments, disc, and elastic portion of the muscles in this model, since the exertions remained in the active range of the muscles (sagittal flexion less than 45°). Secondly, the exertions performed were not completely free-dynamic. The lifting/lowering style could have been influenced by the restriction of the hips and pelvis. These two limitations will be addressed in the current study.

2.3.5 Models with passive components

McGill and Norman's biomechanical model (1986) included the contribution to the restorative moments from passive components, such as ligaments and disc but they found the passive contribution to be negligible as compared to the muscles. The lifting exertions in this study did not reach full trunk flexion. The height of the load was 32cm above ground and the subject used squat posture (bend knee) to perform the lifts, which kept the subject away from full flexion posture. In some of the recent Marras group models, such as Davis et al. (1998), the maximum flexion angle was 45°. The minimal contribution of ligaments could be attributed to the fact that the motion range of previous models was out of the ligaments activation range.

The effects of passive components in generating the restorative moments must be considered when the subject is in a near full flexion posture. As previously noted, in these postures the EMG activities of the erector spinae muscles are reduced to near zero which indicate that passive components including the elastic proportions of the muscles, ligaments and disc may take the role of supporting the trunk. Under these conditions, the simple linear relationship between muscle force and the normalized EMG activity turned out to be invalid for several reasons. Firstly, EMG activities of the erector spinae muscles are near zero.

Secondly, the passive force of the muscle is now the majority source of the tension which is not related to the muscle activities (McGill and Norman 1986; McGill and Kippers 1994). Thirdly, the ligaments and disc are also activated to provide restorative torque.

Several studies have attempted to quantify the near full flexed posture with EMG-assisted biomechanical models. In 1994, McGill and Kippers conducted a study about the distribution of load between lumbar tissues during the FRP. This study can be viewed as an expansion of the previous McGill models (McGill and Norman 1986; McGill 1992). As described above, the myoelectric silence of the erector spinae muscles indicated the transfer of loads from active muscles to passive components. In this model, the force generated by a muscle included two parts, the active portion which depended upon EMG activities and the passive elastic portion which was related to the stretched length of the muscle. The same procedure described in McGill (1986) was used to partition the external load to trunk tissues. The restorative moment from the ligaments was also included. The ligament forces were calculated based on the cross-sectional area and the percent strain from the rest length of each ligament. There were a total of 11 ligaments involved. The parameters for the lines of action of the ligaments were determined from fluoroscopic measurements in the previous study (Cholewicki and McGill 1992). Eight subjects participated in this research by performing three flexion-relaxation maneuvers starting from a fully upright standing posture to a fully flexed posture with a load of 8kg held symmetrically in the hands. The results show that the muscles were deactivated at full flexion posture and generated elastic forces. The major source of restorative moment was the ligaments. For example, in one trial when the external moment was 171 Nm, 113Nm was generated by ligaments while only 38Nm was generated by muscles. An important observation was that the L4/L5 joint compression and

shear force were mainly from ligaments due to shorter moment arms as compared to trunk muscles. Therefore, the effects of ligaments should not be ignored in lifting activities that require almost full flexion postures. However, their study was limited by the lack of interaction between the compression force on the disc and the length of the ligaments (Dolan and Adams 2001). The disc becomes thinner with increasing compression force during trunk flexion, and ligament length becomes shorter. At full flexion posture, the ligaments were stretched far beyond their resting length. Small changes in ligament length may significantly affect the force generated by these ligaments. However, in McGill and Kippers model, the force from ligament was calculated from the strain only, which would not reflect the effects of the varied compression forces on the disc during trunk flexion which would reduce the accuracy of the model. Another limitation was that the authors did not consider the flexibility of the subjects. In this study, only one of the subjects showed FRP in the experimental trials while most other subjects demonstrated erector muscle activities up to 26% of MVC. The reason could be the diversity of the subjects' flexibility. Thus, while the McGill and Kippers model might be suitable to analyze the load distribution at the static full flexion posture, the usage of this model in eccentric and concentric motions at near full flexion postures might not be appropriate.

The calculation of restorative moments from ligaments is sensitive to the accuracy of the measurements on the ligaments strain. A small amount of change in the ligament strain when the ligament is stretched far beyond its resting length could cause a large amount of change in force production. In addition, other restorative components, (e.g. disc, facets) were not considered in McGill's model. One method of avoiding these problems is to use the overall stiffness value of the spine to represent the effects of the passive components. In 1996,

Nussbaum and Chaffin introduced a scalable and deformable geometric model of the human torso. The model incorporated the thoracic and lumbar spine, sternum, ribcage and sacrum, represented as rigid bodies interconnected by a set of spring and beam elements (Nussbaum and Chaffin 1996). Muscles were incorporated into the model as several point-to-point connections. Muscle force was described by the active and passive length-tension properties and calculated by a fourth-order polynomial and exponential curves respectively. The passive moment was estimated based on the L3/L4 rotational angle and the uniaxial stiffness values of the spine reported from previous research. The output of this model was the displacements and rotations of each segment of the model and it was validated by the values measured by the surface triad markers. This model revealed that in full flexion posture, the passive moment including the elastic portion of the muscles and that overall stiffness of the spine explained 94% of the required moment necessary to equilibrate body segment weights.

Finite element analysis is another approach used to study the role of passive components in the near full flexed posture (Arjmand and Shirazi-Adl 2005; Arjmand and Shirazi-Adl 2006; Bazrgari, Shirazi-Adl et al. 2007). A recent thoraco-lumbar finite element model by Arjmand and Shirazi-Adl (2005) studied human trunk load partitioning to ligaments and muscles at a near full flexion posture (65° symmetric flexion). It was a sagittally symmetric beam-rigid body model comprising six deformable beams to represent T12–S1 discs and seven rigid elements to represent T1–T12 (as a single body) and lumbosacral vertebrae (L1–S1). A sagittally symmetric muscle architecture with 46 local (attached to lumbar vertebrae) and 10 global (attached to thoracic cage) muscles was used. The ligaments were not modeled individually. The overall nonlinear stiffness of T12–S1 motion segments (i.e., vertebrae, disc, facets and ligaments) at different directions and levels

were modeled. Using the kinematics (total lumbar rotation) and external load as input, the finite elemental model was able to predict the muscle forces and restorative moments from passive components. The results show that the passive ligaments and muscles resisted more than 77% of the net moment at 65° trunk flexion angle. Later, Bazrgari et al. (2007) used this model to study muscle forces and spinal loading in squat and stoop dynamic lifting. Fifteen subjects were asked to perform sagittally symmetric squat and stoop lifts with or without a 108N load on a bar in front at 20cm height from the floor. The rotation of the spine was captured and input to the model to predict the muscle forces and spinal load. This study found a significantly larger rotation of lumbar and pelvis (70° and 45° in stoop versus 37° and 25° in squat respectively), hence larger internal spinal loads (maximum compression force: 2355N versus 2159N) in stoop lifting posture than in squat lifting posture. These results indicated that knee posture significantly affected the spinal load. However, in this study, the load was 20cm above the floor and the author reported “no flexion relaxation was observed which would otherwise have influenced the results in the final periods of the lowering phase of the study”. Thus, the effects of knee posture on spinal load in full flexed posture are still unclear.

The viscoelastic behavior of the passive components is an important factor that affects the restorative moment generated by the passive components in the full flexed posture. Shin (2005) conducted a study that considered this characteristic of the passive components of the spine in a long duration stooping (full flexion) posture using finite element analysis. He developed and validated a three-dimensional nonlinear viscoelastic finite element model of a whole lumbar spine that could simulate time-dependent mechanical responses of the spine. This model consisted of five vertebrae (L1 to L5), five intervertebral discs (L1/L2 to

L5/S1), posterior ligaments (posterior longitudinal ligament (PLL), capsular ligament (CL), ligament flavum (LF), intertransverse ligament (ITL), interspinous ligament (ISL), and supraspinous ligament (SSL)) and lumbar extensor muscles (multifidus and erector spinae). The vertebrae were modeled as a linear elastic material. The intervertebral discs consisted of three components: nucleus pulposus, annulus matrix and annulus fibers. The viscoelastic properties of the different materials of these components were defined respectively and incorporated into the model. Spinal ligaments were added to each vertebra according to their insertion points and cross-sectional areas. The viscoelastic property of the ligaments was represented as a nonlinear stress-strain curve (see Figure 3).

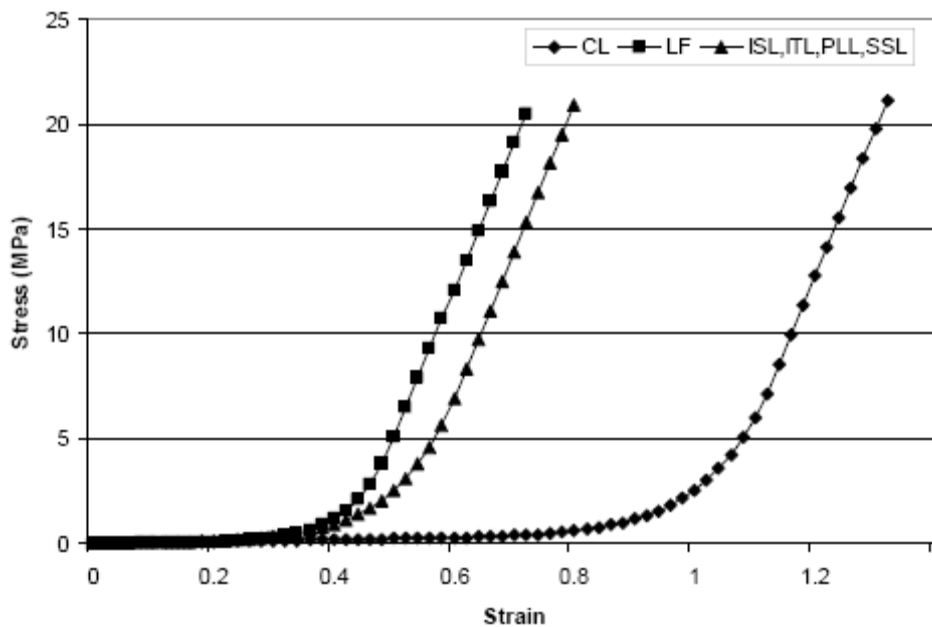


Figure 3. Nonlinear stress-strain curves of spinal ligaments (from Shin, 2005)

Major lumbar extensor muscles were included and the passive stretch of the muscle elements was considered in the model. After the model was constructed, the author used this model to simulate several conditions of the spine in various simulated tasks, including quiet upright standing, flexion to full flexion posture, stooping, extension to upright posture and weight holding. The lumbar extensor muscles activity level were affected by the creep

displacement of the viscoelastic components (the intervertebral discs and ligaments) due to the force from the weight of the body and load. To verify the predictions of the model, ten subjects were recruited to perform tasks that were simulated in the model. The EMG activity of the lumbar extensor muscles of the subject was recorded. The model predicted muscle force was compared with the measured empirical force estimated from the EMG activities of the lumbar extensor muscles (see Figure 4). High correlation coefficients ($R>0.9$) with relatively small mean absolute errors, indicated good performance of the model.

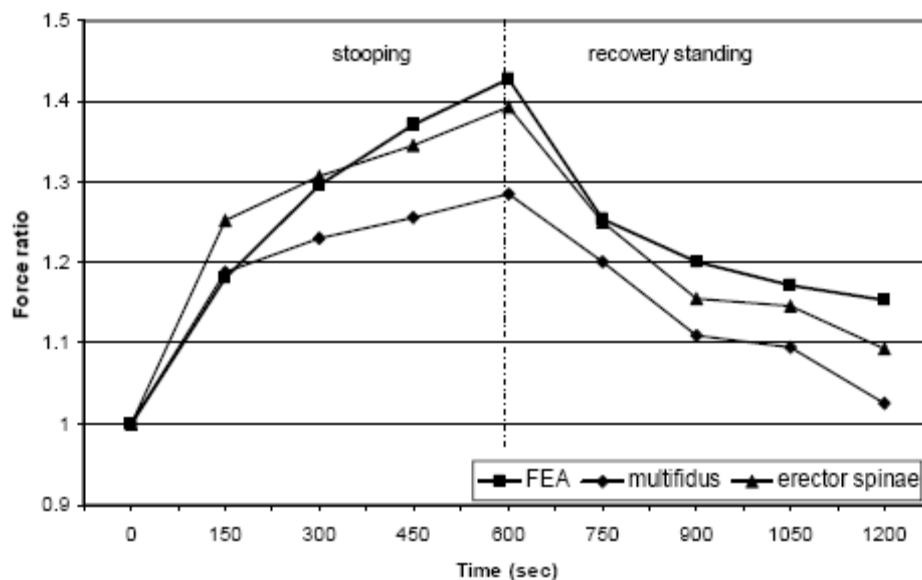


Figure 4. Measured muscle force verses model predicted muscle force in different tasks (from Shin, 2005)

Collectively, these studies indicate that the passive components of the trunk, especially the ligaments, are important factors in determining the load on the spine. Because of the relatively short moment arms, the compression force from ligaments are much higher than that generated by active or passive muscles (McGill and Kippers 1994). Thus, the effects of ligaments as well as other passive components should be included in studying the spinal load during lifting/lowering exertions with near full flexion postures. Table 1 presents a summary of the important EMG assisted biomechanical models

Table 1. List of important EMG-assisted biomechanical models

Author and year	Strengths	Limitations
Morris, Lucas et al. 1961	One of the earliest biomechanical models	Single force vector represents back muscles, sagittal symmetric, static
Schultz and Andersson 1981	Included 10 major spine muscles with detailed structure	Not a real three dimensional model
McGill and Norman 1986	Landmark one, detailed spine muscle structure, considered both disc, ligaments and muscles, anatomically accurate muscle structure	Muscle stress value varied between trials
Reilly and Marras 1989	EMG assisted	Only ratio, no real force values
McGill and Hoodless 1990	Twisting	Muscle stress value varied between trials
Marras and Sommerich 1991a,b	Uses muscle cross section area and stress value to predict real load	Muscle structure sub-optimal
McGill 1992	Lateral bending was first modeled	Passive tissues not considered, concentric exertions only
Mirka and Marras 1993	Stochastic modeling approach used, provides simulated distributions of muscle forces and spine loading	Passive tissues not considered, concentric exertions only
Granata and Marras 1993	Constant muscle stress value	Passive tissues not considered, concentric exertions only
McGill and Kippers, 1994	Included spinal ligaments in the model, investigated the flexion-relaxation phenomenon	Only studied static full flexed posture, no interaction between muscles and passive components
Marras and Granata 1995	More accurate muscle structure, twisting	Passive tissues not considered, concentric exertions only
Davis, Marras et al. 1998	Eccentric and concentric motions	Not validated in full trunk flexion range, passive tissues not included

3 PILOT WORK

The study conducted by Shin, Shu et al. (2004) is included in this section as it provided a strong foundation upon which much of the current work was built. The objectives of this work were to quantify the interactive effect of trunk angle and knee angle on the lumbar extensor activity and to quantify the effect of individual trunk flexibility in this response. Since the knee flexion angle can affect the rotation of the pelvis in the trunk flexion motion, the muscle activities of back extensors were expected to change as the knee angle changed. Also, flexibility was expected to be related to the ligament tension in the flexed posture and it was reasoned that this might influence the muscle activity level in large flexion postures. Results of this previous work were used to provide some empirical data that support the idea of passive components generating extension moment in full flexion postures

3.1 Subjects

Eight male subjects with a mean (and standard deviation) age of 27 years (2.3), height 1.74 m (0.03), body mass 68.5 kg (4.9) were recruited from the university community and participated voluntarily. All subjects were free from chronic and current back problems and gave written informed consent after being introduced to the nature of the study. After a period of brief warm up and light stretching, the flexibility level of each subject was assessed by having the subject flex his trunk forward and reach towards the ground with knees straight. Subjects were categorized as low-flexibility (finger tip reach greater than +5 cm from floor, two subjects) (group 3), mid-flexibility (finger tip reach between -5 cm and +5 cm, three subjects) (group 2), and high-flexibility (finger tip reach below -5 cm from floor, three subjects).

3.2 Apparatus

Eight pairs of surface Ag-AgCl electrodes (Model E22x, In-Vivo Metric) were used to collect the EMG muscle activity of the sampled muscles. These data were pre-amplified (1000×) and then carried via shielded cable to the main amplifiers that filtered (60 Hz, and low-pass 1000 Hz) and further amplified (50×) the EMG data. An isokinetic lumbar dynamometer was used to provide the necessary static resistance for the collection of the angle-specific maximum voluntary contraction (MVC) EMG data from the lumbar extensors. This dynamometer system was also able to provide a measure of the angle-specific peak moment generated by the subject, necessary for the calculation of the hand-held loads as discussed later. A stationary chair system was developed to capture the angle specific MVC EMG data for the knee flexors and extensors.

3.3 Independent variables

Independent variables in this study included sagittally symmetric trunk flexion angles (30°, 50°, 70°, and 90°), knee flexion angles (0° (knees straight), 20°, and 40°), static moment on the L5/S1 joint (no external load, and 50% of the subject- and angle specific trunk extension moment), and subject flexibility level (high, medium, low). The angle between a vertical reference line and the line joining the acromion process and greater trochanter was defined as trunk flexion angle. The angle between the line joining the greater trochanter and center of rotation of the knee and the line joining the center of rotation of the knee and the lateral malleolus of the ankle was defined as knee flexion angle.

3.4 *Dependent variables*

Dependent variables were the normalized EMG from lumbar extensors (multifidus, iliocostalis, and longissimus), knee extensors (rectus femoris, vastus lateralis, and vastus medialis) and knee flexors (gastrocnemius, soleus and biceps femoris). All data were collected on the right side only.

3.5 *Experimental procedures*

Surface electrodes were placed over eight muscles on the right side of the body of the subjects. The muscles sampled (and sampling location) were: 1) multifidus (1.5 cm to the right of the vertebral midline at L4 level), 2) longissimus (3.5 cm to the right of the vertebral midline at L2 level), 3) iliocostalis (4.5 cm to the right of the vertebra midline at L2 level), 4) vastus medialis (8–9 cm above the knee joint cleft), 5) rectus femoris (9–10 cm above the knee joint cleft), 6) vastus lateralis (8–9 cm above the knee joint cleft), 7) biceps femoris (10–12 cm above the knee joint cleft), and 8) gastrocnemius-soleus group (medial side, 10–12 cm below the knee joint cleft) with a fixed inter-electrode center to center distance of 2.5 cm. While the signal collected from the three trunk extensors almost certainly contained cross-talk from adjacent trunk extensors muscles, the electrode placement locations were chosen to maximize the contribution of the named muscle based on the relative cross-sectional areas of the muscles in the region (L2–L4). Prior to placement, the electrode placement area was shaved, abraded and cleansed with isopropyl alcohol absorbed cotton ball to lower the electrical impedance. All EMG data were collected at 1024 Hz. After the experimental setup, the maximum voluntary trunk extension moment and lumbar extensor MVC EMG data were collected using an isokinetic dynamometer as the subject performed

the isometric trunk extension exertions at each of the four different trunk flexion angles (30°, 50°, 70°, and 90°). The maximum EMG of knee extensors and flexors were then collected at 0° (knees straight), 20°, and 40° knee flexion angles as the subject sat on the stationary chair system and pulled against a secure harness. The MVC exertion for the gastrocnemius-soleus group was accomplished by having the subject exert a maximum plantar flexion force against a stationary surface while seated in the chair. Each exertion was maintained for three seconds. All MVC trials were collected only after the subject completely understood and performed consistent pre-test trials. Between consecutive MVCs, a one minute rest break was given. In the subsequent trials, subjects experienced loading conditions of no load (simply holding the weight of the torso) and a condition that required the subject to produce an extension moment (about L5/S1) equal to 50% of their posture specific capacity. This 50% condition was accomplished by having the subject hold a barbell loaded with the appropriate amount of weight. The procedure used to calculate the required hand-held weight required the development of a simple biomechanical model to derive the static moment of the upper body mass as well as the posture-specific trunk extension maximum that occurred in the isokinetic dynamometer. Using these two inputs, the posture-specific moment was calculated and the appropriate hand-held weights were calculated for each trunk flexion condition for that subject. Subjects performed a total of 48 trials (two repetitions of all combinations of four trunk flexion angles, three knee flexion angles, and two load conditions). At each trial, the subject bent his torso forward and flexed (or straightened in the case of 0° condition) both knees and held the barbell using both hands. The experimenters used goniometers to establish when the subject had achieved the appropriate knee and trunk angles. The subject was then asked to hold that position and keep his heels in contact with floor. As soon as the posture

was stable, the muscle activities were collected for 3 seconds. There was a 20 second rest break between consecutive trials during which the subject stood up in a relaxed posture. Task order was fully randomized.

3.6 Data processing

The raw data were filtered using a 10–500 Hz pass filter as well as a notch filter that eliminated 60 Hz and its aliases. Once filtered these signals were rectified (full-wave) and averaged across the three second data collection period. This processing occurred in both the data collected during the experimental trials, as well as during the maximum voluntary contractions. The EMG data collected during the maximum exertions were then partitioned into 1/8 s windows and the maximum of the 24 windows for each muscle in each posture were identified and were used as the denominator in the process of normalizing the experimental data.

3.7 Data analysis

The data set was partitioned into two subsets by load condition and then each set was analyzed using ANOVA to examine the effects of trunk flexion angle, knee flexion angle and subject flexibility and their interactions. This preliminary ANOVA was performed to get a sense of the global effects of these variables. To test the specific hypotheses of the current study, further partitioning of the data was necessary. In an effort to be more refined in the analysis of the effect of individual flexibility and knee angle on the flexion–relaxation response, these datasets were further partitioned by trunk angle and an ANOVA was performed on each of these trunk angle-specific datasets to identify those particular trunk

angles at which the flexion–relaxation response was influenced by individual flexibility and knee angle.

3.8 Results

The mean values of the normalized EMG activities of the erector spinae muscle are shown below (see Figure 5, Figure 6 and Figure 7). These results indicate that the effect of knee angle is particularly important when the subject nears the end of their range of motion (90° trunk flexion) where the slight changes in pelvis rotation can have a significant impact on the passive contribution to the extensor moment (see Figure 5). On the other hand, the effect of individual flexibility appears to have a more consistent response across trunk angles. Figure 6 shows that at every trunk angle, the low flexibility group generated less muscle activity and relied more on the passively generated extensor moment. Further exploration of this flexibility response in the extreme flexion positions (70° and 90°) showed that the knee angle response was affected by the flexibility of the subject (see Figure 7). This figure illustrates that for the high flexible subjects, there was a strong knee angle effect on the flexion-relaxation response at the 90° trunk flexion angle but there was no knee angle effect at the 70° position. In the middle flexibility group, it appears that this knee angle effect is also seen at the 70° position, indicating that the transition point from passive to active occurs around this point for this group. In the low flexibility group, there does not appear to be any knee angle effect on the flexion-relaxation response indicating that, for this group, the transition point is less than 70° and regardless of knee angle, the passive contribution is still high.

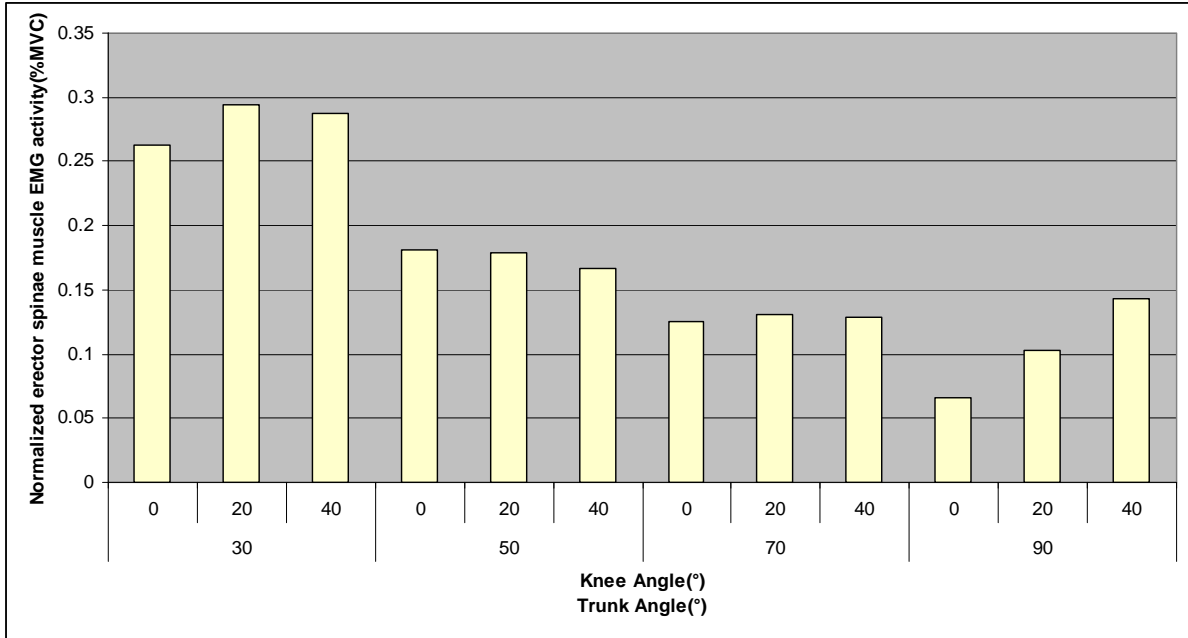


Figure 5. Normalized EMG of lumbar extensors vs. knee angle and trunk angle (50% MVC)

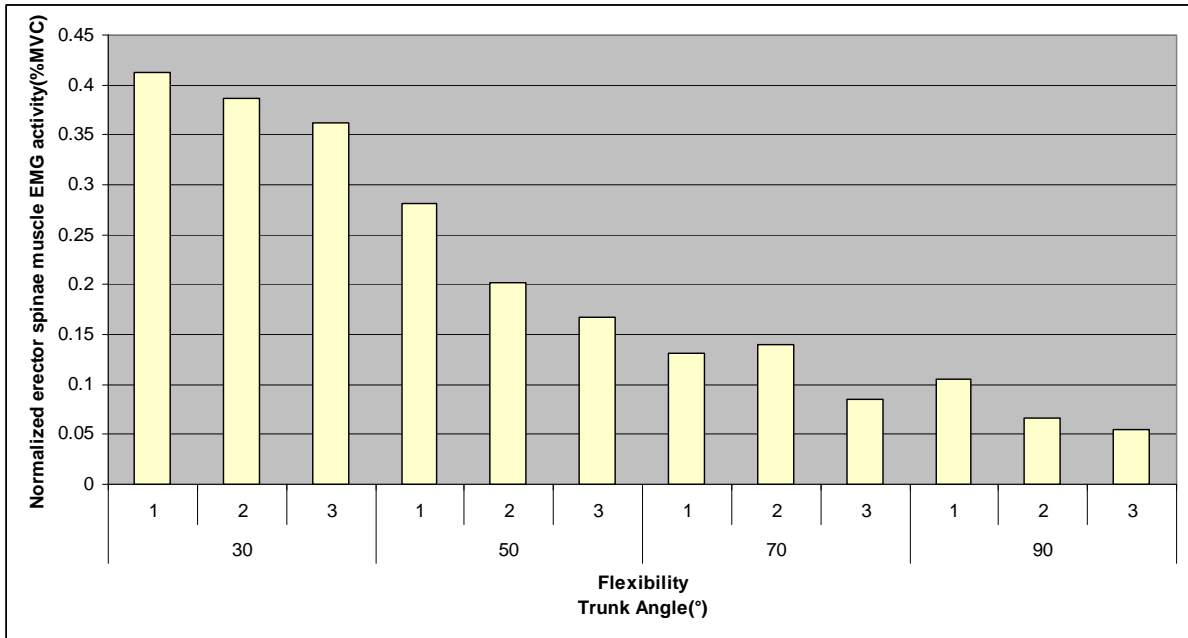


Figure 6. Normalized EMG of erector spinae muscle vs. flexibility and trunk angle (50% MVC condition) (group 1 : high-flexible, group 2 : mid-flexible, group 3 : low-flexible)

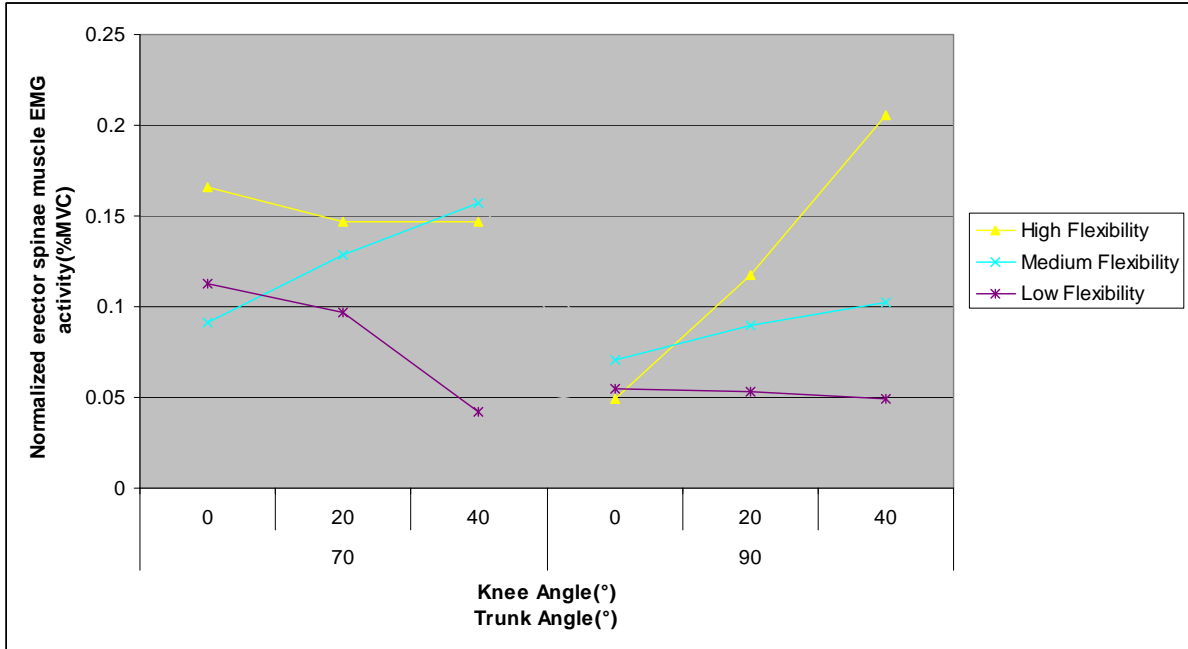


Figure 7. Normalized EMG of lumbar extensors vs. knee angle, trunk angle, and flexibility (50% MVC condition)

The results of the model predicted L5/S1 joint compression force and torque from muscles alone are shown in Figure 8. There is a clear difference in compression force and torque between the high and low flexibility subjects. The compression force and torque of high flexibility subjects are about 70% larger than those of low flexibility subjects. This indicates that this EMG-assisted model is sensitive to the flexibility of the subjects. Therefore, the estimation of spinal load maybe inaccurate at near full flexion posture when the contribution of passive components is ignored.

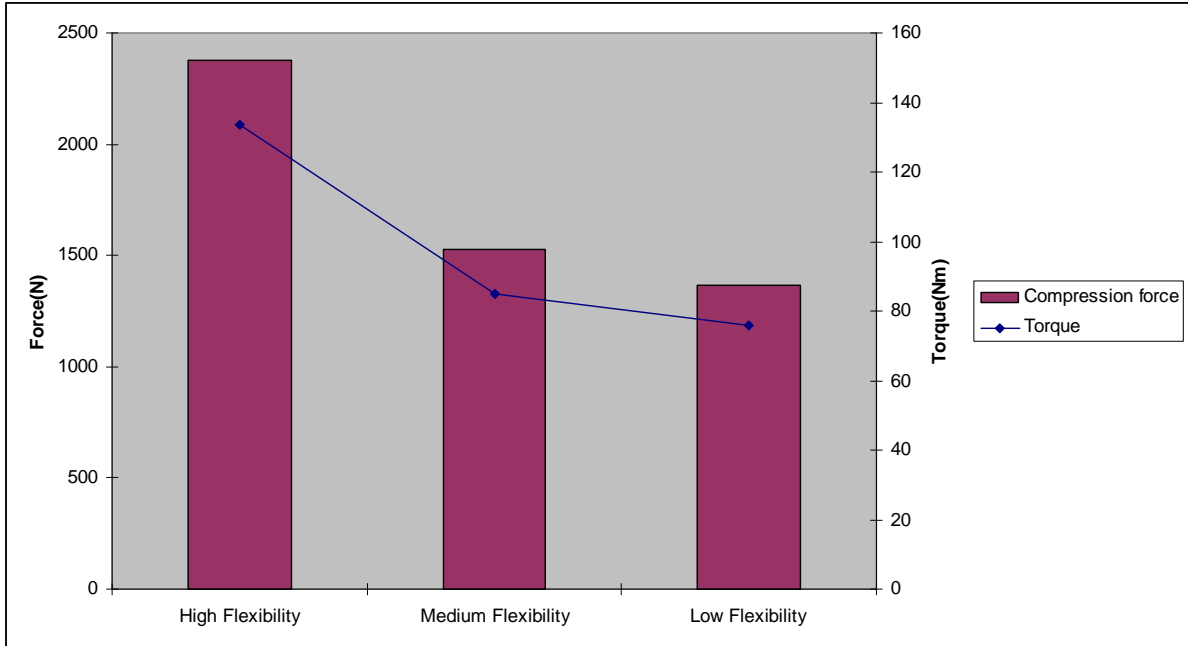


Figure 8. Model predicted L5/S1 joint compression force and torque from muscles vs. flexibility

4 MODEL DEVELOPMENT

The goal of this research is to develop an EMG-assisted biomechanical model that is able to accurately predict the spinal loading during the entire range of motion of trunk extension (concentric)/flexion (eccentric) movements and then apply this model to explore the differences between concentric and eccentric lifting exertions. In preparation for this research, significant preliminary work was conducted to develop the individual components that are to be employed in this model. The following is a description of those efforts.

The basic components and the flow of the model are outlined in Figure 6. The output of this model includes the time-dependent stress changes on the L5/S1 joint during these trunk movements, while the inputs include subject anthropometry, a description of the lifting kinematics/kinetics and finally the EMG data describing the relative activation levels of the major muscles of the torso. The methods used in each step of the model are presented in the following sections.

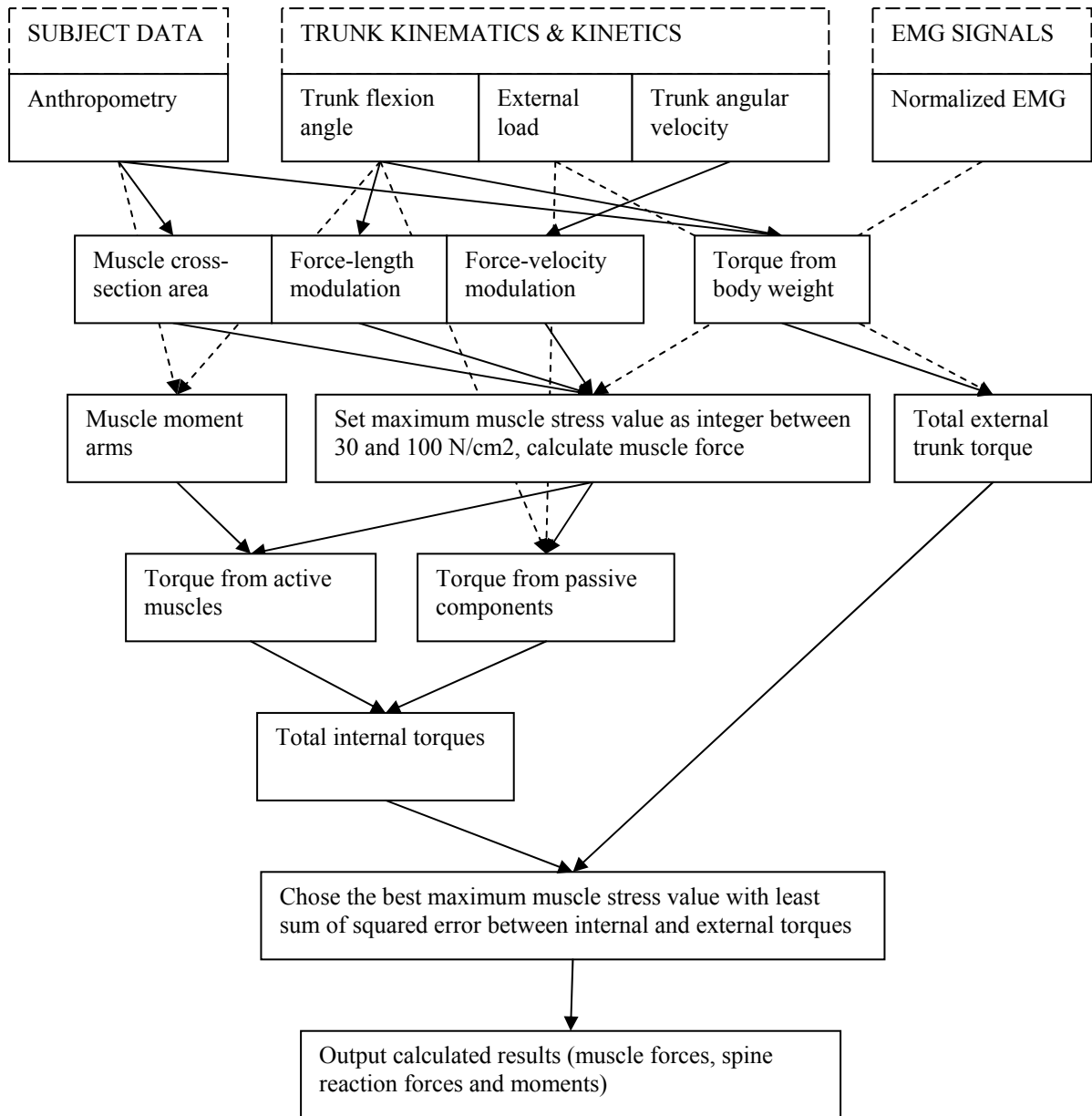


Figure 9. Inputs and flow of the model

4.1 Input data

There are three kinds of inputs for this model: the subjects' anthropometric characteristics, the trunk kinematics and kinetics, and normalized (to maximum) EMG activity data of ten primary trunk muscles. The anthropometric data of the subject include subject's weight, stature, width and depth of the torso at the level of the umbilicus. The

weight of the subject is measured by a scale. The stature, waist width and depth of the subject are measured by a straight ruler. This information is used to estimate the cross-section area of each of the ten trunk muscles, moment arm of each of these muscles about the spine (Marras and Granata 1995), and external moment created by the weight of the upper body (McGill and Norman 1985).

The trunk kinematics and kinetics data include the time-dependent trunk flexion angle, angular velocity, angular acceleration and total external torque. In this study, trunk kinematics/kinetics are captured by a dynamometer or motion analysis system and these data are used in the calculation of the force-length factor, the force velocity factor as well as in the calculation of the external torque due to the trunk weight. The total external torque is the sum of the torque due to the loads lifted and the torque from trunk weight. These components are described in greater detail in Section 4.2.

The normalized to maximum EMG data contain the time-dependent muscle force generation information for measured trunk muscles, including antagonist muscles. This indicates the percent of capacity exerted by each muscle to counter the external loads. The ten muscles included in this model are: the right and left pairs of the erector spinae, the latissimus dorsi, the rectus abdominis, the external obliques and the internal obliques. These components are described in greater detail in Section 4.3.

4.2 External moment calculation

There are three components in the external moment about the spine. The first one is moment generated by the external load, either hand-held load or a force applied onto a transducer on a dynamometer. This torque is calculated as the force times the moment arm about the L5/S1 joint. For the hand-held load, the torque is the load weight times the

horizontal distance between the center of the weight and the L5/S1 joint. The perpendicular distance of the L5/S1 joint to the center of the load is calculated based on the anthropometric data of the subject and the trunk flexion angle. The formula is:

$$M_{load} = \text{Load mass} \times (\alpha + g) \times l \times \sin(\theta)$$

where α is the vertical acceleration of the load (m/s^2), g is gravitational constant (9.8 m/s^2), l is the length from the L5/S1 joint to the shoulder joint (m), and θ is the trunk flexion angle ($^\circ$).

For the torque as measured by a dynamometer, the moment is the force measured by the force transducer multiplied by the distance between the force transducer and L5/S1 joint:

$$M_{load} = 0.22 \times F$$

where 0.22 (m) (constant) is the moment arm from the transducer to L5/S1 joint, and F is the force (N) measured by the transducer.

The second component is the moment generated by the weight of the upper body. It is a function of trunk flexion angle. The upper body weight and location of the center of mass are estimated from Clauser et al. (1969). The moment created by the upper body weight is calculated as:

$$M_{body} = \text{torso mass} \times g \times 0.47 \times \text{torso length} \times \sin(\theta)$$

where torso mass is the total mass of the upper body above L5/S1 joint, calculated as the 38% of the total body mass of the subject (Clauser, McConville et al. 1969); g is gravitational constant, 9.8 N/kg ; 0.47 is the percent location of the center of torso mass along the total torso length from L5/S1 joint (Clauser, McConville et al. 1969); torso length is the distance between the L5/S1 joint to top of head, and θ is the flexion angle.

The third component is the moment from the angular acceleration of the trunk. This component will only exist in dynamic exertions when the velocity is not held constant. The moment by the rotational acceleration of the upper body is calculated as:

$$M_{acc} = 0.0010 \times \text{torso mass} \times \text{torso length}^2 \times \alpha \\ + \text{torso mass} \times (0.34 \times \text{torso length})^2 \times \alpha$$

where 0.0010 is the dimensionless moment of inertia of the torso (Cheng, Chen et al. 2000), torso mass (kg) is the total mass of the upper body above L5/S1 joint, calculated as the 38% of the total body mass of the subject (Clauser, McConville et al. 1969), torso length (m) is the distance between the L5/S1 joint to top of head, 0.34 is the percent location of the center of torso mass along the total torso length from L5/S1 joint (Clauser, McConville et al. 1969), and α is the angular acceleration of upper body (rad/s²).

The total external moment (Nm) is calculated as:

$$M_{ext} = M_{load} + M_{body} + M_{acc}$$

4.3 Internal moment calculation

The total internal moment includes two parts: the moment from passive components and the moment from active muscles. The passive moment in this model is directly related to the trunk flexion angle and reaches maximum value at full flexion postures. The flexibility of the subject, the compression force from active muscles, and load also modify the calculation of the passive moment. The moment from active muscles is related to the EMG activities and lines of action of these muscles. The force-length and force-velocity factors are incorporated to reflect the changes in force generation capacity due to varied muscle length and contracting/lengthening velocity.

4.3.1 Calculating the moment from the passive components

First, the lumbar flexion angle and load relationship is determined from the full flexion trial data of the subject. The maximum trunk flexion angle and the angle between the L5 and S1 vertebrae are measured. The weight of the upper body is the only external load in this scenario. The external moment is calculated as the weight of the torso times the moment arm as the distance between the center of torso mass and the L5/S1 joint. The formula is:

$$M = \text{torso mass} \times g \times 0.47 \times \text{torso length} \times \sin(\theta)$$

where torso mass is the total mass of the upper body above L5/S1 joint, calculated as the 38% of the total body mass of the subject (Clauser, McConville et al. 1969); g is gravitational constant, 9.8 N/kg; 0.47 is the percent location of the center of torso mass along the total torso length from L5/S1 joint; θ is the trunk flexion angle.

This external load and the flexion angle between L5 and S1 joints are then imported into the Finite Element Analysis (FEA) model developed by Shin (2005). As previously described, this model consists of the major posterior trunk muscles, the vertebra, and the passive components including the ligaments and disc. Using the external vertical load and trunk flexion angle as input, this model is capable of estimating the force and moments generated by the passive components. In order to avoid the time consuming computational procedure of the FEA, various combinations of the external load and lumbar flexion angle have been processed and the relationship between the moments from passive components and the combinations of external load and lumbar flexion angle is represented as a three-dimensional surface (see Figure 10).

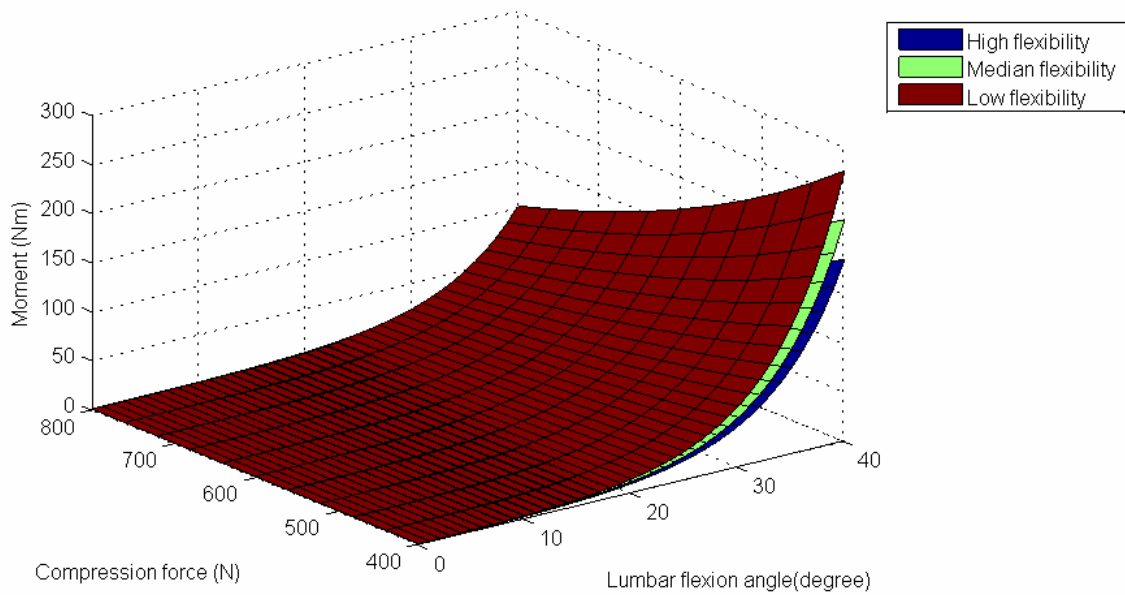


Figure 10. Illustration of the 3D surface of passive moment vs. load and lumbar flexion angle

In this figure there are three surfaces representing the theoretical response of the passive tissues of the subjects with different flexibility. Assuming two subjects have the same weight, the one with higher flexibility can bend further than the one with lower flexibility, resulting in a larger lumbar flexion angle. The flexibility level of the subject is determined based on the maximum flexion angle using the method described in previous research (Shin, Shu et al. 2004). The values of these three variables in the full flexion posture for a specific subject determines the unique 3D surface that will be used to estimate the restorative moment from passive tissues in other postures. For example, the trunk flexion angle for one subject at full flexed posture is 60° and the lumbar flexion angle is 26° . The restorative moment generated from the passive components must be the same as the external moment calculated based on the weight and length of the subject's torso since the muscles are relaxed in this posture. Assuming the subject's upper body weight is 400N and the distance from the center of gravity of the upper body to the L5/S1 joint is 0.3m, the total external load will be

$400 \times 0.3 \times \sin(60^\circ) = 104 \text{ Nm}$. This is also the total internal load from the passive components. The lumbar flexion angle (36°), total upper body weight (400N) and the total internal moment (104Nm) determine one unique point as well as a unique response surface in the 3D space as shown in Figure 10. The moments from passive components at other lumbar flexion angle and load combinations can be picked out on this surface. For example, at another trunk flexion angle during one lifting exertion, the lumbar flexion angle is measured as 24° , and the force from the load and the weight of the upper body is 450N. The height of the only point on the 3D response surface of this subject at 24° lumbar flexion angle and 450N external load is found to be 90Nm, which is used as the restorative moment from passive components of the spine (M_p) and added into the total internal torque.

Using the same method, the 3D surface for the compression force on L5/S1 joint from the passive components can be established and the forces at any trunk flexion angle can be estimated.

4.3.2 Calculating the moment from the active muscles

There are several factors that will affect the calculation of the moment generated by active muscles, including the muscle cross-sectional area, muscles lines of action, muscle force-length and force-velocity modifiers, normalized EMG activity, and the maximum muscle stress value. The details of these factors are discussed below.

Muscle cross-sectional area

Muscle force is assumed to be proportional to muscle size as described by the cross-sectional areas (Bogduk, Macintosh et al. 1992). Two kinds of muscle cross-sectional areas are mentioned in the literature. Anatomical area is the real muscle area at a transverse cutting

plane, usually measured *in vitro* or by a CT scan *in vivo*. Because the anatomical area is directly related to the location of cutting plane and is not constant for a specific muscle, the other kind of muscle's area, physiological cross-sectional muscle area (PCSA), is usually used in the spinal biomechanical models. It is defined as the total volume of the muscle divided by the length of the muscle. PCSA is used in this study because it is more accurate in determining the force generating capacity of a specific muscle.

Muscle areas used in early models, e.g. Schultz, Andersson et al. (1982), were based on cadaver studies which might differ from each other and so could not represent the real working area *in vivo* (McGill, Patt et al. 1988). The computerized tomography (CT) and magnetic resonance imaging (MRI) technologies were used to measure the *in vivo* muscle cross-sectional areas in several studies (McGill, Patt et al. 1988; Tsuang, Novak et al. 1993; Marras, Davis et al. 2001). Some of these studies also used regression to predict the muscle areas from simple human variables such as height and weight (McGill, Patt et al. 1988; McGill, Santaguida et al. 1993).

In this study, the physiology cross-sectional areas are calculated from the subject's waist width and depth measured at the umbilicus as described in Marras and Granata (1995). The equation is:

$$Area = coefficient \times depth \times width$$

The coefficients for the ten muscles are listed in Table 2.

The CT and MRI methods are also capable of measuring the origin, the insertion and line of action for muscles (McGill, Patt et al. 1988; Bogduk, Macintosh et al. 1992; McGill, Santaguida et al. 1993). The line of action of a muscle is defined by one of three approaches: straight origin-insertion line, bony landmark line and centroid line (Van der Helm and

Veenbaas 1991). The first two kinds of line are straight lines connecting the origin and insertion sites or landmarks for a muscle, which is simple and easy to measure by CT and MRI. The centroid line is created by joining the centroids of varying cross-sectional areas along the length of a muscle. There are several assumptions for the concept of muscle line of actions. First, the force vector derived from the muscle line of action at a certain cross-section of the muscle is representative of the forces transmitted by the muscle at that particular cross-section. Second, the force is exerted along the line so no moment is exerted by the muscle around the muscle line of action. Finally, no shear force exists in the particular cross-section area (Van der Helm and Veenbaas 1991).

Muscle lines of action

In this study, the muscle lines of action data from Marras and Granata (1995) are used. This method has been used and validated in several studies (Marras and Granata 1997; Davis, Marras et al. 1998; Marras, Granta et al. 1999) and has been proven to be accurate. Table 2 contains the coefficients of these origin-insertion data, adapted from Marras and Granata (1995).

Table 2. Coefficients of muscle coordinates and cross-sectional areas (Marras and Granata, 1995)

Muscle Equivalent	Area	Origins			Insertions		
		X	Y	Z	X	Y	Z
Right latissimus dorsi	0.0351	.25	-.30	0	.60	.10	0.0275
Left latissimus dorsi	0.0351	-.25	-.30	0	-.60	.10	0.0275
Right erector spinae	0.0389	.20	-.30	0	.30	-.30	0.0275
Left erector spinae	0.0389	-.20	-.30	0	-.30	-.30	0.0275
Right rectus abdominis	0.006	.10	.55	0	.10	.55	0.0275
Left rectus abdominis	0.006	-.10	.55	0	-.10	.55	0.0275
Right external abdominis oblique	0.0207	.10	.55	0	.45	-.19	0.0275
Left external abdominis oblique	0.0207	-.10	.55	0	-.45	-.19	0.0275
Right internal abdominis oblique	0.0215	.45	-.30	0	.45	.20	0.0275
Left internal abdominis oblique	0.0215	-.45	-.30	0	-.45	.20	0.0275

Area = coefficient × depth × width
Right lateral moment arm: X = coefficient × width
Anterior moment arm: Y = coefficient × depth
Elevation moment arm: Z = coefficient × height

These origins and insertions were measured at standing upright posture (Marras and Granata 1995). The relative position of the origin and insertion of a particular muscle may change during flexion as the curvature of the spine changes. These changes may also affect the moment arms of the spine muscle. Jorgensen et al. (2003) reported that the moment arms of erector spinae muscles decreased with increasing flexion angle at all levels of the lumbar spine. The sagittal moment arm of erector spinae muscle for male subjects decreased from 64.0 mm to 57.8 mm. To account for the changes in value of the moment arms, the insertion and orientation of a muscle must be modified according to the torso flexion angle. McGill and Norman (1986) used a three-dimensional skeleton comprised of a pelvis, rib cage and five lumbar vertebrae to simulate the changes in lordosis during flexion. The total lumbar rotation was allocated to the five vertebrae according to the linear-decline relationship:

$$R_{(i)} = c_{(i)} \times \alpha$$

where $R(i)$ is the rotation of the i th vertebra, i is the lumbar level (L1, L2, L3, L4 and L5), $c(i)$ is the percentage of flexion attributed to the i th vertebrae (L1 and L2 13.2%, L3: 21%, L4: 29%, L5: 23.6%), and α is the lumbar flexion angle (in degrees).

Marras and Granata (1995) used a two-plate lumbar mechanical model to address the flexion, lateral bending and rotation of the spine. One plate at the level of the iliac crest represented the head of the force vector coplanar where the three-dimensional positions of the muscles origin were located. The other plate was located at the level of the 12th rib, represented the tail of the force vector coplanar where the insertions of the muscles were located. Using this approach, the change of muscle orientations and lengths throughout a movement can be simulated as the relative movement of these two plates.

Marras and Granata (1995) did not describe the procedure to calculate the relative position of the two plates in flexion since the only motion they studied was twisting. Therefore, a combination of McGill and Marras's methods are used in this study. The flexion angle of the spine is attributed to five vertebrae, which are assumed to have the same length. From the rotation of each vertebra, the relative movement from the upper end of the vertebra to the lower end of the vertebra is calculated and added, representing the linear movement of the upper plate. The flexion angle is then applied to the upper plate. The origins of the muscles are adjusted to fit on the angled upper plate. Through this procedure, the origins and insertions, as well as the moment arms and lines of action, are coordinated with the dynamic movements of the torso.

Muscle force-length and force-velocity modifiers

It has been shown in the literature that the muscle force capacity is not constant, but rather varies as the length and the velocity of lengthening/shortening of the muscle changes

(Sutarno and McGill 1995; Raschke and Chaffin 1996; Hoyt, Wickler et al. 2005). Raschke and Chaffin (1996) found a linear relationship between the muscle length and the muscle force. As the muscle length increases, the muscle tension force also increases. It is noticeable that in this study “no evidence was found to reject the hypothesis for a linearly increasing length-tension relationship toward full flexion” (p.1061). McGill provided an equation for the active muscle force-length relationship based on Hill’s (1938) muscle formula (McGill 1992), but stated that passive tissue force should also be included since the muscle length was more than 40% of resting length. Therefore, in his equation he added an extra part for passive force. Marras and Granata (1995) solved this problem by measuring the empirical force-length relationship and using the regression method to obtain the equation relating muscle force to muscle length. This method did not distinguish the active and passive muscle components. This force-length modifier equation is used in the current study and is shown below:

$$f(l) = -3.2 + 10.2l - 10.4l^2 + 4.6l^3$$

where $l=(L_{(t)}/L_0)$, the relative length of the muscle at time t , calculated as the ratio of the instantaneous length of the muscle $L_{(t)}$ and the resting length of the same muscle L_0 at 20° of trunk flexion.

For the force-velocity modifier, the most important feature is the distinction between lengthening (eccentric) and shortening (concentric) motions. The force generation capacity will decrease quickly as the shortening speed increases, but it is constant for a large range of lengthening speed (Sutarno and McGill 1995; Raschke and Chaffin 1996; Hoyt, Wickler et al. 2005). To capture this feature, the force-velocity module has different functions depending on the instantaneous velocity. For a static condition when the velocity is zero, the modifier

must be equal to 1. For the slow eccentric speed condition (up to $-0.05L_0/s$, where L_0 is muscle's resting length), the module is a linear function from 1 to 1.2. For the eccentric conditions where muscle lengthening velocity is faster than $-0.05L_0/s$, the module is a constant, 1.2. The force-velocity module used in this study is adapted from Marras (1995) and McGill (1986) as shown below:

$$f(v) = \begin{cases} 1.2 & (v \leq -0.05, \text{ fast eccentric}) \\ 1 - 4v & (-0.05 < v \leq 0, \text{ slow eccentric \& isometric}) \\ 1.2 - 0.99v + 0.72v^2 & (v > 0, \text{ concentric}) \end{cases}$$

where $v=(L_{(t)}/L_0)'$, the relative velocity of muscle lengthening.

Calculation of muscle force and moments

After the muscle cross-sectional area, the force-length and the force-velocity modifiers are calculated, the followed equation is used to estimate the amount of force generated by a given muscle at any point in time during the trunk movements.

$$Force(t) = \text{muscle stress value} \times \text{PCSA} \times NEMG_{(t)} \times F(l_{(t)}) \times F(v_{(t)})$$

where *Force* is the instantaneous magnitude of force generated at time t , PCSA is the muscle physiological cross-sectional area (m^2), $NEMG(t)$ is the instantaneous normalized EMG activity for the muscle, $F(l_{(t)})$ is the force-length modifier to account for the force generation capacity according to the length of the muscle at time t , and $F(v_{(t)})$ is the force-velocity modifier capturing the changes in force because of muscle shortening/lengthening velocity.

From the equation above, the time-dependent force values of each individual muscle are calculated and applied to the lines of actions of these muscles to form the force vector for each muscle. For example, a muscle-generated force with a value of F , along the line of

action with θ_x , θ_y , and θ_z angles with the coordinate axes, form the force vector representing this muscle that is:

$$\begin{aligned}\mathbf{F} &= F \cos \theta_x \mathbf{i} + F \cos \theta_y \mathbf{j} + F \cos \theta_z \mathbf{k} \\ &= F_x \mathbf{i} + F_y \mathbf{j} + F_z \mathbf{k}\end{aligned}$$

The origin position vector of the muscle on the cutting plane from the L5/S1 is $\mathbf{r} = r_x \mathbf{i} + r_y \mathbf{j} + r_z \mathbf{k}$. The moment of the force about the L5/S1 is the cross product of \mathbf{r} and \mathbf{F} with is denoted as $\mathbf{r} \times \mathbf{F}$. The cross product can be expressed using unit coordinate vectors \mathbf{i} , \mathbf{j} , \mathbf{k} by calculating a matrix determinant as shown below:

$$\begin{aligned}\mathbf{M}_{L5/S1} = \mathbf{r} \times \mathbf{F} &= \begin{vmatrix} \mathbf{i} & \mathbf{j} & \mathbf{k} \\ r_x & r_y & r_z \\ F_x & F_y & F_z \end{vmatrix} \\ &= (r_y F_z - r_z F_y) \mathbf{i} + (r_z F_x - r_x F_z) \mathbf{j} + (r_x F_y - r_y F_x) \mathbf{k} \\ &= M_x \mathbf{i} + M_y \mathbf{j} + M_z \mathbf{k}\end{aligned}$$

The total spine load from muscles is the sum of all forces and moments on the L5/S1 joints. They are calculated as:

$$\begin{aligned}\mathbf{F}_m &= \sum F_x \mathbf{i} + \sum F_y \mathbf{j} + \sum F_z \mathbf{k} \\ \mathbf{M}_m &= \sum M_x \mathbf{i} + \sum M_y \mathbf{j} + \sum M_z \mathbf{k}\end{aligned}$$

The total internal load includes two parts, the moments from all active muscles (M_m) and the moments from passive components (M_p). The total internal load is calculated as:

$$M_{\text{int}} = M_m + M_p$$

Calculation of muscle stress value and output results

The muscle stress value is the force generation capacity per unit area for a muscle. In this EMG assisted biomechanical model, the muscle stress values were predicted from the

performance data of each individual subject. Thus, the muscle stress values were different between subjects but the same muscle stress value is applied to all muscles and all trials for the same subject. This is consistent with the nature of the muscle stress value that it is “highly variable between subjects, based on subject condition and natural ability. On the other hand, the muscle stress value predicted for a given subject must be constant throughout each of the experimental trials.” (Granata and Marras 1995, p.1310)

The muscle stress value of each subject is found by comparing the total internal moment (M_{int}) to the external moment (M_{ext}) in the sagittal plane. Only the moments in the sagittal plane were considered because the motions in this study are purely flexion/extension with no lateral bending and/or twisting. Hence the moments of side bending and rotation are minimized and are not used to predict the muscle stress value. Allowing the muscle stress value to vary within its physiologically feasible region, allows the model to generate a best least squares fit between the internal and external load.

The first time the model is run for a given subject, the muscle stress value for this subject is unknown. So for each of the trials for this subject, the integers between 30 and 100 are considered and the one that minimizes the sum of squared error between external and internal sagittal moments is identified as the muscle stress value for that trial. Then, the mean muscle stress value of all the trials is calculated as the error minimized “best muscle stress value” for this subject. This predicted best muscle stress value must be physiologically valid. In the literature, the maximum muscle stress value has been reported to be in the range of 30 to 100 N/cm² (see Table 3).

Table 3. Range of maximum muscle stress values (gain) found in the literature

Studies	Maximum muscle stress value(N/cm²)
Morris et al (1961)	39.2
Ikai and Fukunaga (1968)	63.0
Farfan (1973)	34.3-82.3
Weis-Fogh and Alexander (1977)	100
Schultz et al. (1982)	Up to 100
Reid and Costigan (1987)	48
McGill and Norman (1987)	30-90

Finally, this muscle stress value is applied to all of the trials for this subject to predict the overall spinal reaction forces and moments. For example, the total compression force on the L5/S1 joint is the sum of compression force from muscles, passive components, the gravity and acceleration of the load and the subject's upper body.

5 EXPERIMENTAL METHOD

5.1 Summary of literature review

The most important finding from the literature review was the importance of considering the contribution of the passive components at the full flexion posture. Some of the previous biomechanical models have considered the effects of passive components of the spine. However, none of them studied the interplay between active muscles and passive components continuously in the full range of trunk flexion/extension motion during both concentric and eccentric exertions. Figure 11 illustrates the summary of the previous EMG-assisted biomechanical models and the main contribution of this study.

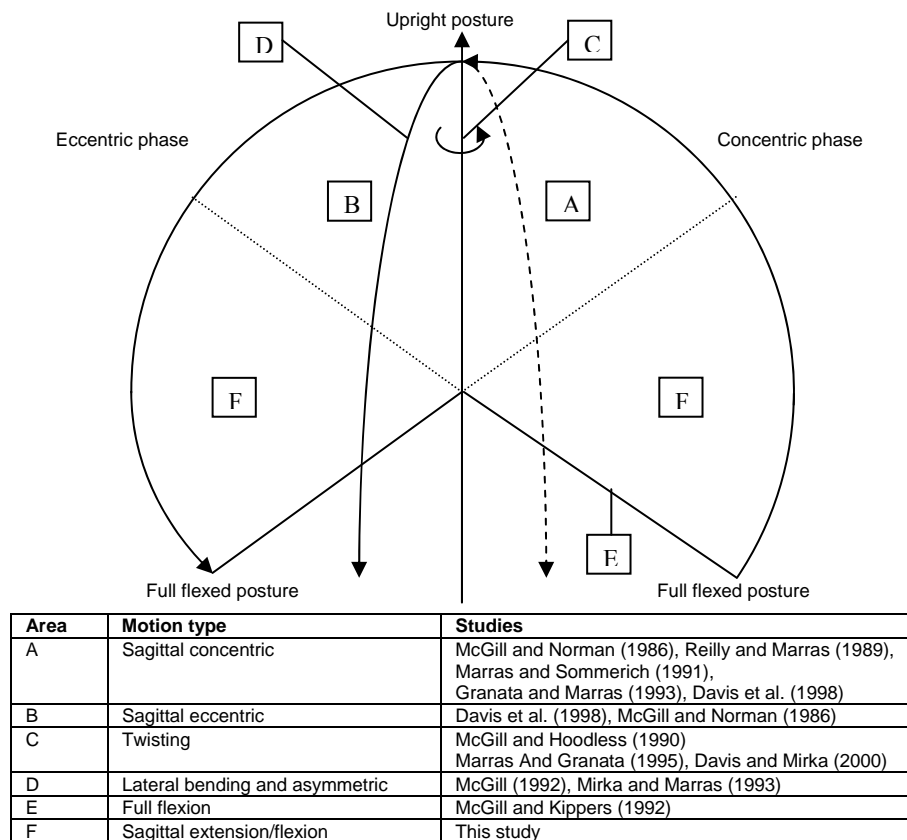


Figure 11. Illustration of the range of trunk motion in previous models and current study

The goal of this study was to develop and validate an EMG-assisted biomechanical model that is capable of estimating spinal reaction forces resulting from both the active muscles and passive components in the full range of trunk flexion/extension motions. This study included two experiments. Each experiment required that human subjects perform concentric and eccentric lifting motions while the experimenter gathered empirical data on their performance. In the first experiment, the subjects performed controlled concentric/eccentric trunk extension exertions in the ARF lumbar dynamometer. As they performed these exertions, the muscle activity of the major trunk muscles was collected and used in the EMG-assisted biomechanical model to predict spine reaction forces. In the second study, the subjects performed free dynamic lifting and lowering tasks. The kinematics of the subject and EMG data of the trunk muscles were gathered and imported into the EMG-assisted biomechanical model to test the performance of the model in free dynamic lifting/lowering exertions.

5.2 Experiment one: dynamometer study

The goals of the first experiment were to 1) gather the empirical data for the development and validation of the EMG-assisted biomechanical model and 2) use this EMG-assisted biomechanical model to compare spinal loading during eccentric and concentric lifting exertions.

5.2.1 Subjects

Subjects were selected from the university undergraduate and graduate student population. To control many of the inter-gender differences in the lumbar anatomy and physiology, this study used a relatively homogenous pool of subjects to evaluate this model.

Only male subjects were tested. All subjects were fully informed volunteers who were in good health with no previous back injuries or current back pain. Each subject signed a consent form approved by the IRB of NCSU.

Table 4. Anthropometric data of the subjects in experiment one

Number	Age	Stature (m)	Weight (kg)	Waist width (m)	Waist depth (m)
6	25 (2.6)	1.76 (0.06)	69.9 (11.6)	0.29 (0.028)	0.21 (0.030)

5.2.2 Equipment

Electromyography

The EMG signal processing system was used to collect ten trunk muscle activation levels. These data were collected at 1024Hz. Five pairs of major trunk muscles (symmetrically on left and right side) including erector spinae, latissimus dorsi, rectus abdominis, external obliques and internal obliques were captured (Brown and Potvin 2007). Silver-chloride (6 mm-diameter, bipolar) electrodes were used to capture the EMG activity of these ten sampled bilateral muscles. The data were pre-amplified (1000x) and then carried via shielded cables to the main amplifier that filtered (notch filter of 60 Hz, and low pass 1000 Hz) and further amplified (50x) the EMG data. The EMG signals were converted to a 16bit digital signal through an A/D data acquisition module (DT9834, Data Translation, USA) and recorded on a computer.

Asymmetric Reference Frame

The Asymmetric Reference Frame (ARF) is a device that allows a researcher to isolate the motions/forces of the lumbar spine in human subjects (Figure 12). It was used to precisely control the subjects' sagittal position, extension/flexion velocity and angle. The KIN/COM isokinetic dynamometer was used to control the velocity of motion and magnitude

of torque. The target torque was graphically displayed on a computer monitor screen as a red line. The instantaneous torque measured by the dynamometer was also displayed on the screen, as a shifting blue line. The subject was asked to control his extension torque during trunk movements so that the blue line (generated torque) was as close to the red line (target torque) as possible. The velocity, acceleration and torque of the trunk flexion/extension data were collected from ARF simultaneously with EMG signal at 1024Hz.

5.2.3 Experimental design

Independent variables

The controlled dynamometer study had three independent variables including two levels of motion direction (eccentric vs. concentric), three levels of velocity (10°/s, 20°/s and 30°/s) and three load levels (10%, 20% and 30% of maximum lifting capacity).

Dependent variables

The dependent variables in the controlled dynamometer study included predicted maximum compression and anterior-posterior shear forces of the spine at L5/S1 joint. The measured EMG activities of the trunk muscles were used as the input for the EMG assisted biomechanical model to predict these spinal reaction forces. In addition to these maximum values, we were also interested in the degree of variability in these measures across trials. To accomplish this, the variability across trials was calculated as the deviation of the individual trial values (6 observations) from the median for that particular condition and these variables are called the median deviation values. The calculation of these median deviation values is more fully described in Section 5.2.5.

5.2.4 Procedure

When the subject entered the laboratory, he was given an informed consent form and was informed of the requirements of the experimental procedure. Then the subject was given a five-minute warm-up and stretching period designed to prepare the trunk muscles for the experiment. Several anthropometric data of the subject were collected. The stature, waist width and depth were measured by a straight ruler. The weight of the subject was measured by a weight scale.

The subject was then fitted with electrodes secured to the skin with double sided tape. Before placement of electrodes, the skin of the abdomen and low back were cleaned with alcohol. Five pairs of electrodes were placed over the measured muscles, including the rectus abdominis, external oblique, internal oblique, latissimus dorsi and erector spinae. The placement of the electrodes followed the instructions described by McGill and Norman (1986) and McGill (1992).

The subject was then secured in the ARF with the pelvis restrained by the fixture around the waist. The subject then performed two maximum effort trunk extensions and flexions respectively at 45° and 55° trunk flexion angle on the ARF. In each extension trial, the subject was asked to generate maximum extension torque against the bar of the ARF by gradually increasing to maximum, hold for 1 second, and then gradually relaxing. In each flexion trial, the subject was asked to generate maximum flexion torque by pulling against a strap that was wrapped around the subject and around the bar of the ARF. Between the maximum exertions there was 1 minute rest break. The maximum extension torque displayed on the screen of the KIN/COM dynamometer was recorded. This value was used to set the 10%, 20% and 30% of maximum load line displayed on the screen.

The subject then performed a randomized sequence of trunk extension exertions. These included isokinetic eccentric/concentric exertions and isometric exertions. The setup of this experiment is shown in Figure 12.



Figure 12. Controlled flexion/extension exertions in ARF

The range of motion of the subject was determined first. The start angle was 0° when the subject stood upright in the ARF. The end angle was the subject's full flexion angle when the myoelectric silence of the erector spinae muscles was observed. The subject performed a random sequence of the isometric or isokinetic trunk exertions. For isometric exertions, there were three trunk angles: 45° , full flexion angle and the median angle between 45° and full flexion angle, and three load levels: 10%, 20% and 30% of the maximum torque at the 30° trunk flexion angle. The subject bent to the target angle, and gradually generated extension torque to the target level, maintained the torque for three seconds, and gradually released.

There were two trials for each combination of the three flexion angles and three load levels. Totally there were eighteen trials and their orders were fully randomized. These data were only used for the model evaluation phase of the study. For isokinetic exertions there were three levels of speed: 10°/s, 20°/s and 30°/s and three levels of load: 10%, 20% and 30% of the maximum torque. In each trial, the subject performed both concentric and eccentric trunk exertions. He started from full flexion, extended to upright, and then flexed to full flexion again or he started from the upright position, bent to full flexion and back to upright. Each trial included two repetitions. In both extension and flexion, the subject generated extension moment. The order of the eccentric and concentric exertions were balanced and randomized. During the movements, a monitor was set in front of the subject displaying a red line representing the simultaneous extension moment generated by the subject and a blue line representing one of the target load (10%, 20% and 30%). The subject was asked to control the extension moment carefully so that the red line matches the blue line as accurately as possible. The trials last about 24, 12, and 8 seconds for speed level of 10°/s, 20°/s and 30°/s respectively. Each combination of speed and load was repeated two times making a total of 18 trials (2 replications \times 3 speed levels \times 3 load levels). These data were used for both the model evaluation phase and statistical analysis phase of the study.

5.2.5 Data processing

The EMG signal was filtered (high pass 10Hz, low pass 1000Hz), rectified, and integrated into a time-dependent (20 milliseconds) moving average data which was used as the numerator in the normalization process. Maximum EMG values were established as the peak values for the averages of MVC exertions from discrete 1/8th-second windows. The EMG data in each isometric trial was normalized by the maximum EMG value in the MVC

exertions at the same angle. The maximum EMG values for the angles that were not measured in the MVC exertions were calculated from linear interpolation (as a function of trunk angle) based on the peak values of the MVC exertions and the EMG data in the isokinetic trials were normalized to these interpolated maximum EMG values according to the corresponding angle of the EMG data. The data of velocity, angle and force in voltage from the sensors on ARF were converted to data in their real units based on the equations obtained in calibration of the ARF prior to the studies. All data was collected simultaneously with the EMG data so that they were synchronized. The normalized EMG data and the trunk flexion angle/velocity data were input into the EMG-assisted biomechanical model. For each trial the maximum muscle stress value that minimized the sum of squared error between the predicted and actual torques were calculated. The mean of these values across all trials for one subject was then calculated and used as the maximum muscle stress value for that subject in the EMG-assisted biomechanical model. For the model evaluation phase of this research, the predicted internal moment could then be calculated at each point in time throughout the lift which could then be compared with the actual external moment about the L5/S1 joint.

For the statistical analysis phase of this experiment, the EMG-assisted model was used to calculate the peak spine compression and the peak anterior-posterior shear forces for each trial (a total of six observations per condition). The dependent variables describing the variability of these measures (compression force and A/P shear force on L5/S1 joint), were calculated as the absolute deviation from the median (of the six) of each condition. For example, there were six observations (two trials \times three repetitions) in each of the combination of load level, motion direction and lifting techniques. The median value of these six observations was found, and six absolute deviations from this median value were

calculated. The mean of these absolute deviations represented the variance of this variable. This approach was an adaptation of the modified Levene's test. (Montgomery 2001, p.82)

5.2.6 Model evaluation

The performance of the model was evaluated in several ways following the established techniques proposed by Marras and Granata (1995). First, using the mean maximum muscle stress value computed for each subject, the measured moment (from the weight of the body and load) and model predicted moment (from the active muscles and passive components) in sagittal plane were compared. The average absolute error between the measured and model predicted moment was the calculated for each trial. The model with passive components was compared with the model without passive components to quantify the improvement by involving the passive components in the model. The coefficient of determination (R^2) value of the measured and model predicted moment in the sagittal plane was also calculated. The R^2 value of the measured and model predicted moment was calculated as the square of the correlation coefficient:

$$R^2 = \rho^2 = \left(\frac{n \sum y \hat{y} - \sum y \sum \hat{y}}{\sqrt{n \sum y^2 - (\sum y)^2} \sqrt{n \sum \hat{y}^2 - (\sum \hat{y})^2}} \right)^2$$

where y is the measured moment in sagittal plane, \hat{y} is the model predicted moment in sagittal plane. A larger R^2 value (close to 1) demonstrates the good prediction of the model. These two measures provided information about the quality of the fit of the model using one single maximum muscle stress value per subject.

The accuracy of the model was also evaluated by considering the individual maximum muscle stress values as computed on the trial-by-trial basis. First, the maximum

muscle stress values for each individual trial were computed. Next, the standard deviation of the maximum muscle stress values across trials for a given subject (including both isokinetic and isometric trials) was calculated. A relatively small standard deviation showed consistent performance of the model under various speed, load and trunk flexion angle conditions.

5.2.7 Statistical analysis

The statistical model for the controlled dynamic flexion/extension exertion in ARF had a factorial design with blocking on subject. The model was created by including the three main effects (load level, flexion/extension velocity, and motion direction), all two-way interactions and the three way interaction. Multivariate analysis of variance (MANOVA) was conducted to assess the effects of the dependent variables collectively (by the Wilks' Lambda criterion ($p < 0.05$)). The analysis of variance (ANOVA) F statistic was used to test the significance of the model and specific factors. The linear design for this model was:

$$y_{ijklm} = \mu + \tau_i + \lambda_j + \beta_k + \delta_l + \tau\lambda_{ij} + \tau\beta_{ik} + \lambda\beta_{jk} + \tau\lambda\beta_{ijk} + \varepsilon_{ijklm}$$

where:

y corresponds to the response variable

μ corresponds to the overall mean

τ corresponds to velocity and $i=1,2,3$

λ corresponds to load level and $j=1,2,3$

β corresponds to motion direction and $k=1,2$

δ corresponds to subject and $l=1$ to 6

$\tau\lambda$ corresponds to the interaction between velocity and load level

$\tau\beta$ corresponds to the interaction between velocity and motion direction

$\lambda\beta$ corresponds to the interaction between load level and motion direction

$\lambda\beta\gamma$ corresponds to the interaction between velocity, load level and motion direction
 ε corresponds to the error term and $m=1$ to 6

The normality of residuals and the equality of variance from the statistical models were checked graphically to validate the adequacy of the MANOVA and ANOVA models (Montgomery, 2001). The normality assumption was tested by examining normal probability plots of residuals (difference between observed value and fitted value). The equality of variance assumption was tested by plotting the residuals versus the fitted values.

5.3 Experiment two: free lifting/lowering study

The goal of this study was to investigate the performance of the new EMG-assisted biomechanical model in free dynamic lifting/lowering exertions. Once the model was validated under these conditions, the output of the model was used to study the effects of lifting motion direction (eccentric versus concentric) and lifting technique (squat versus stoop) on spinal loading parameters (similar to Experiment 1) and variability of the lifting motions. The following were hypotheses related the effects of eccentric vs. concentric lifting motions:

H1: The spine reaction forces are greater in the eccentric exertions than in the concentric exertions.

H2: The variability in the spine reaction forces is greater in the eccentric exertions than in the concentric exertions.

H3: The variability in lifting kinematics will be greater in eccentric exertions than in concentric exertions.

5.3.1 Subjects

Subjects were selected from the university undergraduate and graduate student population. As in Experiment 1, inter-gender differences in the lumbar anatomy and physiology were controlled for by only recruiting male subjects. All subjects were fully informed volunteers who were in good health with no previous back injuries or current back pain. Each subject signed a consent form approved by the IRB of NCSU. The experiment was conducted in less than two hours.

Table 5. Anthropometric data of the subjects in experiment two

Number	Age	Stature (m)	Weight (kg)	Waist width (m)	Waist depth (m)
12	26 (4.8)	1.74 (0.05)	70.8 (12)	0.29 (0.026)	0.21 (0.031)

5.3.2 Equipment

EMG and ARF system

This experiment also used the EMG and ARF system. The EMG system was used to measure the activities of the major trunk muscles. The ARF system was used for the subject to perform maximum voluntary contractions. The details of these systems are the same as those for the Experiment 1.

Motion tracking system

The three-dimensional posture data of the subject was captured by the Ascension MotionStar position and orientation measurement system (Ascension Technology, VT, USA) and recorded at the frequency of 100Hz with the Innovative Sports Training Motion Monitor software (version 4.10). Motion track sensors were placed on the back, shoulder and hand of the subject. Four sensors were placed along the center line of the spine at T6, T12/L1, L5 and

S1 levels respectively (see Figure 13). One was placed on the lateral aspect of the left shoulder. The other one was placed on back of the right hand.



Figure 13. Motion sensors placed on the back of the subject

Force plate

The ground reaction forces and moments were measured by the force plate (Bertec corporation, Ohio USA). Six channels of data including the net ground reaction forces (F_x , F_y and F_z) and moments (M_x , M_y and M_z) were measured at 1024Hz, processed through the same data acquisition module simultaneously with the EMG data and recorded on the computer.

5.3.3 Experimental design

Independent variables

The free dynamic lifting/lowering study has three independent variables including two levels of motion directions (eccentric vs. concentric), two levels of lifting techniques (squat or stoop) and three load levels (10%, 20% and 30% of maximum lifting capacity). In the stooped posture the subject must keep the knees straight during the lifting/lowering process. In squat posture, the subject must bend the knees, but he can choose between fully flexing the knee (full squat posture) or a less flexed knee posture (semi-squat posture).

Dependent variables

The dependent variables in the free dynamic lifting/lowering study include measures of the mean and variability of the peak flexion/extension velocity in each lifting/lowering exertion. The measured EMG activities of the trunk muscles were used as the input for the EMG assisted biomechanical model to predict spinal reaction forces and moments. The peak spine reaction forces (compression and anterior-posterior forces on L5/S1 joint) were included in the set of dependent variables in this experiment and were used to test the first hypothesis of this experiment. The variability of the dependent variables was measured as the absolute deviation from the median in each motion direction, lifting technique and control strategy combinations. The variability of the spine reaction forces was used to test the second hypothesis of the experiment. Finally peak velocity was identified in each lifting motion (both concentric and eccentric) and these peak velocity values were used to test the third hypothesis of this experiment.

5.3.4 Procedure

The preparation activities for this experiment were the same as those followed in Experiment 1. The subject was informed of the requirements of the study, signed the informed consent form, followed five-minute warm-up/stretching routine and then the same anthropometric measurements were collected. The surface EMG electrodes were placed and the maximum voluntary contractions were performed in the ARF following the procedures outlined for Experiment 1. The maximum extension torque measured on ARF was used to determine the weight of the load (10% 20% and 30% of the maximum lifting capacity) to be lifted, following the same procedure described in Shin, Shu et al.(2004).

Motion tracking sensors were placed on the subject as described in the equipment section. The upright, quiet standing posture (with the load) for the subject was recorded first and set as the 0° neutral position. All the trunk flexion angles were derived as deviations from this position. The subject was then asked to hold a full flexion posture for three seconds. The myoelectric silence of the erector spinae muscles was read on the screen of the computer recording the EMG data to confirm the flexion relaxation of the trunk extensor musculature.

The subject then moved to the force plate on which the subsequent lifting trials were performed. The force plate was placed on a one foot high wooden platform which allowed the handle of the load to be about the same height as the force plate (see Figure 14). The height of the load was adjusted so that the subject was in full trunk flexion to pick up the load. After that, the subject performed dynamic lowering and lifting activities under six conditions as the combinations of three levels of load (10%, 20% and 30% of maximum lifting capacity) and two levels of posture (squat and stoop). In each trial, the subject started by grasping the load on ground, lifted it up to the upright posture, and lowered it back to ground again (see

Figure 14). In order to compare the free lifting/lowering study with the dynamometer study, the subject was asked to perform controlled lifting/lowering exertions. To limit the unnecessary acceleration during exertions, a small bottle filled with water was placed on the load so that the subject could see the bottle. The subject was asked to lift and lower the load without disturbing the water. If the water spilled, the subject was asked to repeat the trial again to ensure smooth performance in lifting and lowering. In the stoop posture the subject was asked to keep the knees straight during the lifting/lowering process. In squat posture, the subject was asked to bend the knee, but he could choose between fully flexing the knee (full squat posture) or a less flexed knee posture (semi-squat posture). The lowering and lifting procedure were repeated three times per trial. Between the lifting and lowering exertions there was a three second interval when the subject maintained a full flexed posture or upright standing posture to reduce the influence of the previous exertions. Each of the six conditions (three levels of load \times two levels of lifting techniques) consisted of three repetitions. Totally there were 18 trials in this experiment. The order of these 18 trials was fully randomized.



Figure 14. A dynamic lifting exertion at full flexion posture

5.3.5 Data Processing

Trunk flexion angle, velocity and acceleration in the sagittal plane were recorded as the difference between the motion sensors at T6 and S1 level. The lumbar flexion angle was the difference between the sensor at T12/L1 and S1 level. As the lifting task was symmetric, motion in coronal and transverse plane was negligible. As noted in the procedures section above, the subjects performed three repetitions of the concentric/eccentric lifting motion per trial. For data analysis purposes the first concentric exertion and the last eccentric exertion

were not included in the analysis because of the potential for differences in strategy at the end points of the bout of lifting.

The eccentric phase of the lift was defined as the interval start from the time point with the smallest trunk flexion angle (near upright) to the time point with largest trunk flexion angle (near full flexion). The concentric phase of the lifting motion was defined as the interval start from the time point with the largest trunk flexion angle to the time point with smallest trunk flexion angle. The variable “peak velocity” was calculated as the maximum trunk flexion angular velocity in the eccentric phase and the maximum extension angular velocity in the concentric phase.

The EMG data processing procedures employed in Experiment 1 were used to process the EMG data for this experiment. The output from the EMG-assisted biomechanical model were the spinal reaction forces including the compression and anterior-posterior shear forces on L5/S1 joint. The peak compression and shear forces were calculated as the maximum compression and shear force that occurred in each of the eccentric and concentric phases during the free dynamic lifts. The calculation of the the dependent variables describing the variability of these spine reaction force measures used the same procedure to calculate the absolute deviation from the median that was outlined in Experiment 1. Finally, to capture an estimate of the variability in lifting kinematics used in this free dynamic lifting task, the variability of the peak trunk flexion/extension velocity was calculated using the same method.

5.3.6 Model evaluation

The technique used to evaluate the quality of the model predictions follows the approach outlined for Experiment 1. Measures of performance included average absolute

error between predicted and actual moment, R^2 between the predicted and actual moment as described in Section 5.2.6.

5.3.7 Statistical analysis

The model for the kinematics study of free dynamic lifting/lowering had a factorial design with blocking on subject. The model was created by including the three main effects (load level, lifting technique, and motion direction), all two-way interactions and the three way interaction. Multivariate analysis of variance (MANOVA) was conducted to assess the effects of the dependent variables collectively (by the Wilks' Lambda criterion ($p < 0.05$)). The analysis of variance (ANOVA) F statistic was used to test the significance of the model and specific factors. The linear design for this model was:

$$y_{ijklm} = \mu + \tau_i + \lambda_j + \beta_k + \delta_l + \tau\lambda_{ij} + \tau\beta_{ik} + \lambda\beta_{jk} + \tau\lambda\beta_{ijk} + \varepsilon_{ijklm}$$

where:

y corresponds to the response variable

μ corresponds to the overall mean

τ corresponds to lifting technique and $i=1,2$

λ corresponds to load level and $j=1,2,3$

β corresponds to motion direction and $k=1,2$

δ corresponds to subject and $l=1$ to 12

$\tau\lambda$ corresponds to the interaction between lifting technique and load level

$\tau\beta$ corresponds to the interaction between lifting technique and motion direction

$\lambda\beta$ corresponds to the interaction between load level and motion direction

$\lambda\beta\gamma$ corresponds to the interaction between lifting technique, load level and motion direction

ε corresponds to the error term and $m=1$ to 6

The normality of residuals and the equality of variance from the statistical models were checked graphically to validate the adequacy of the MANOVA and ANOVA models (Montgomery, 2001). The normality assumption was tested by examining normal probability plots of residuals (difference between observed value and fitted value). The equality of variance assumption was tested by plotting the residuals versus the fitted values.

6 RESULTS

6.1 *Experiment one: dynamometer study*

6.1.1 Model Evaluation

Recall that there were three measures that were to be used to evaluate this new approach to the EMG-assisted biomechanical modeling. For each measure a comparison between the EMG-assisted model with the passive tissues and the EMG-assisted model without the passive tissues is performed. These three measures include 1) the consistency of the predicted maximum muscle stress value, 2) the average absolute error between the predicted and actual moments about L5/S1, and 3) the coefficient of determination (R^2) between the predicted and actual moments about L5/S1.

The maximum muscle stress values were calculated for each trial performed by each subject following a process that minimized the error between the predicted and actual moment for that individual trial. It would be expected that if the model was well-formulated that these maximum muscle stress values would be relatively constant across conditions. A comparison of variability of these values provides some insight into the quality of the model. In this study trunk angle was a particularly relevant independent variable because of the potential impact of extreme flexion angles on the predictive ability of the model. Figure 15 shows the clear difference of the effects of trunk flexion angle on the mean and standard deviation of the maximum muscle stress values between the model with and without passive components. The mean maximum muscle stress value from the model with passive components slightly increased as the trunk flexion angle became larger (62.2 N/cm², 61.7

N/cm² and 62.7 N/cm² at 45°, medium and full trunk flexion angles respectively). On the other hand, the mean and standard deviation of the maximum muscle stress value in the model without passive components greatly increased at larger the trunk flexion angles. The mean (standard deviation) maximum muscle stress value increased from 67.5 (17.3) N/cm² at 45° trunk flexion angle, to 71.4 (21.0) N/cm² at medium, and to 94.3 (66.2) N/cm² at full trunk flexion angle. Statistical analysis showed that there was no significant difference between the maximum muscle stress values at different trunk flexion angles from the model with passive components, (p=0.9614) while there was significant difference of these values at different trunk flexion angles from the model without passive components (p=0.0077). This result provides the first evidence of a positive impact of the inclusion of the passive tissues in the EMG-assisted model.

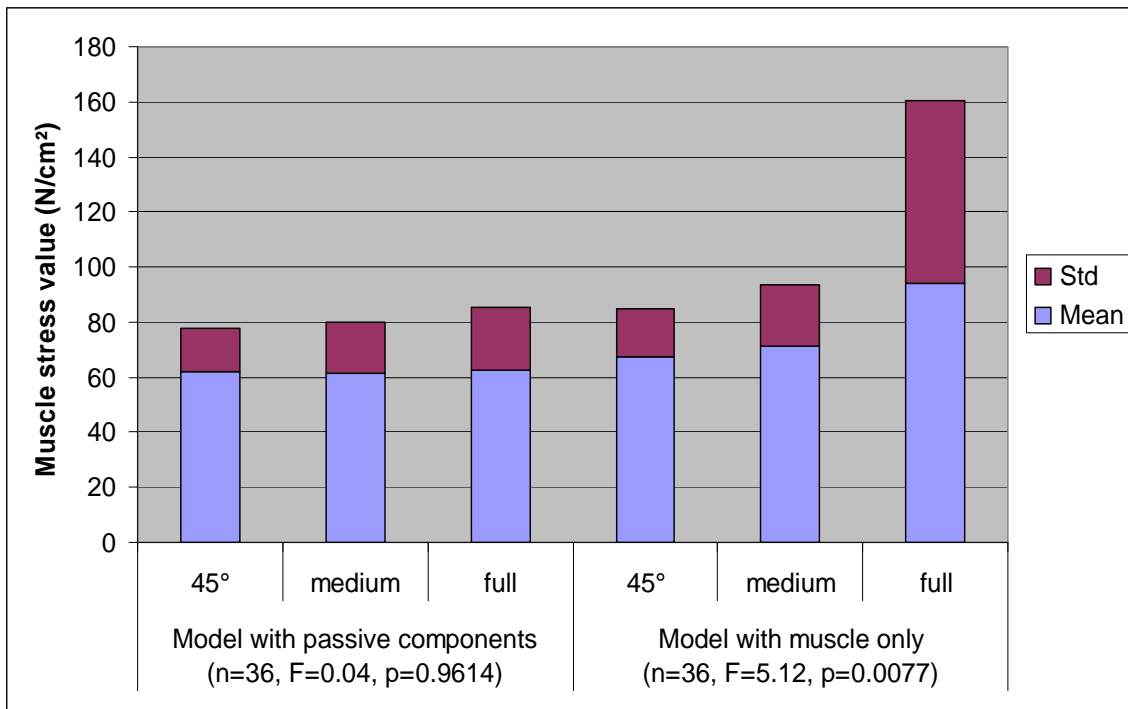


Figure 15. Mean and standard deviation of the maximum muscle stress value versus trunk flexion angle.

To better understand the remaining two measures used to evaluate the model, we begin with some sample graphical representations of these data. Three examples of the measured external moment and model predicted internal moment in the controlled static trials were compared in the following figures (Figure 16, Figure 17 and Figure 18). In these figures the trace labeled “External moment” was the measured net external moment that needed to be countered by the internal moments predicted by the model. The trace labeled “Muscle only” means the predicted moment from the model without passive components. The trace labeled “With passive components” illustrated the predicted moment from the full model with both muscles and passive components. Finally, the trace labeled “Moment from passive components” was the predicted moment generated by the passive tissues as part of the moment predicted by the full model.

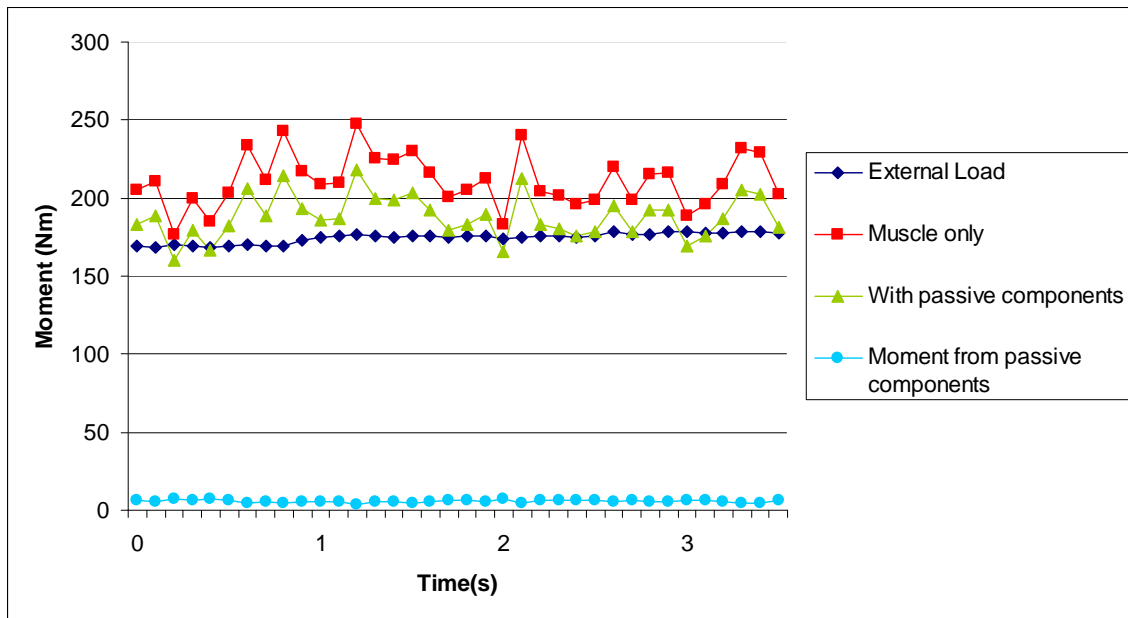


Figure 16. Measured and model predicted moment at 45° trunk flexion angle in controlled static exertion.

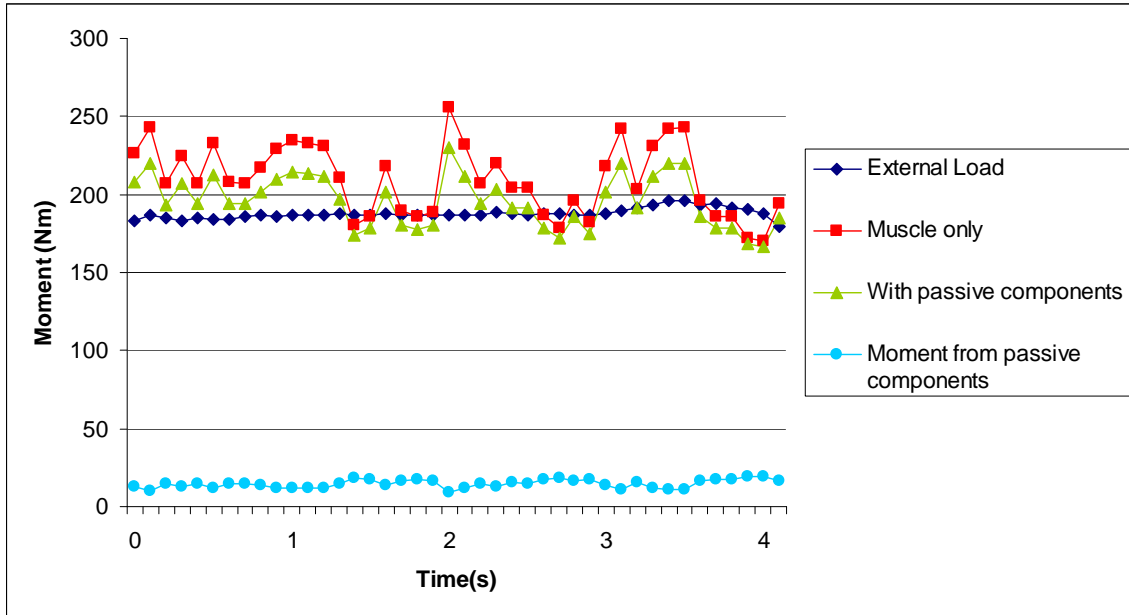


Figure 17. Measured and model predicted moment at medium trunk flexion angle in controlled static exertion.

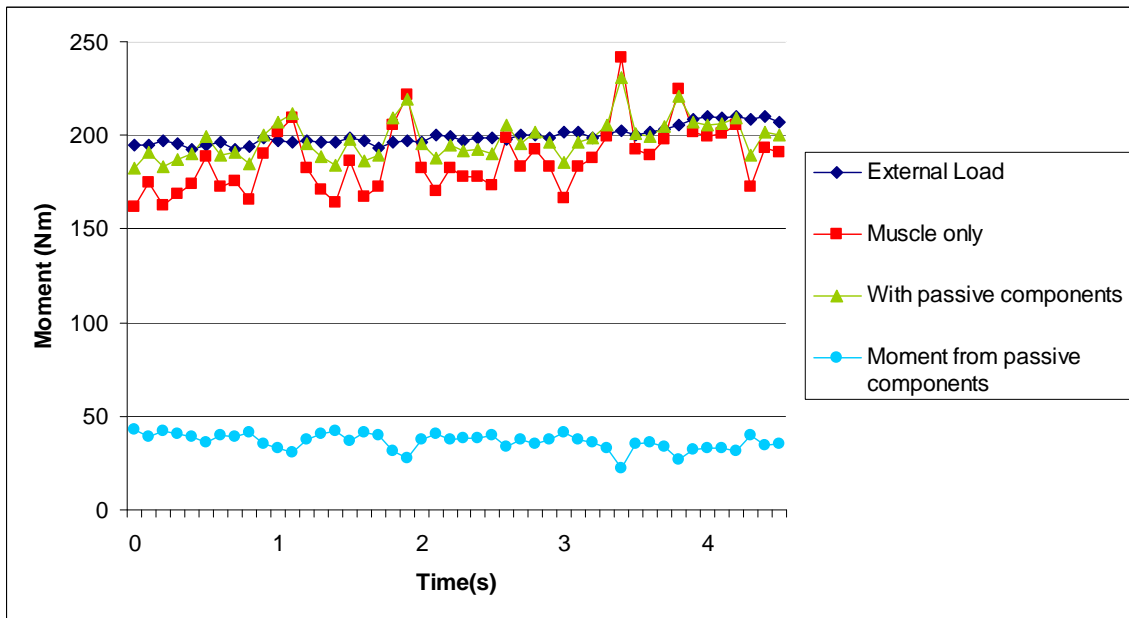


Figure 18. Measured and model predicted moment at full trunk flexion angle in controlled static exertion.

These three figures are examples of measured and model predicted moments at three trunk flexion angles during isometric exertions. Generally, the predicted internal moment

from the model with passive components fitted the external moment more accurately than the model without passive components. As Figure 15 previously illustrated, the maximum muscle stress value from the model without passive moments significantly increased as the trunk flexion angle increased. Thus, when using the mean value of these varied maximum muscle stress values as the input for one subject, the prediction could be significantly biased at different trunk flexion angles. At 45° and medium trunk flexion angle, the model without passive components predicted internal moment clearly higher than the measured internal moment. While at full trunk flexion angle, the model without passive components notably under predicted the internal moment. The model with passive components performed relatively better at all three trunk flexion angles.

Figure 19 shows the measured and predicted moments in two full dynamic flexion/extension exertions. The subject started from upright, bent to full flexion (about 6 seconds), extended to upright (about 12 seconds) and repeated the motion. The EMG activities of the back muscles notably reduced at near full flexion angle, as the passive components stretched long enough to support the upper body. The model without passive components failed to track the measured moment at near full flexion angles as its prediction depended only on active muscle forces. Because the model used the mean maximum muscle stress value from all trials to predict the internal moment, the prediction was biased at different trunk flexion angles similarly to the controlled static trials on dynamometer. The model without the passive component over-predicted the internal moment at small trunk flexion angles, and under-predicted at near full flexion angles. In this situation when the subject bent to full flexion, the moment generated by passive components must be considered. The model with passive components correctly predicted the internal moment accordingly.

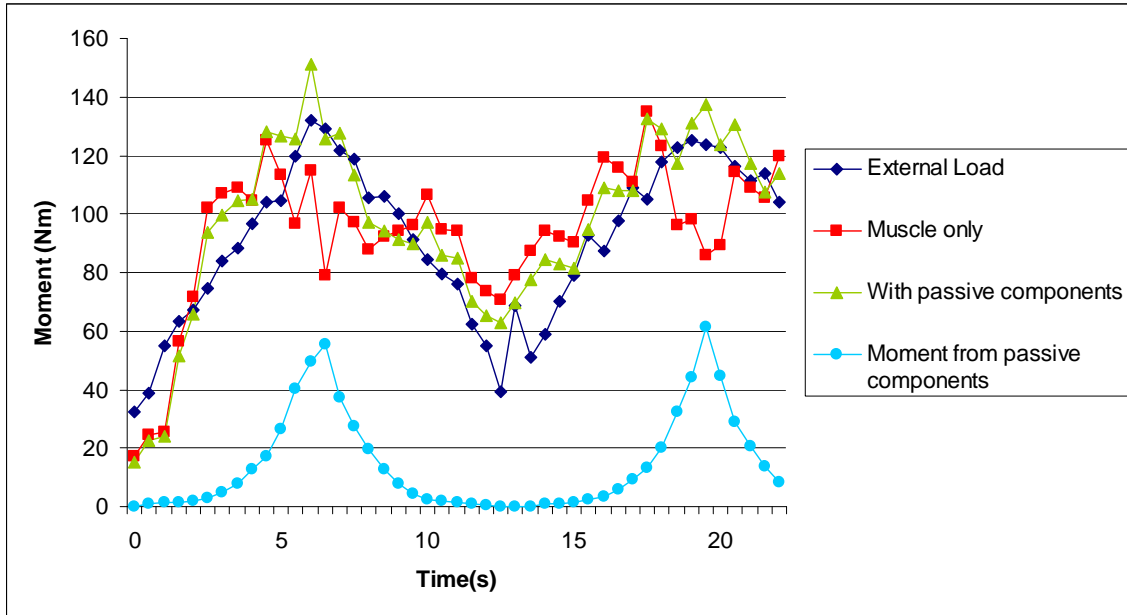


Figure 19. External and internal moment in controlled dynamic exertion on dynamometer.

The data presented graphically in Figure 16 to Figure 19 provide some qualitative evidence of the effects of the new modeling approach. The more quantitative approach to making this assessment is provided by considering the average absolute error and the R^2 value for each modeling approach. Table 4 presents these quantitative results and shows that, across conditions, the mean absolute error from the model with passive components was smaller than that from the model without passive moments. The R^2 values show a similar trend with the model with the passive components included accounting for an average of 66% of the variance, while the model without the passive components only accounting for 37% of the variance. The smaller mean absolute error and larger R^2 values indicate significant improvement.

Table 4. Comparison of mean absolute error and R² values in controlled trials on dynamometer.

		Mean absolute error (Nm)		R ² value	
		Model with passive components	Model with muscle only	Model with passive components	Model with muscle only
Load	10%	20.7(5.6)	25.5(7.9)	68.3%(16%)	47.1%(15%)
	20%	18.5(6.4)	24.9(6.3)	68.2%(16%)	34.5%(25%)
	30%	19.1(4.9)	26.6(5.8)	63.0%(12%)	28.1%(20%)
Speed	10°/s	19.1(5.7)	25.3(5.6)	68.9%(14%)	37.9%(22%)
	20°/s	18.3(5.3)	23.8(5.6)	69.7%(11%)	39.9%(22%)
	30°/s	20.9(5.9)	27.9(8.0)	60.8%(17%)	31.9%(20%)
Mean		19.6(6.5)	25.5(7.1)	66.2%(14%)	36.6%(22%)

6.1.2 Comparison of eccentric versus concentric exertions

Using the EMG-assisted model that included the passive tissues, a comparison of biomechanical measures collected during the concentric and eccentric phases of the lifting motion was performed. There were four dependent variables: 1) the model predicted maximum compression force on the L5/S1 joint, 2) the model predicted maximum shear force on the L5/S1 joint, 3) the median deviation values of these compression force and 4) the median deviation values of these shear forces. Due to the differences in the nature of the dependent variables, analysis of Variables 1 and 2 are conducted separately from the analysis of Variables 3 and 4.

Prior to conducting the statistical analysis, the assumptions of the ANOVA procedure (normality of residuals and the homogeneity of variance assumptions) were checked graphically to validate the adequacy of the MANOVA and ANOVA models (Montgomery, 2001). This analysis revealed that there were instances where homogeneity of variance and the normality of residual assumptions were violated. Log transformations were applied to the data. The transformed data was then used in the statistical analysis. The plots of the normality and residuals versus predicted values for the transformed data validated the

assumptions of the model. These plots, including both the original data and the transformed data, are shown in the Appendix B.

The results of the statistical analysis are presented in Table 6. The MANOVA tests found significant effects from the Load, Velocity, Direction, and the interaction between the Load and Velocity. The trunk extension Velocity significantly affected the maximum shear force but not the maximum compression force. Direction significantly affected both dependent variables. There was no significant three-way interaction effect.

Table 6. MANOVA and ANOVA results of the maximum spine reaction forces in the dynamic exertions.

	MANOVA	ANOVA	
		Maximum compression force	Maximum shear force
Load (L)	F=18.5, p<0.0001	F=38.38, p<.0001	F=28.61, p<.0001
Velocity (V)	F=7.28, p<0.0001	F=2.69, p=0.0706	F=13.7, p<.0001
Direction (D)	F=100.8, p<0.0001	F=177.25, p<.0001	F=162.99, p<.0001
L*V	F=2.51, p=0.0116	F=4.56, p=0.0015	F=3.72, p=0.0061
L*D	F=1.01, p=0.4043	NT	NT
V*D	F=1.83, p=0.1218	NT	NT
L*V*D	F=0.66, p=0.7288	NT	NT

NT –not tested because of non-significant MANOVA.

There were significant differences in the maximum compression and shear force on the spine between the eccentric and concentric exertions (see Figure 20, Figure 22, Figure 23 and Figure 25). On average, the eccentric exertions generated higher compression and shear force on spine than the concentric exertions. Even through the difference between the eccentric and concentric exertions increased as the Velocity increased, the statistical analysis showed no significant effects of interaction between the Direction and Velocity while there was a significant effect of the interaction between the Load and Velocity on the maximum spinal compression and shear forces (see Figure 21 and Figure 24).

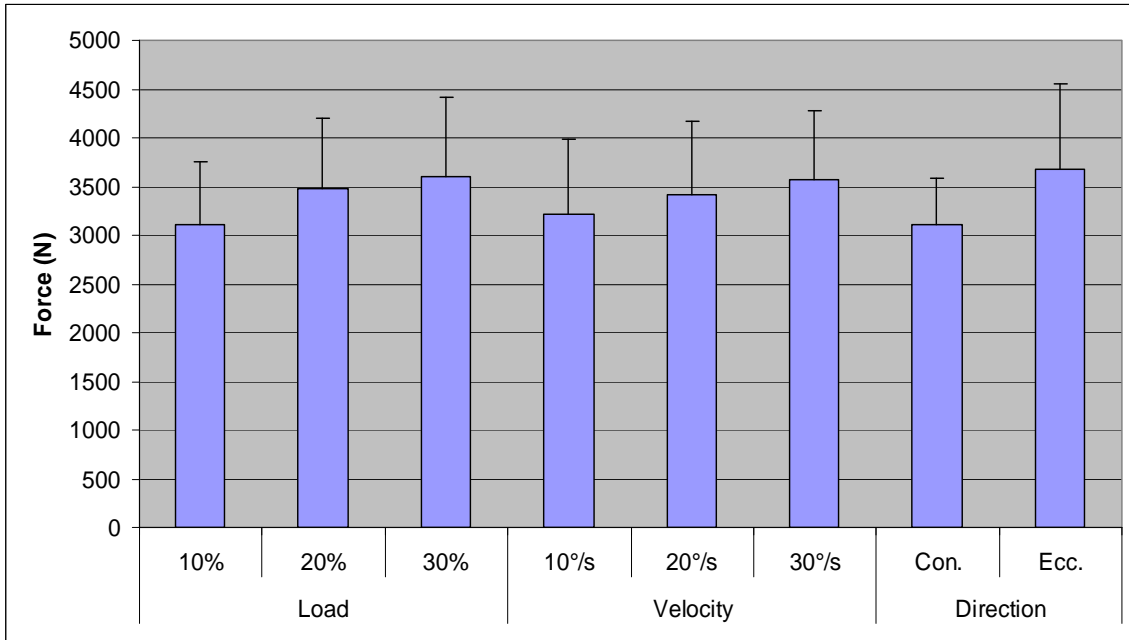


Figure 20. Maximum spinal compression force vs. Load, Velocity and Direction.

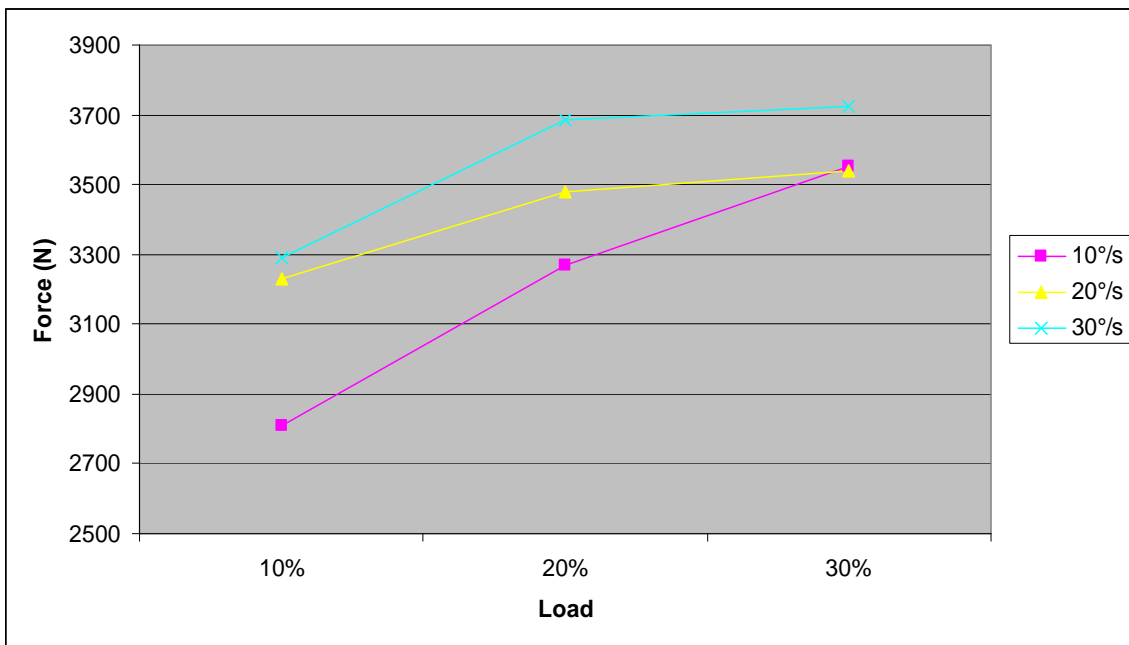


Figure 21. Interaction between Load and Velocity on maximum compression force.

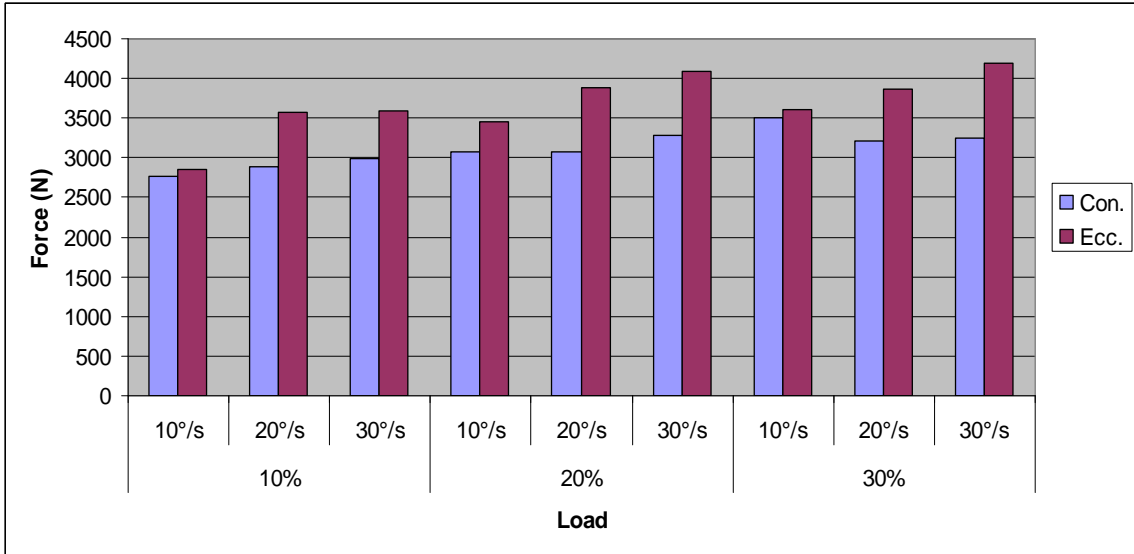


Figure 22. Maximum spinal compression force in dynamic controlled trials.

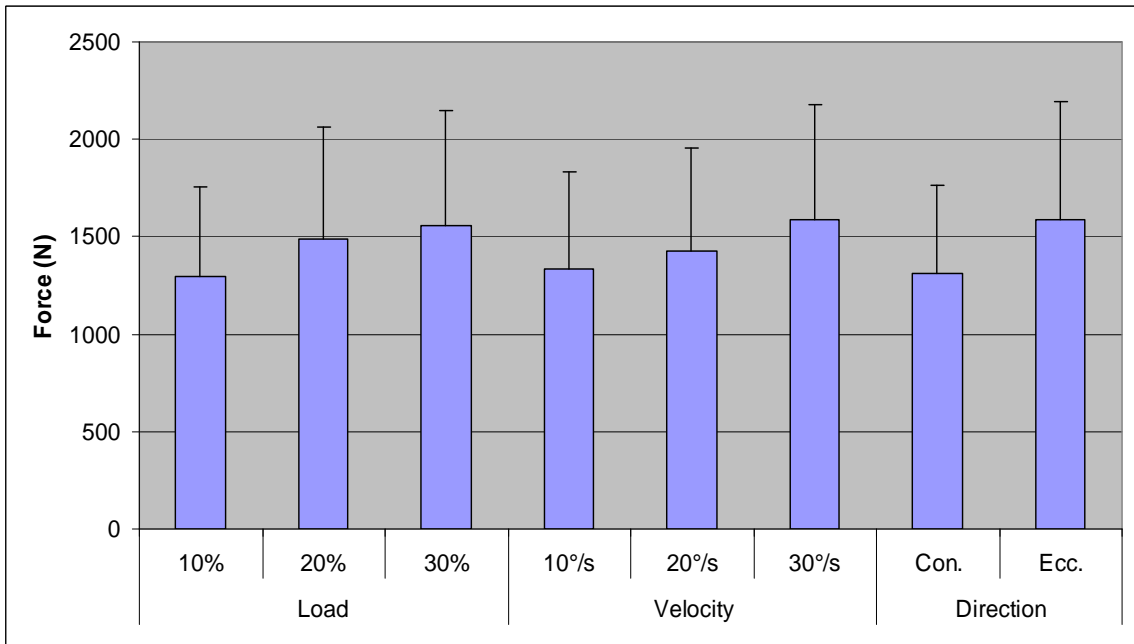


Figure 23. Maximum spinal shear force vs. Load, Velocity and Direction.

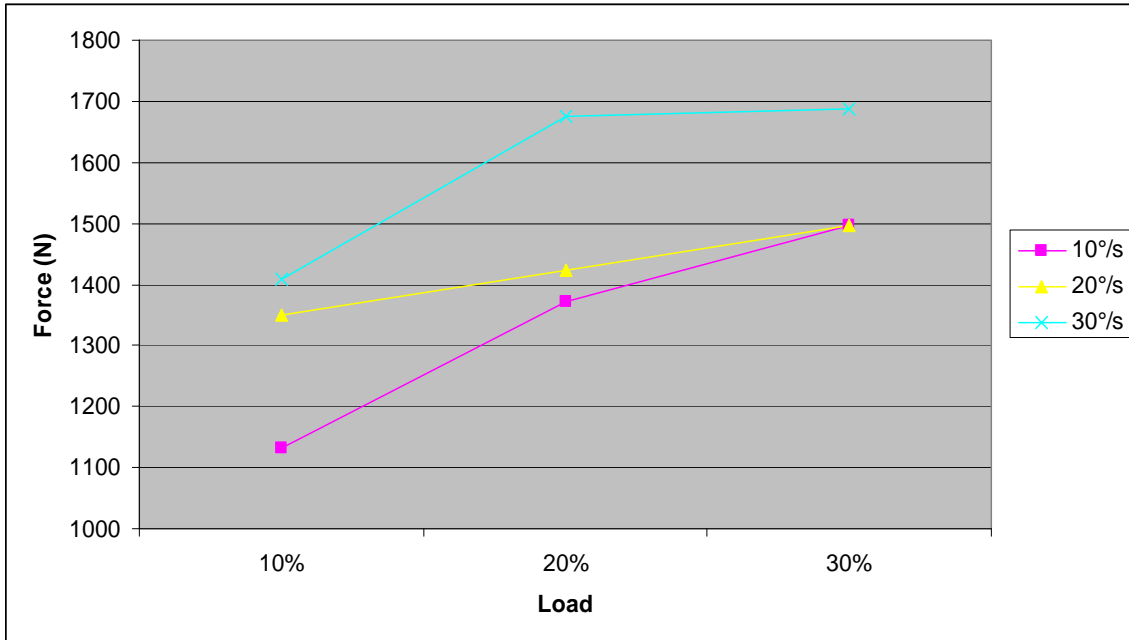


Figure 24. Interaction between Load and Velocity on maximum spinal shear force.

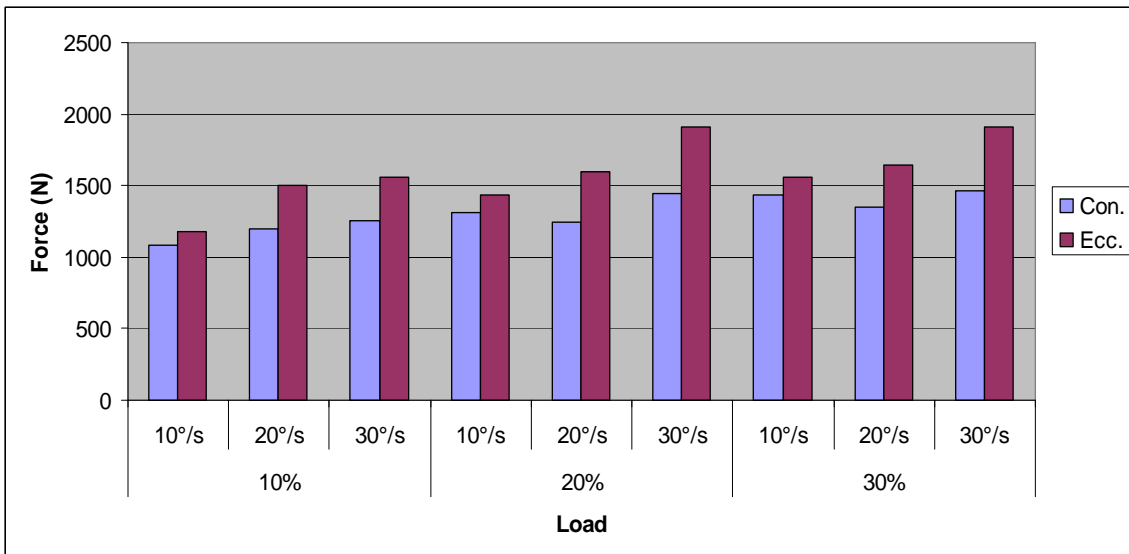


Figure 25. Maximum spinal shear force in dynamic controlled trials.

The median deviation of the maximum compression force and shear force on L5/S1 joint were calculated and used to investigate the differences in variability between concentric and eccentric exertions. The statistical analysis showed that the direction of the motion

(eccentric and concentric) significantly affected the variability of spinal load in terms of median deviation of the spinal compression and shear forces (see Table 7).

Table 7. MANOVA and ANOVA results of the median deviation values

	MANOVA	ANOVA	
		Median deviation of the maximum compression force	Median deviation of the maximum shear force
Load (L)	F=3.78, p=0.0047	F=6.96, p=0.0011	F=3.58, p=0.0288
Velocity (V)	F=1.92, p=0.1045	NT	NT
Direction (D)	F=5.53, p=0.0043	F=7.36, p=0.007	F=8.52, p=0.0037
L*V	F=2.62, p=0.0077	F=2.49, p=0.0424	F=4.81, p=0.0008
L*D	F=3.10, p=0.0150	F=0.05, p=0.9506	F=5.16, p=0.0061
V*D	F=0.88, p=0.4762	NT	NT
L*V*D	F=1.03, p=0.4130	NT	NT

NT –not tested because of non-significant MANOVA.

Figure 26, Figure 27, Figure 29 and Figure 30 present significant effects of the direction of the motion on the median deviation of the maximum compression and shear forces. The eccentric exertions generated larger median deviation values of the maximum compression forces in all Velocity and Load conditions as compared to concentric exertions. Velocity also affected the dependent variables but the trend was not consistent. There was also a clear interaction between the Velocity and Direction (see Figure 28 and Figure 31). The median deviation of the maximum compression and shear force in eccentric exertions decreased as the speed increase. The effect of Direction was not consistent in three levels of Load. In 20% load level, the median deviation of the shear force was even smaller in eccentric than in concentric exertions (see Figure 32).

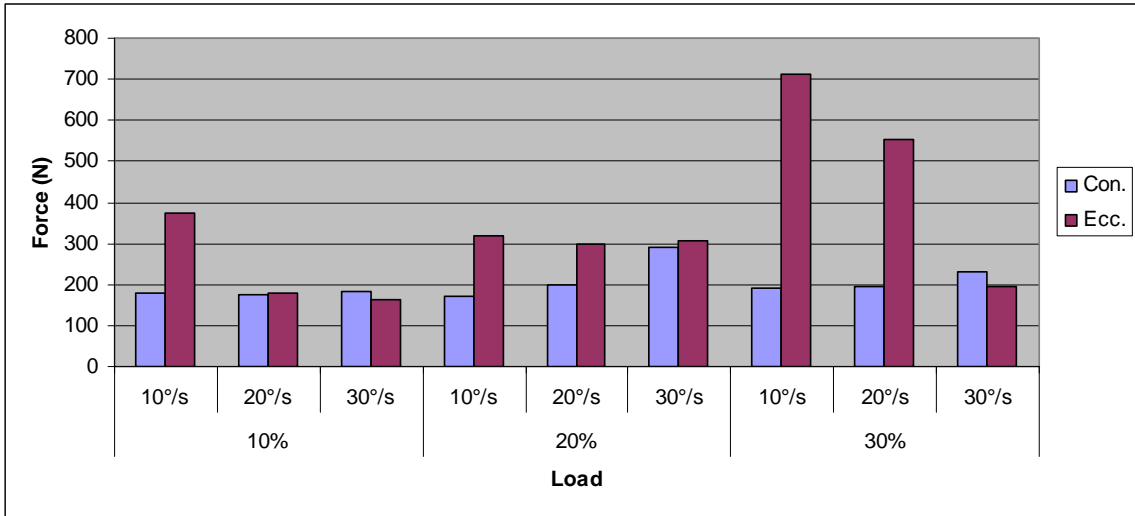


Figure 26. Median deviation of the maximum compression force in controlled dynamic exertions.

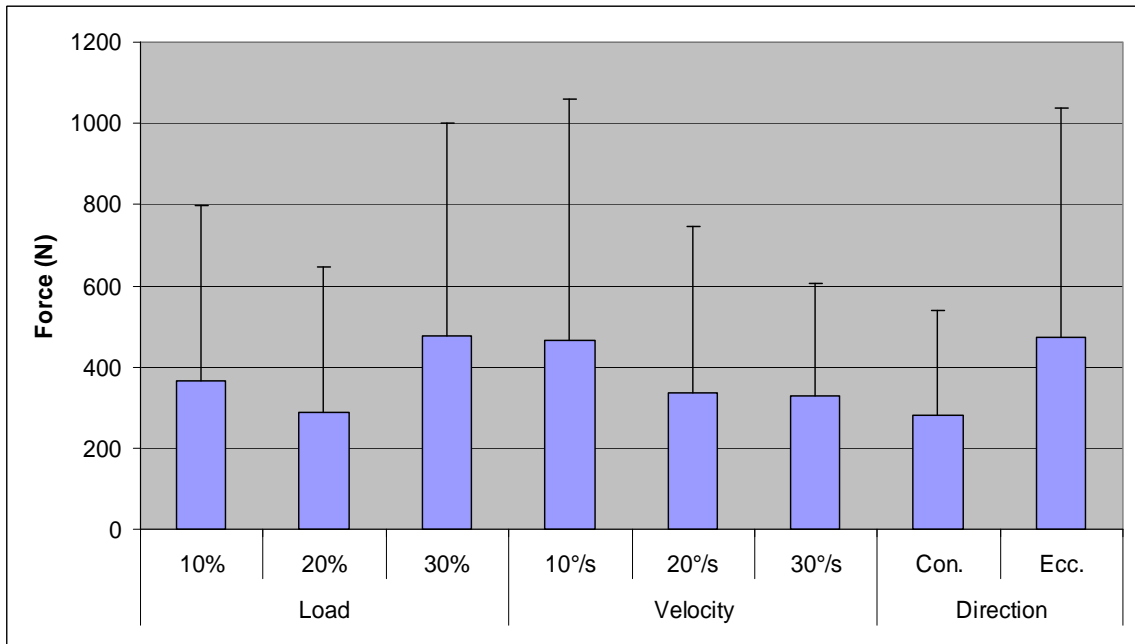


Figure 27. Median deviation of the maximum compression force.

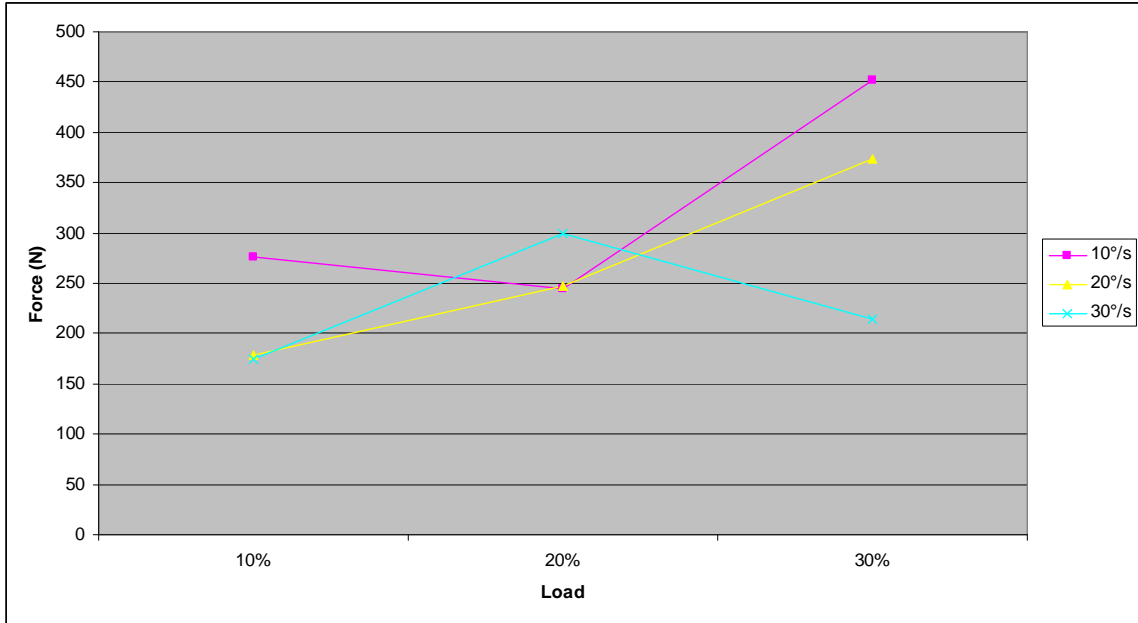


Figure 28. Interaction between Load and speed on median deviation of the maximum compression force.

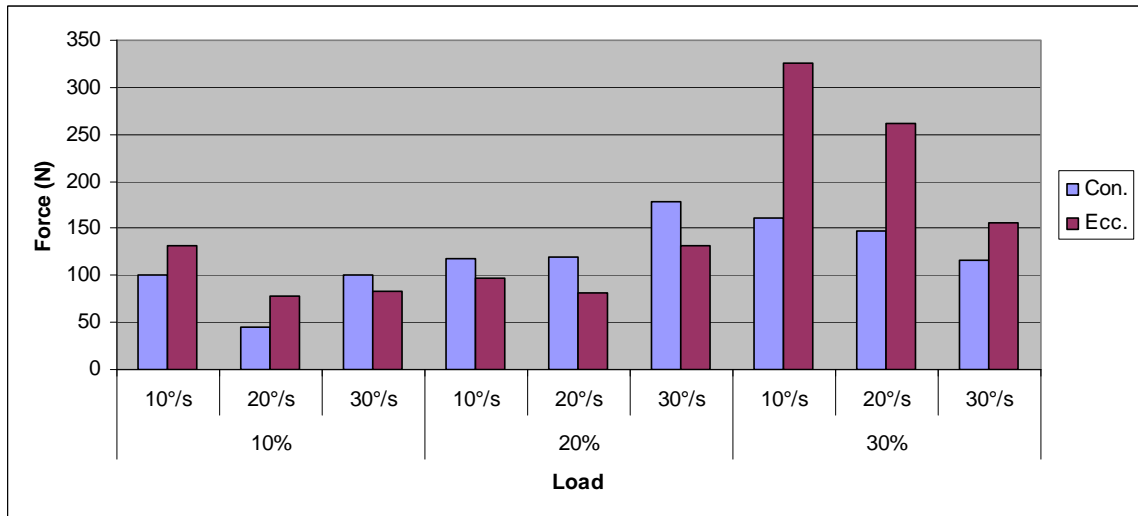


Figure 29. Median deviation of the maximum shear force in controlled dynamic exertions.

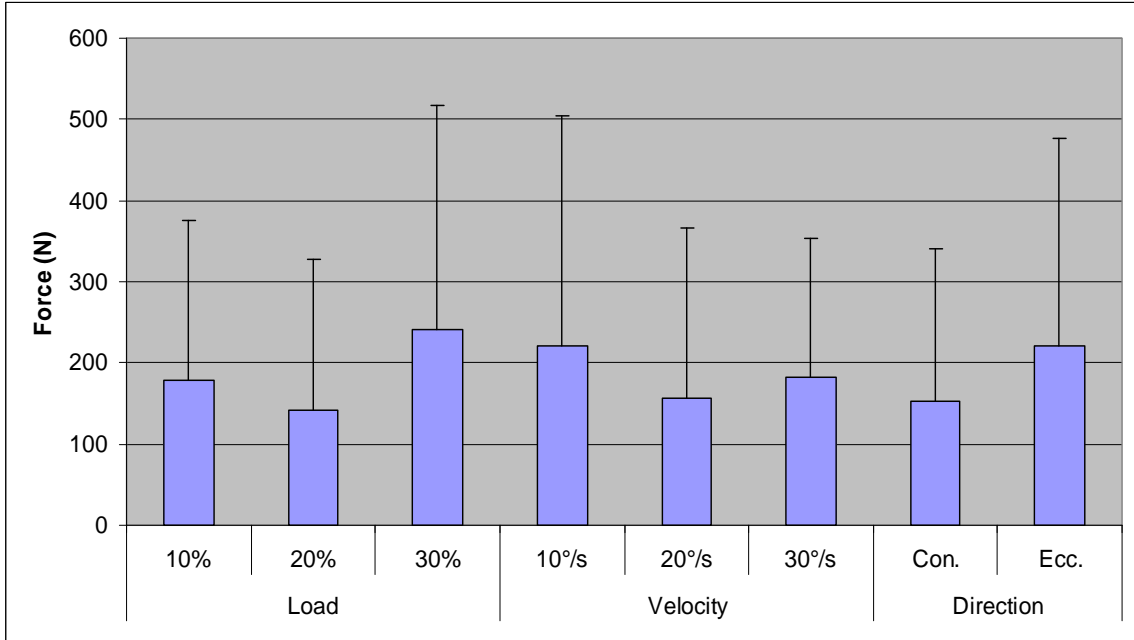


Figure 30. Maximum spinal shear force vs. Load, Velocity and Direction.

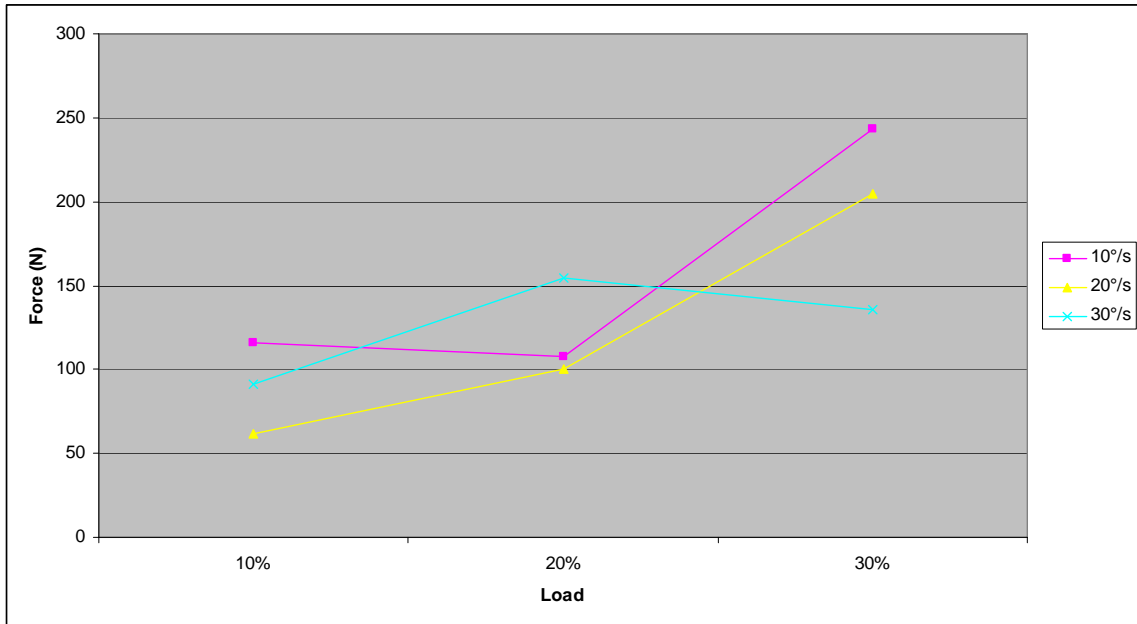


Figure 31. Interaction between Load and Velocity on the median deviation of the maximum shear force.

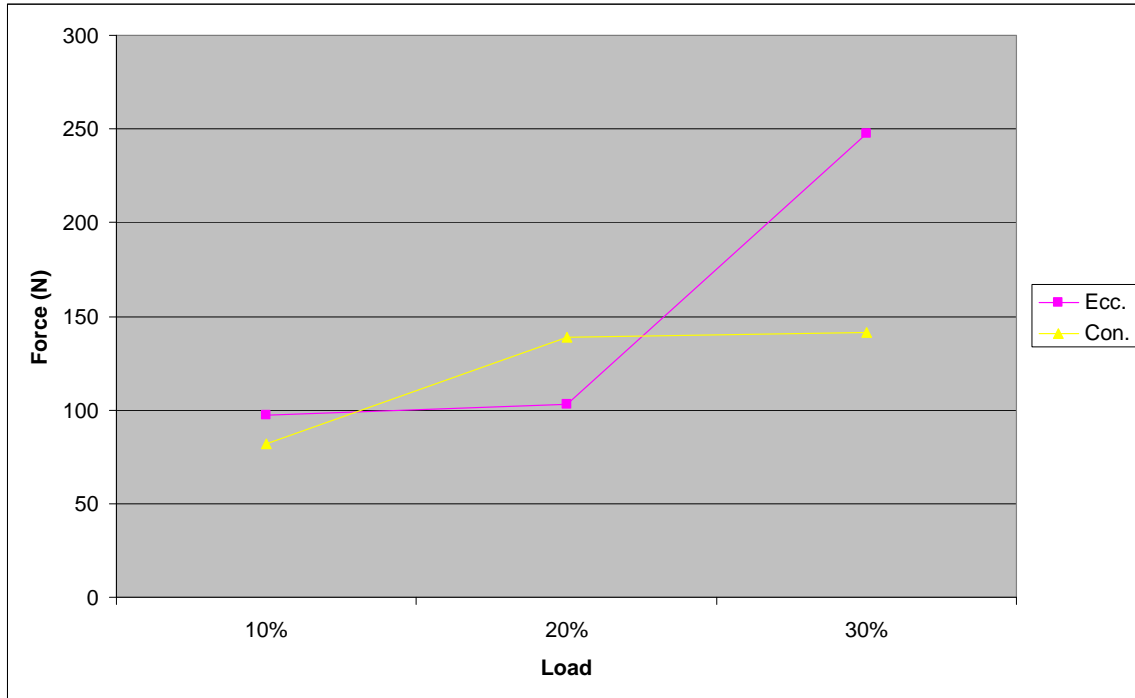


Figure 32. Interaction between Load and Direction on the median deviation of the maximum shear force.

6.2 Experiment two: free lifting/lowering study

6.2.1 Model evaluation

As in the Results section for Experiment 1, we begin with a graphical presentation of the data (Figure 33). This figure presents one example of three lifting/lowering exertions from one subject. The subject started from full flexed posture, lifted the load to the upright posture (about 7 seconds), lowered the load (about 13 seconds), and repeated the lifting motion two more times. The trace from the “Muscle only” model shows the flexion relaxation phenomenon with the muscle activity diminishing as the subject reached the full flexion posture. The muscle activities decreased at full trunk flexion angles and the model without the passive components did a poor job of predicting the external moment at the full flexion posture. The “With passive components” model did a much better job of tracking the external moments throughout the full lifting motion.

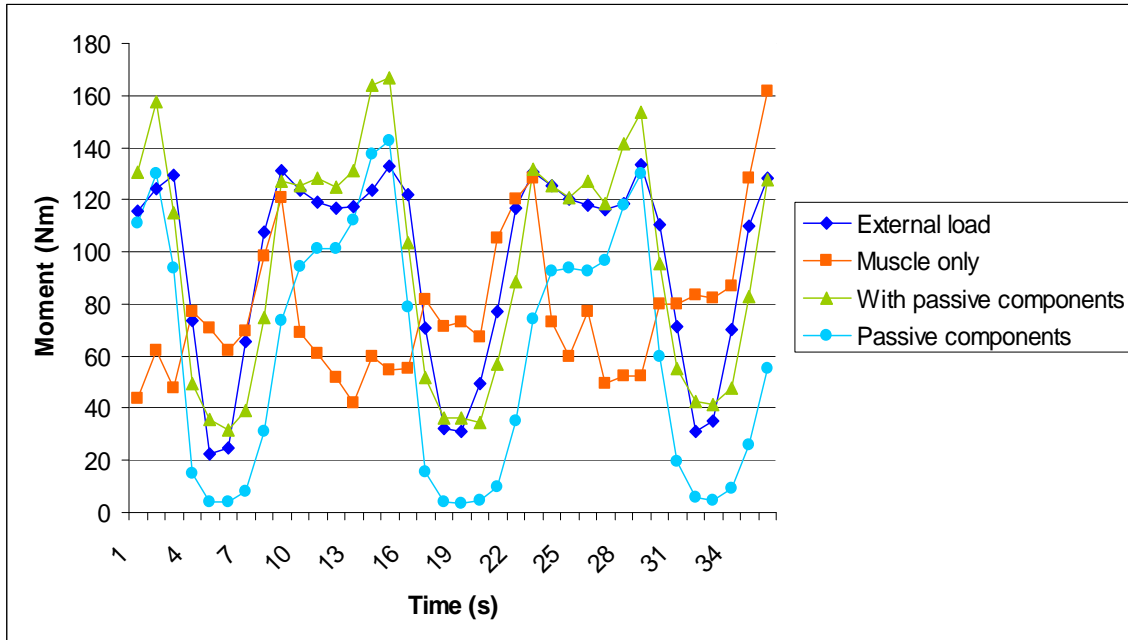


Figure 33. Measured external moment and model predicted internal moment in free lifting/lowering exertions.

The results of the comparison of the mean absolute error and the R^2 values indicated excellent performance of the model with passive components (Table 8). The mean absolute error was less than half for the model with passive components as compared to the model without passive components. The R^2 value for the model with passive components was considerably higher. These results indicate the model with passive components was significantly better than the model without passive components in predicting the total external moment.

Table 8. Comparison of mean absolute error and R² values in free lifting/lowering exertions.

		Mean absolute error (Nm)	R ²
Model with passive components	Bend knee	19.2 (6.8)	76.2% (9%)
	Straight knee	19.6 (7.6)	73.6% (11%)
	All	19.4 (7.2)	74.9% (10%)
Model with muscle only	Bend knee	54.1 (14.2)	12.3% (13%)
	Straight knee	55.7 (17.2)	11.6% (11%)
	All	54.9 (15.3)	11.9% (12%)

These results confirm the results of Experiment 1 that showed the improvements in quality of the predictions of the model that included the passive tissues. This was true in both the bent knee and straight knee condition. Their mean absolute error and R² values were not significantly different. The model correctly addressed the difference of maximum trunk flexion angle between the bend knee and straight knee conditions.

6.2.2 Comparison of eccentric versus concentric exertions

Similar to Experiment 1, an evaluations of the ANOVA assumptions revealed that a log transformation was necessary for the median deviation data of the maximum compression and shear forces. After transformation the data was shown to comply with the normality assumptions of the statistical models (Appendix B). The MANOVA and ANOVA technique revealed several significant effects of Direction on the peak compression and shear values (see Table 9). This included both Direction as a main effect and the interaction of Direction with Posture.

Table 9. MANOVA and ANOVA test results of the maximum values in free lifting/lowering exertions.

	MANOVA	ANOVA	
		Maximum compression force	Maximum shear force
Posture (P)	F=31.79, p<0.0001	F=0.13, p=0.7219	F=45.59, p<.0001
Load (L)	F=10.26, p<0.0001	F=27.22, p<.0001	F=11.23, p<.0001
Direction (D)	F=3393, p<0.0001	F=796.61, p<.0001	F=467.8, p<.0001
P*L	F=0.76, p=0.5998	NT	NT
P*D	F=7.08, p=0.0001	F=19.67, p<.0001	F=6.56, p=0.0106
L*D	F=0.59, p=0.7353	NT	NT
P*L*D	F=0.61, p=0.7226	NT	NT

NT –not tested because of non-significant MANOVA.

Figure 34 and Figure 35 present the effects of Load, Posture and motion direction on the model predicted maximum spinal compression force. Posture did not show a significant effect on spine compression as a main effect, but there was a significant interaction between Posture and Direction (Figure 38). This figure shows that the eccentric exertions generated higher compression force than concentric exertions but the difference between eccentric and concentric exertions were larger in the bent knee condition than that in the straight knee condition.

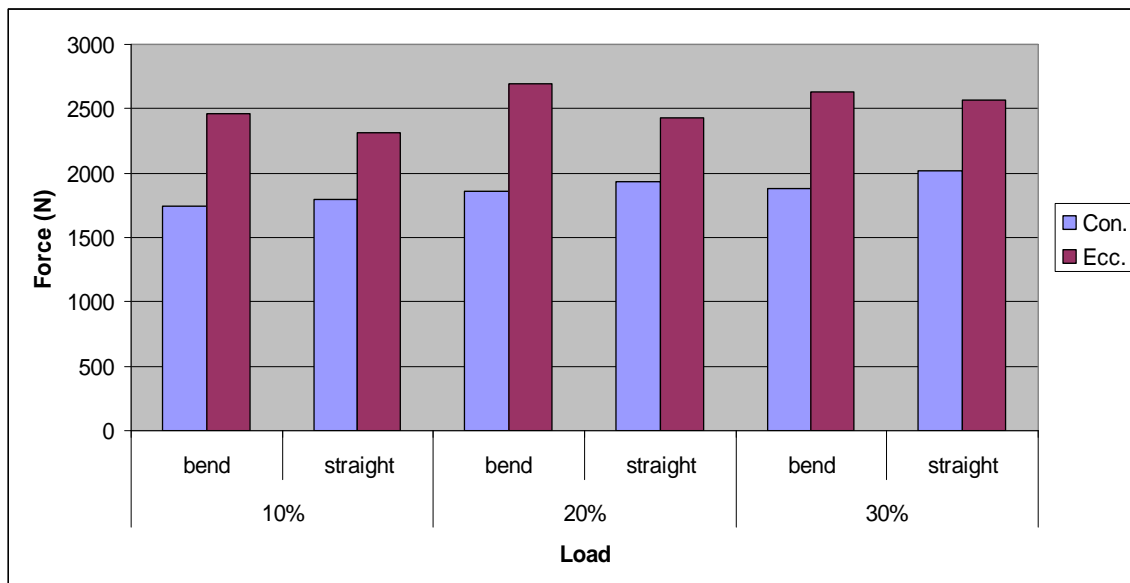


Figure 34. Maximum spinal compression force in free lifting/lowering exertions.

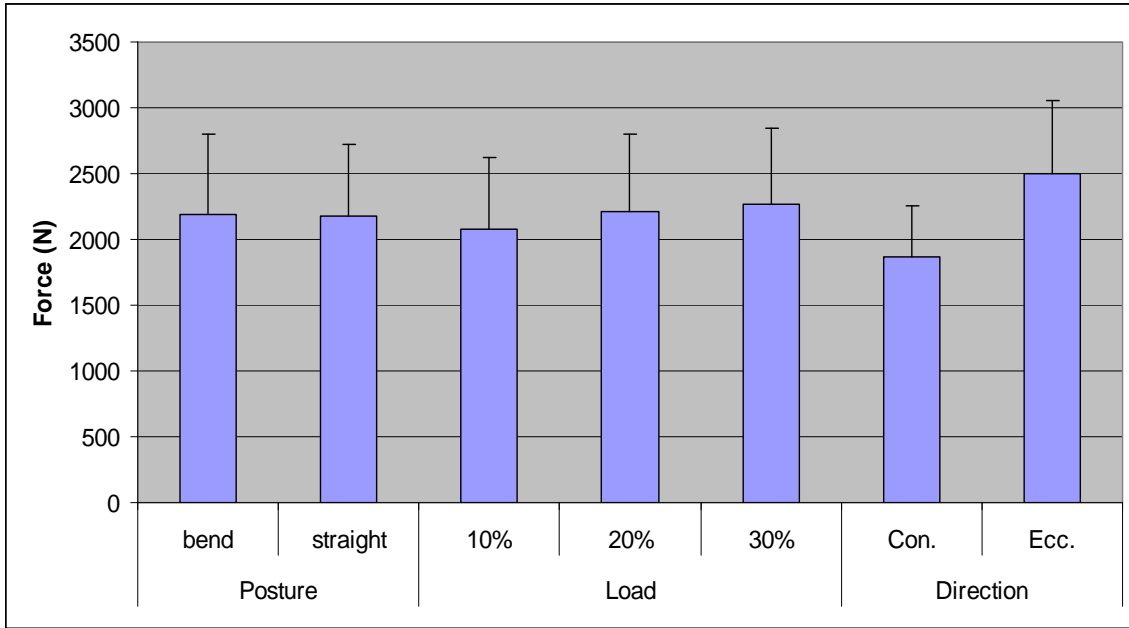


Figure 35. Maximum compression force vs. Posture, Load and Direction.

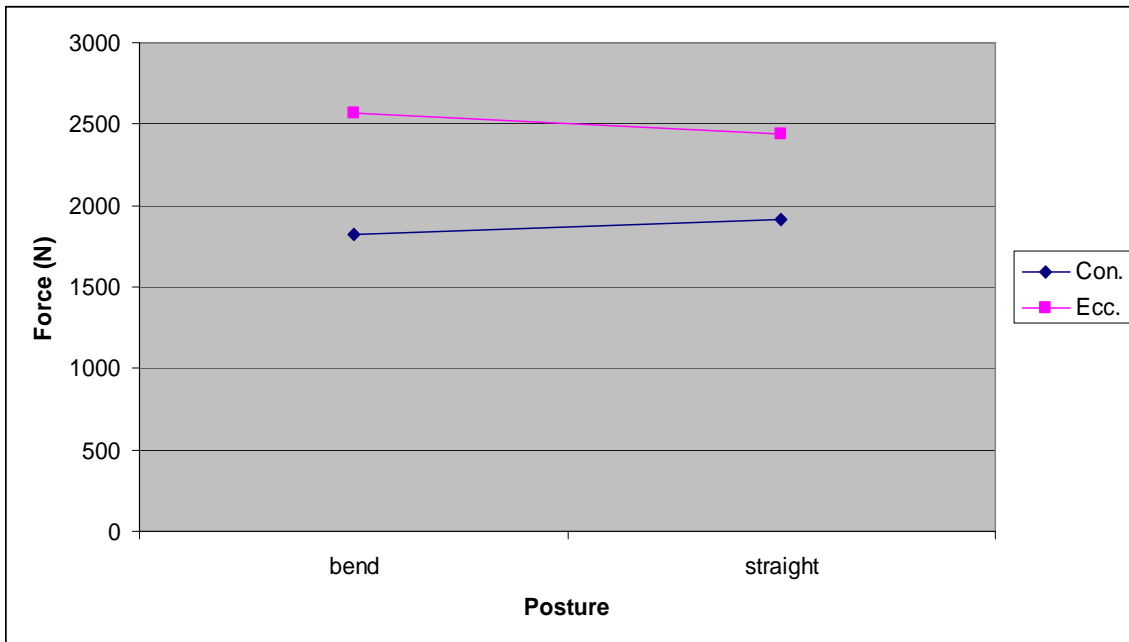


Figure 36. Interaction between Posture and Direction on maximum compression force.

For maximum shear force, only the main independent variables (Load, Posture and Direction) had significant effects (see Figure 37 and Figure 38). The maximum shear force

on spine was significantly lower in the bend knee condition as compared to the straight knee condition. There was a significant interaction between Posture and Direction (see Figure 42).

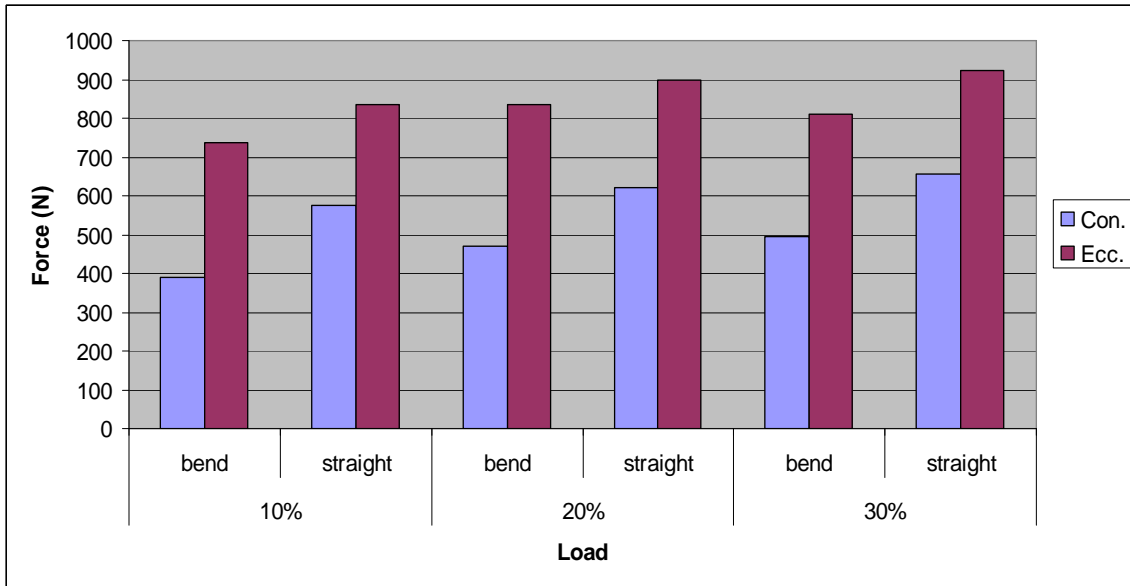


Figure 37. Maximum spinal shear force in free lifting/lowering exertions.

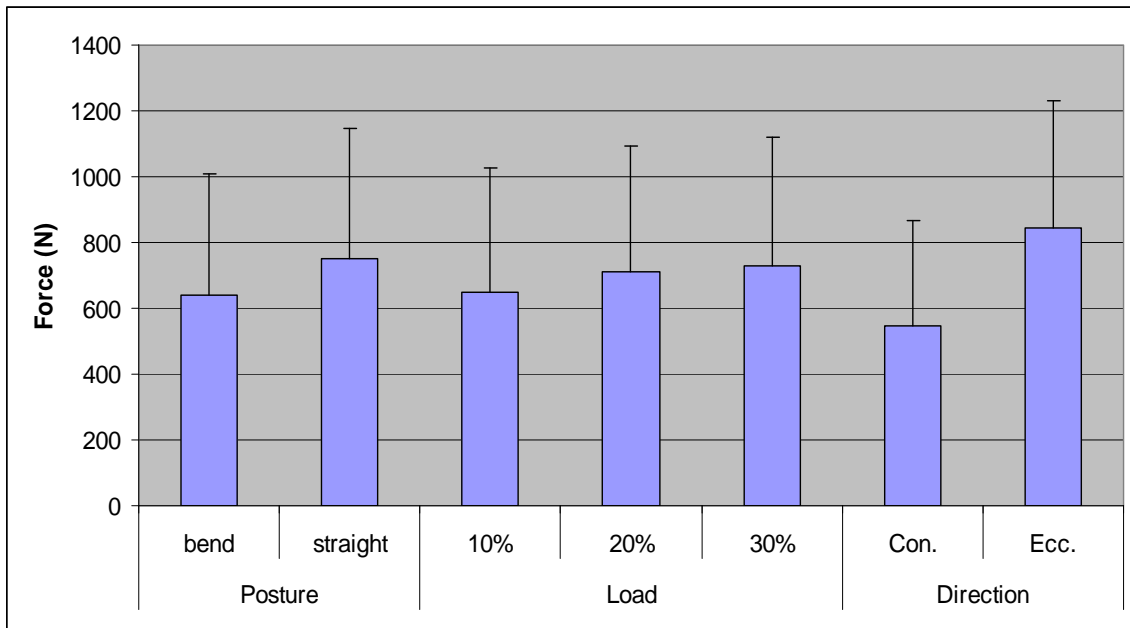


Figure 38. Maximum spinal shear force vs. Posture, Load and Direction.

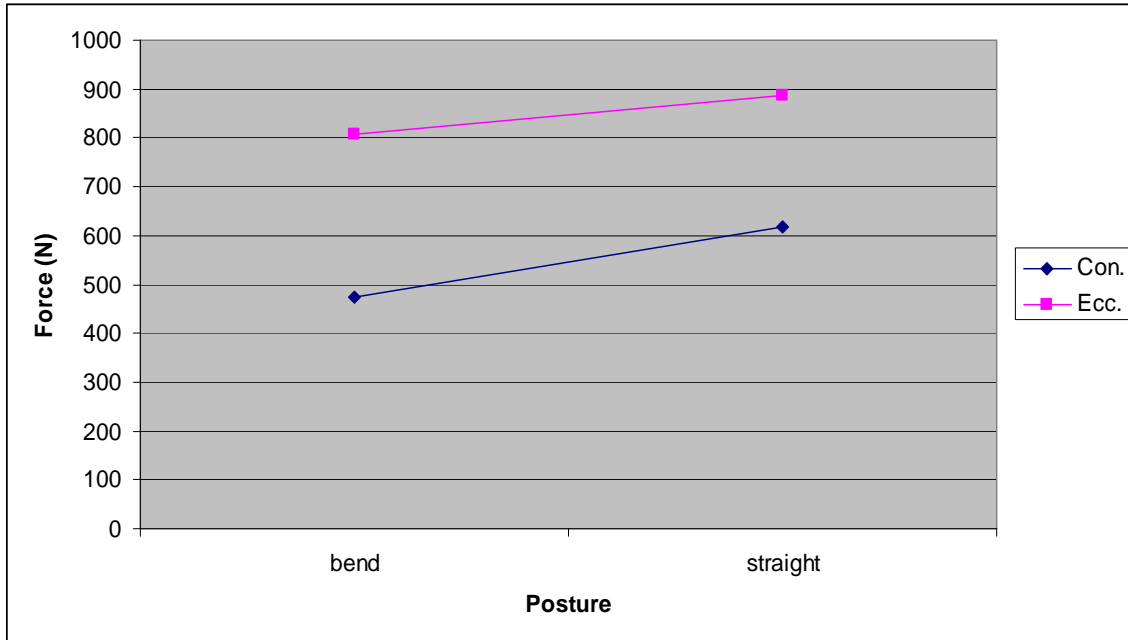


Figure 39. Interaction between Posture and Direction on the maximum shear force.

Similar to experiment one, the same procedure was conducted to investigate the effect of eccentric and concentric exertions on the variability of the dependent variables. Statistical analysis results are presented in Table 10:

Table 10. MANOVA and ANOVA test results of the median deviation of the maximum values.

	MANOVA	ANOVA	
		Median deviation of maximum compression force	Median deviation of maximum shear force
Posture (P)	F=3.05, p=0.0477	F=0.63, p=0.4294	F=3.83, p=0.0507
Load (L)	F=4.87, p=0.0007	F=4.05, p=0.0178	F=7.45, p=0.0006
Direction (D)	F=22.41, p<0.0001	F=44.87, p<.0001	F=4.9, p=0.0271**
P*L	F=0.42, p=0.7945	NT	NT
P*D	F=1.49, p=0.2253	NT	NT
L*D	F=4.03, p=0.0030	F=4.29, p=0.014	F=5.66, p=0.0036
P*L*D	F=0.35, p=0.8465	NT	NT

NT –not tested because of non-significant MANOVA.

** Simple effects analysis revealed that the main effect of Direction was not significant.)

As seen from Figure 42, there was a clear interaction between the Load and Direction. The eccentric exertions generated larger median deviation values of the maximum compression forces than concentric exertions in all load conditions (see Figure 40 and Figure

41). But this difference was mostly noticeable in 10% and 20% load conditions and was decreased in 30% load conditions.

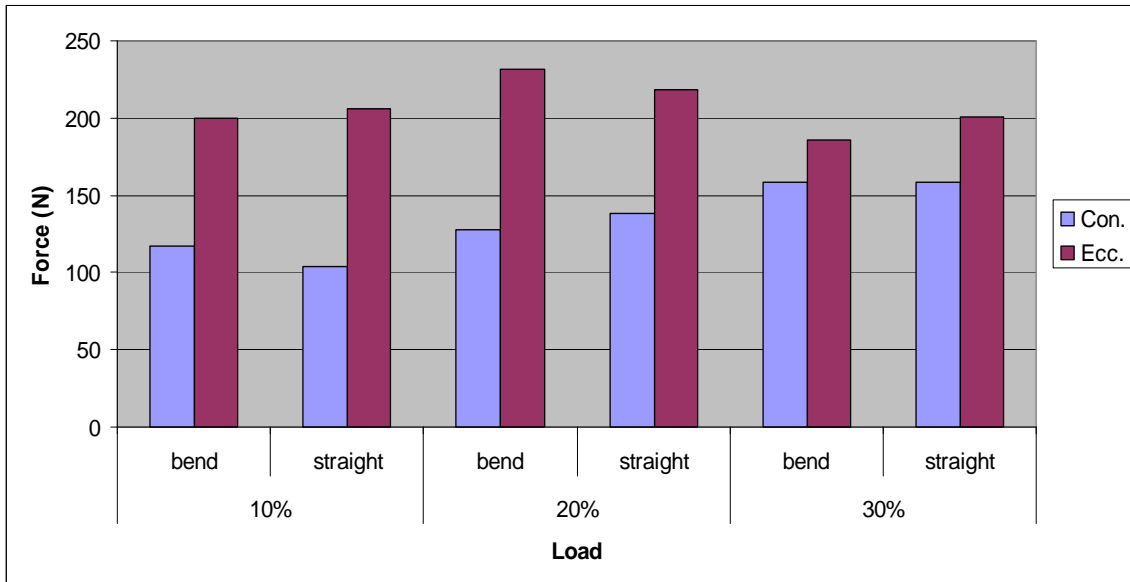


Figure 40. Median deviation of maximum compression force in free lifting/lowering exertions.

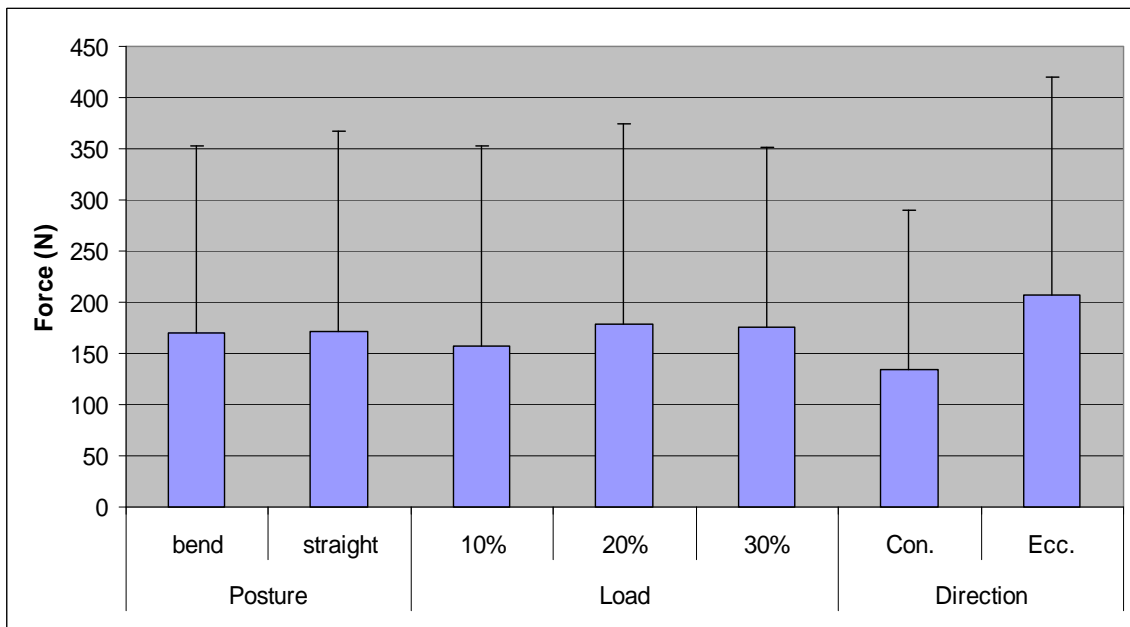


Figure 41. Median deviation of maximum compression force vs. Posture, Load and Direction.

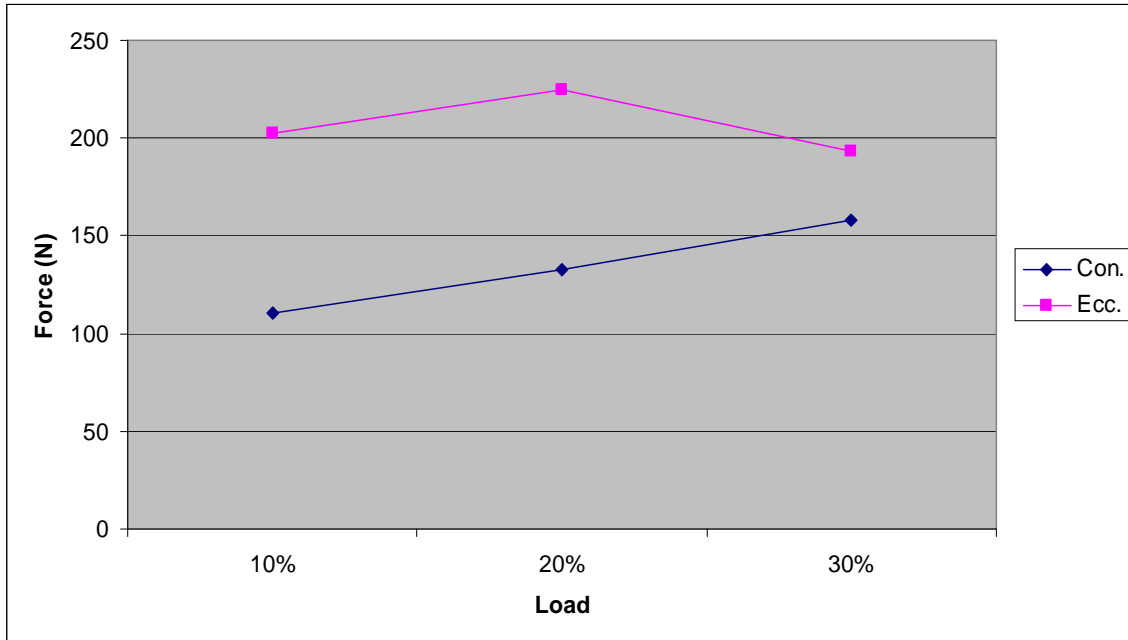


Figure 42. Interaction between Load and Direction on the maximum compression force.

Figure 45 showed a clear interaction between the Direction and Load. The eccentric exertions generated higher median deviation values of the maximum shear force only in 10% and 20% load level conditions. In 30% load level, the concentric exertions generated higher values, but their difference was relatively small. Overall, the median deviation of the maximum shear force was smaller in concentric exertions than in eccentric exertions in low load conditions, but as the load increase, the difference was smaller (see Figure 43 and Figure 44).

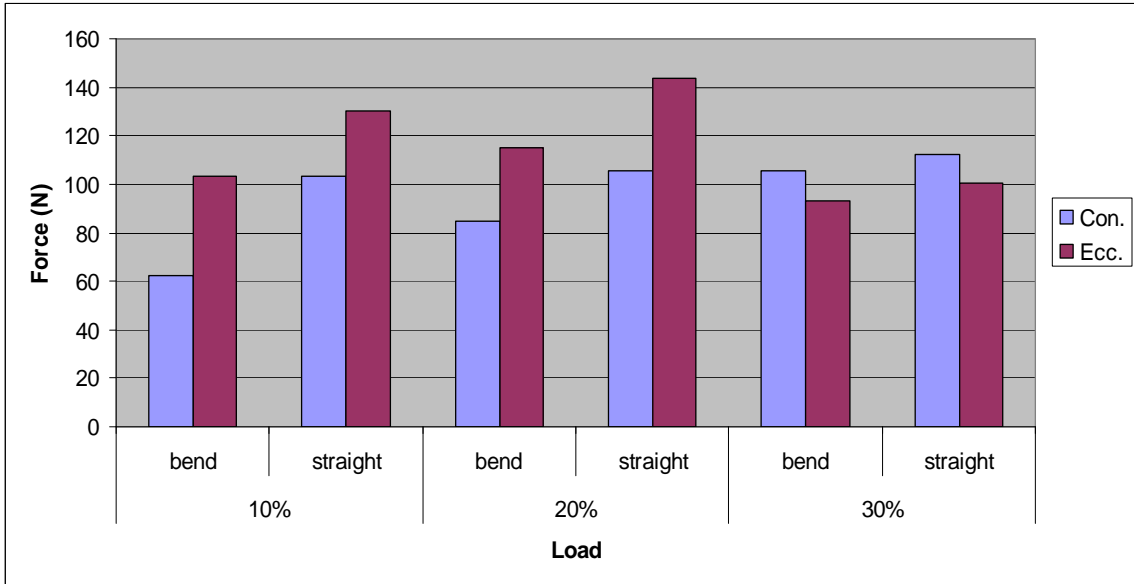


Figure 43. Median deviation of maximum shear force in free lifting/lowering exertions.

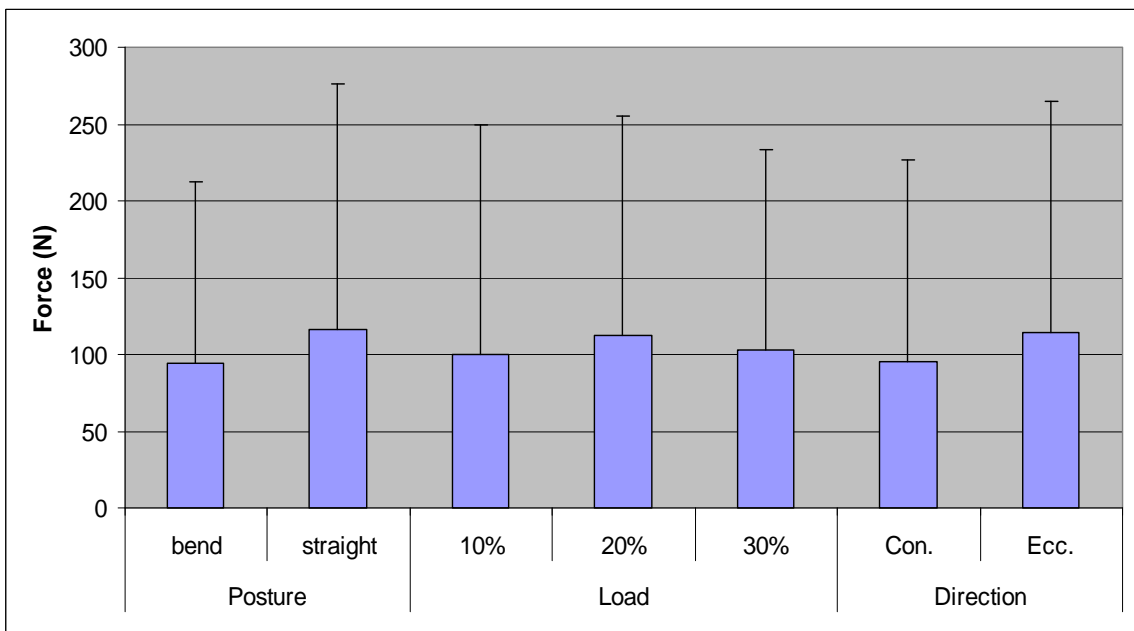


Figure 44. Median deviation of maximum shear force vs. Posture, Load and Direction.

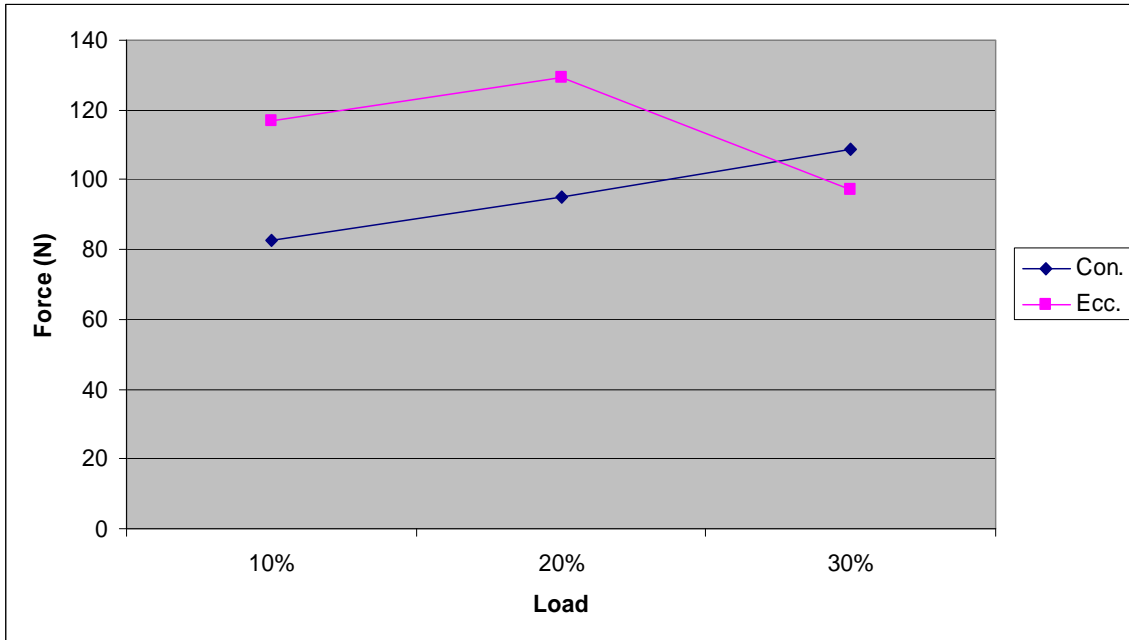


Figure 45. Interaction of Load and Direction on median deviation of the maximum shear force.

7 DISCUSSION

7.1 Assessment of the model

This EMG assisted biomechanical model of the spine provides insight into the complicate operation and interaction of the trunk muscles and passive components. It was useful to help us understand how the trunk operates. For example, this model was capable of distinguishing if the upper body was supported exclusively by the trunk muscles or by passive components, or evenly by both of them. This information can be used to evaluate the status of the trunk musculoskeletal control system. Meanwhile, this model was capable of estimating the spinal load accurately; thus, it can be used to assess the loading on the spine during the performance of various tasks and provide valuable information for tracing the source of low back disorders.

One advantage of this EMG-assisted biomechanical model of the spine is that it provided information about the spinal load in full flexion postures that related to the extreme loads on the spine. There are studies that indicate that it is the extreme, as opposed to the average, loading of the back that define the risk of occupationally-related low back disorders (Marras, Lavender et al. 1993). From a biomechanical view, the load on the spine increases as the trunk flexion angle becomes larger. Extreme loadings of the spine are more likely to happen at extreme trunk flexion angle, which is, the full flexed posture. There are two reasons for this. First, the moment generated by upper body reaches maximum at 90° trunk flexion angle which is usually very close to the full trunk flexion angle. Secondly, as shown in the current study, the passive components generate majority of the restorative moments at this posture. Due to their shorter moment arms (relative to the extensor musculature), the

passive components generate significantly larger forces than the active muscles. Therefore, the load on the spine at full flexion posture is practically largest in the full range of trunk motions.

McGill and Kippers (1994) conducted a study to investigate the distribution pattern of load between lumbar tissues at full flexed posture when flexion-relaxation phenomenon occurred. They expanded one of McGill's previous EMG-assisted biomechanical models (McGill and Norman 1985; McGill and Norman 1986; McGill 1992) by including a new equation to calculate the restorative moment generated by lumbar ligaments. In this model, the forces generated by ligaments were calculated based on the percent strain from rest length, which was related to trunk flexion angle, but not affected by the forces from muscles or the external load. They found that the majority of the restorative moment was generated by the lumbar ligaments (113Nm out of 171Nm total) at full flexed posture. These results were comparable with the results in experiment two of this study (approximately 120Nm from passive components out of 166Nm total), but significantly different from the results in experiment one (approximately 60Nm from passive components out of 130Nm total). The main reason might be the activation levels of the trunk muscles at full flexed posture. McGill and Kippers asked the subject to reach full flexed posture and maintain that posture, similar to the setup in experiment two of this study. The subjects could relax their trunk muscles and rely on the passive components to support upper body. Therefore, the trunk muscles ceased activity. In experiment one of this study, the subject was asked to maintain a certain level of extension moment at the full range of trunk flexion, including the full flex posture. The subject could activate their muscles to generate the extension moment. Sometimes this was necessary since the data from experiment one indicated the antagonist muscles were also

activated. The synergetic activation of both flexor and extensor muscles provided more precise control of the extension moments. When muscles were activated, the distribution pattern of the external load to lumbar tissues should be changed. However, in McGill and Kippers model, the forces generated by lumbar ligaments were not affected by muscle activation level. If their model was applied to the data from the experiment one, they would over estimate the total internal load, or under estimate the maximum muscle stress values of the subjects. The results from experiment one, as compared to experiment two, indicated the importance of considering the complicate interaction between the forces generated by passive components and the muscle forces and external load. As the external load increases, the muscles generated larger forces, thus compressing the intervertebral discs and shorten the length of lumbar ligaments. The forces from passive components were not exclusively related to trunk flexion angle, but also related to the activation level of the muscles and the total compression force on spine. This complicated interaction was successfully addressed by the finite element model used in this study and provided more realistic results in experiment one.

This model was based on the model introduced by Davis et al. (1998) which is an expansion from the previous EMG-assisted biomechanical models developed in Ohio State University (Marras and Reilly 1988; Reilly and Marras 1989; Marras and Sommerich 1991a; Marras and Sommerich 1991b; Granata and Marras 1993; Granata and Marras 1995). In this model, Davis et al. included the empirical relationship between muscle torque and muscle length and velocity. Using this new force-length and force- velocity relationship, they were able to estimate the spinal load in both eccentric and concentric exertions. They found that lowering exertions had significantly lower anterior-posterior shear force than lifting exertions

(680.4±161.4N versus 815.1±281.4N), but the maximum compression forces were greater in lowering exertions than in lifting exertions (3269.1±843.3N versus 2665.2±719.6N). These results were significantly different from the findings in this study (3114±471N versus 3680±879N for maximum compression force, and 1309±454N versus 1589±600N for maximum shear force). First of all, the magnitude of the shear and compression forces was considerably larger in this study. The reason could be the extreme flexion posture used in this study. These results indicated the extreme loadings of the spine occurred at the near full flexion posture. If researchers only investigate postures involving small trunk flexion angles, the risk of low back disorders might be underestimated. Secondly, in this study, the anterior-posterior shear force was significantly larger in lowering exertions than lifting exertions, which was opposite to the results in Davis et al. (1998). This might be explained by the difference in the setup of the experiments between these two studies and the distribution pattern of the load between lumbar tissues. Davis et al. observed that the subjects seemed to hold the load farther away from body in lowering exertions as compared to lifting exertions, which resulted in larger sagittal moment (140.5Nm in lowering versus 113.1Nm in lifting). The subject could abduct their arms to move the load farther away from body, which might induce a more upright posture in lowering exertions. Thus, the forces generated by trunk muscles contributed more to the compression force on the spine, and less to the shear force. In this study, the external load was applied to the consistent position on the back of the subjects in experiment one, which guaranteed the same external moment at the trunk flexion angle between lowering and lifting exertions. Thus, the larger shear and compression force on spine were not from the external load, but possibly resulted from the difference level of co-activation of the lumbar tissues.

In the static controlled exertions on the dynamometer, there was a clear difference in the effects of the trunk flexion angles on the maximum muscle stress value between the models with and without passive components. In the first level of model evaluation we allowed the muscle stress value to vary across conditions within a subject to assess the degree of variability in the predicted maximum muscle stress values. There are several reasons for higher mean and standard deviation of the maximum muscle stress value at full trunk flexion angle in the model without passive components (Figure 15). Firstly, at the full trunk flexion angle in the model utilizing the passive components, the passive components generated the majority of the extension moment, and the muscles were only activated at a low level, resulting in a relatively consistent, low level of predicted maximum muscle stress. In the model without the passive components, this low level activity was the only component available to balance the whole external moment, which required large maximum muscle stress values. Secondly, the higher standard deviation of the maximum muscle stress value may be partly related to larger maximum muscle stress value and partly due to the level of choice in full trunk flexion postures. The subject can choose to activate his back muscles to generate the extension moment. On the other hand, he can relax and let the passive tissues support the trunk and use less muscle force to maintain steady extension torque. In these two contrary conditions the activity level of the muscle could be significantly different. This difference was completely inherited by the muscles in model without passive components as it relied only on muscle activity. The result was the large difference of predicted maximum muscle stress values even in the identical conditions and larger standard deviation of the maximum muscle stress value as compared to the model with passive components. This

increase violated the fundamental assumption that one person's maximum muscle stress value should be constant and should not be varied in different postures.

Returning back to the more accurate physiological reasoning of having only one gain per subject across all conditions, allowed for an assessment of the model from the perspective of the effects of trunk angle on the predicted internal moments. Because a single mean maximum muscle stress value from all trials was used for each subject to predict the internal moment, this mean value was larger than the maximum muscle stress values for some of the trials involving full trunk flexion angles, and less than the ones in the trials involving only small trunk flexion angles. The model without passive components was only accurate at the medium trunk flexion angles. As shown in Figure 16 to Figure 19, the model without passive components tended to over predict at small trunk flexion angles, and under predict at near full trunk flexion angles. This finding that including passive components in the model would affect the prediction of the maximum muscle stress value at different trunk flexion angles had significant implication to the previous EMG-assisted biomechanical models. McGill and Kippers (1994) introduced a model included the passive components. They studied the distributions of the spinal load to trunk tissues in flexion-relaxation phenomenon. Their focus was the static full flexed posture so they made no quantitative comparison between external moment and internal moment during the full range of trunk flexion. Thus the effect of trunk flexion angle on the prediction of maximum muscle stress value (in their study it was the maximum muscle force) was not addressed.

Despite visually inspecting the output figures and qualitatively studying the improvement from involving passive components in the biomechanical spinal model, we could also find improvements in performance of the model with passive components

quantitatively, as the smaller mean absolute error and larger R squared values. There were two components that contributed to the mean absolute error, the fluctuation of the EMG signal and the error from the model prediction. Because the EMG signal is the combination of the electrical impulses of numerous muscle motor units, the output signal was not as smooth as the measured external force. When the external moment calculated from the measured smooth force and the internal moment calculated from the fluctuating EMG signal were compared, the mean values could be the same, but each individual data point might not be fit. For example, in Figure 18 when the model with passive components accurately predicted the internal moment, there were several data points that the internal moment was clearly higher or lower than the measured external moment. All these errors will be additive and represented in the mean absolute error not matter how good the model prediction would be. The second part of the mean absolute error was the error of the model, which was the focus of this study. The difference between these two models was the passive components, which generate significant effects only in large trunk flexion angles, so the difference of the mean absolute error generated from these two models was also significant at large trunk flexion angles. Thus, only in the trials that included full trunk flexion angles, the difference in mean absolute error between these two models was significant. However, when comparing this model's results with previous EMG-assisted biomechanical models, such as Davis et al. (1998), the difference in mean absolute error was smaller, because Davis's model could be viewed as using a subset data in which the trunk flexion angles was less than 45°. Since the trunk muscles were still in active range, the predictions of the maximum muscle stress values as well as the internal moment base only on muscle activities were still reliable.

R squared values represent the percentage of the variability of the measured external moment that can be explained by the model predicted internal moment. As described above, R squared values can also be affected by the fluctuation of the EMG signal. For example, in Figure 18 the R squared value for the model with passive components was only 18%, even though the model with passive components correctly predicted the external moment. This was because the variance of the measured external moment was small as the subject was doing a static extension exertion. The fluctuation of the EMG signal could significantly affect the R squared values in this situation. In the dynamic trials on the dynamometer and the free lifting/lowering exertions where the external moment varied during the trials, the R squared values were larger and more meaningful. These results agree with the findings of the Marras and Sommerich (1991) when the authors reported the mean R squared values from their model were around 70%.

The improvement in the mean absolute error and R squared values confirmed the necessity of involving passive components when studying the lifting/lowering exertions that include full trunk flexion angles. At the full flexion posture, the passive components supported the majority of the extension torque. But the passive components (the ligaments and the discs) usually have smaller moment arms relative to L5/S1 joint as compared to the trunk muscles. Thus, they generated much higher compression and shear force than muscles to support the same torque from upper body. If the model without the passive components was used in this situation, the spinal load would be underestimated and the risk of low back injuries might be likewise underestimated.

This EMG assisted biomechanical model of spine was compatible with both controlled flexion/extension exertions on ARF and free dynamic lifting exertions, in both

bent knee and straight knee conditions. This was a great advantage as compared to previous EMG assisted spinal models. In experiment one, the subjects were fixed in the ARF while their hip was restricted by the fixture. The rotation of the pelvis was limited thus the trunk flexion angle was directly related to flexion of the lumbar. The trunk flexion angle was used to calculate both the torque of the upper body and the restorative moment from passive components. In experiment two, there were two postures. In the straight knee condition, the rotation of the pelvis was still limited. In the bent knee condition, there was no restriction on the pelvis of the subjects. Thus, the trunk flexion angle was also affected by the rotation of the hip and the flexion of knee joint. This introduced more freedom in the performance of the subjects. For example, to reach 60° trunk flexion, the subject could maintain a relatively straight lumbar spine and knees and pelvis rotate to reach 60° . Alternatively, he could bend his knees to a greater degree, rotate his pelvis and flexion his lumbar spine 30° to reach the 60° flexion angle. In both conditions, the external moments generated by the weight of the upper body were the same, but the curvature of the lumber was smaller in bend knee condition than in straight knee condition. Therefore, the elongation of the passive components was smaller and the moment generated was also smaller. This EMG-assisted biomechanical model captured this difference by using two flexion angles, the trunk flexion angle and the lumbar flexion angle. The trunk flexion angle was used to calculate the external torque from the weight of the load and upper body, the lumbar flexion angle was used to calculate the restorative moment from passive components. The good performance of the model in both controlled and free dynamic exertions, and in both bent knee and straight knee conditions indicated this was a correct approach.

The results of this study provided new evidence for the debate about the comparison between squat (bent knee) and stoop (straight knee). The literature has not yet come to conclusion about which posture is safer (van Dieën, Hoozemans et al. 1999). A recent study conducted by Bazrgari, Shirazi-Adl et al. (2007) used a finite element model that included passive components to study the spinal load in squat and stoop lifting conditions. They found that the compression and shear forces on the spine were significantly larger in squat posture than in stoop posture. However, in this study, the posture had no significant effect on the maximum spinal compression force. Only the maximum shear force in bend knee condition was smaller than that in straight knee condition. This might be explained by the extreme maximum trunk flexion angles in this experiment. As the subjects were asked to reach full flexed posture, the maximum trunk flexion angles were over 90° (averaged 97° under bend knee condition, and 116° under straight knee condition). Thus, the total external moment was actually smaller under straight knee condition than under bent knee condition. Meanwhile, from a mechanical point of view, part of the weight of the upper body and the load actually contributed to reduce the compression force on the spine. Beyond 90° , the total compression force from the weight of the upper body and load and forces generated by the muscles and ligaments were actually smaller as compared to 90° flexion posture. Thus, the finding that the maximum compression forces in squat posture was not different from that in stoop posture might be induced by the full flexed posture used in this study.

Using EMG data as input, this model was able to describe the range of muscle activities and the variability of the spinal loadings associated with a particular motion or activity. As discussed before, the extreme loading of the spine is an important explanation to occupational low back disorders. The stochastic feature of the trunk muscle activities

indicates that the trunk exertions with identical load, velocity, flexion angle etc., may introduce different spinal load. Thus, the variability of the spinal load is important factor when considering the risk of low back disorders. If two trunk exertions introduce a spinal load with the same average value, the one with larger variability is more likely to cause larger extreme spinal load and is more dangerous. Mirka and Marras (1993) introduced a stochastic model of trunk muscle during trunk bending. They investigated the effects of load, velocity and trunk flexion angle on the mean and variability of the spinal load. They found that the load and velocity were not only affected by the mean of the spinal load, but also the variability. The range of the model predicted compression force was 220N for the average of all the isometric conditions. This result was confirmed in this study (see Figure 20, Figure 23, Figure 35 and Figure 38). The median deviation of the spinal compression force increased from 674N to 811N as the load increase. These results indicate this model is capable of providing information about variability in spinal load which was used in the next step to study the difference in variability between eccentric and concentric exertions.

7.2 Comparison of eccentric and concentric exertions

Due to the stochastic nature of human performance, identical lifting tasks under the same condition (e.g., load, speed, posture and motion direction) generated a wide range of spinal load. It is necessary to recognize the biomechanical variability associated with a lifting task as well as the risk of low back disorders related to this variance. Granata (1999) et al. investigated the variability in lifting motions with repeated lifting. The authors stated that one task could have an average compressive load with a narrow distribution of loads resulting in a low probability of exertion exceeding spinal tolerance levels. And another lifting task may have an identical mean spinal load with a wide distribution, which results in a high

probability of exertion exceeding the spinal tolerance levels. However, since the mean values of these two tasks are same, the task with wide distribution may be assessed as a safe one by traditional interpretation. Thus, to fully estimate the risk, the magnitude as well as the variance of the spinal load must be addressed.

Previous studies have investigated the influence of load, coupling, speed, posture and previous manual material handling experience on the variability of the spinal load during controlled lifting exertions (Mirka and Marras 1993) or free lifting exertions (Mirka and Baker 1996; Granata, Marras et al. 1999). Mirka and Marras (1993) introduced the stochastic model of trunk muscle coactivation during trunk bending. The subjects were fixed in the ARF and performed isometric, isokinetic and isoinertial (constant accelerations) exertions sagittally while the EMG activities of their trunk muscles and the force, velocity and acceleration were recorded. The experimenter modeled the critical features of these data in varied conditions (EMG of trunk muscles, speed, load, range of motion etc.). Then, they used these features to generate EMG activities that were suitable for a specific condition. In this step, the EMG activities were generated from a translated standard normal distribution which fitted the empirical distribution modeled in the first step best. After that, the authors used these generated EMG values as inputs to an EMG-assisted biomechanical model. The output of the model not only included the usual mean and standard deviation values of the spine load, but also the distributions, which provided quantitative information about the potential relationship between LBP and variability of the spine load. Their results indicate the spinal load was influenced by the load and velocity conditions. Because in their study the subjects were restricted in the ARF, which does not represent the way that real free dynamic lifting exertions happen in a real working environment, the study for unrestricted lifting exertions

was necessary. In 1995, Mirka and Baker conducted a study to investigate the variability of human performance in terms of angular position, angular velocity and angular acceleration of the lumbar spine and the torque about the lumbosacral joint during sagittally symmetric lifting tasks. The subjects performed simple lifting tasks repeatedly by three levels of coupling and seven levels of load. The kinematics and kinetics of lumbar spine were monitored and modeled to estimate the torque about the L5/S1 joint in the sagittal plane. The results showed significant variability in the magnitude of peak velocity and acceleration in the sagittal plane. The kinetic analysis showed both the magnitude and variability of the peak dynamic torque increased as the level of load increased.

The results of this study indicated that load, speed, posture and motion direction significantly affected the spinal load, but not all of them affected the variability. The main finding was that the motion direction significantly affected the variability of the spinal load which in terms of median deviation of the maximum spinal compression force and shear force were always higher in eccentric exertions than in concentric exertions, in controlled dynamic exertions or free lifting/lowering exertions.

In experiment one, the subjects were asked to maintain the target torque as accurate as possible. In experiment two, the subjects were asked to lift and lower the load without disturbing the cup of water on the load. Under both conditions, the goal was to smooth the motion of the subjects thus the variability within each trial was restricted. Though Fang et al. (2001) found that standard deviation of the force measured in forearm eccentric exertions was significantly larger than that in concentric exertions, in this study, the variability of the eccentric and concentric exertions was mainly between trials. This study used the mean of the median deviation of the maximum spinal compression and shear values to compare the

difference in variability between eccentric and concentric exertions. The results agree with Fang et al. (2004), when the authors studied the standard deviation of the mean forearm force values and found eccentric tasks had larger variability.

There were four components that contributed to the compression and shear forces on the spine: the external force exerted on the ARF, the weight of the subjects' upper body, the force from trunk muscles and the force from passive components. But not all of them were related to the variability of the spinal load. The weight of the subject was constant, thus the torque from the weight of the upper body relied only on trunk flexion angle and didn't change between trials. The variability of the compression and shear force mainly related to how steady the subjects performed their exertions and fundamentally how good their nervous systems control their muscles (Aagaard, Simonsen et al. 2000; Fang, Siemionow et al. 2004).

In experiment one, the external moment was always present, even when the subject was in the upright posture. The flexion/extension speed was controlled by the ARF accurately but the load could be varied. The maximum compression force and shear force on L5/S1 joint were larger in eccentric exertions than concentric exertions. The median deviation values of the spinal compression and shear force represented the variability between trials. The variability of the maximum compression force and shear force were significantly affected by direction. This might have resulted because the subjects could maintain the extension torque with the help of abdominal trunk muscles. The subject could just use back muscles or activate both abdominal and back trunk muscles to generate extension torque. If the subject kept a good balance of the activating level between back and abdominal trunk muscles, the extension torque could be the same but the compression and shear force could be varied. This could be the reason that the median deviation of the

maximum compression and shear force were higher in eccentric exertions than in concentric exertions.

In experiment two, the weight of the load was constant but the net external moment increased as the trunk flexion angle increased. The speed of the lifting and lowering was controlled by the subjects and in general the subjects lowered more slowly than they lifted. The reason might be that the subjects were more cautious in lowering exertions and slowed their speed. Interestingly, the maximum spinal compression force and shear force were all larger in lowering than in lifting. Considering these results together, we might conclude that the subjects used both abdominal and back trunk muscles to lift and lower the load. But in lowering exertions, the extensor muscles were elongating while generating force. It was harder for the subject to control the extension torque. Thus, the subject activated the abdominal muscles more to help maintain the stability of the trunk. So in lowering exertions, the speed was smaller as the motions were steadier, but the maximum compression and shear force was higher. This might also explain why the median deviation of the maximum compression and shear force were larger in lowering exertions as compared to lifting exertions.

In this EMG-assisted biomechanical model, the difference between eccentric and concentric exertions was addressed by the function of force-velocity relationship, where in eccentric exertions the function was a constant, and in concentric exertions, the function was related to the value of the muscle contraction speed which is directly related to the trunk flexion/extension velocity. It is reasonable to expect that the variability of the trunk flexion velocity might increase the variability of the predicted muscle forces in concentric exertions but not in eccentric exertions. However, the results of this study indicated that even through

the maximum trunk flexion/extension velocity was smaller in eccentric exertions, there was still more variability of the spinal load in eccentric exertions as compared to concentric exertions. Therefore, the variability of the velocity in the exertions might not be the main reason for the variability of the spinal load. The difference of the performance from the subjects between eccentric and concentric exertions was the direct reason for the difference of the variability of the spinal load, this EMG-assisted biomechanical model did not change this difference through this model treat eccentric and concentric exertions differently. Previous study has indicated that the variability of the spinal load might be induced by the variability of the EMG activity of the trunk muscles. Granata et al. (1999) studied the variation in spinal load and trunk dynamics during repeated lifting exertions. They asked five experienced and seven inexperienced manual material handlers to perform 10 repeated lifting at each combination of load weight, task asymmetry and lifting velocity. The EMG activities of the trunk muscles of the subjects were imported to an EMG-assisted biomechanical model to compute the dynamic loads on the spine. They found that weight and asymmetry significantly affected the spinal load variability. But it was outside of their expectation that the experienced manual material handlers generated larger spinal load variability as compared to inexperienced ones. They carefully investigated the data and found the EMG activity of the trunk muscles, including both agonist muscle (erector spinae and latissimus dorsi) and antagonistic muscles (rectus abdominis and external obliques), were significantly larger from experienced subjects than inexperienced subject (e.g., normalized activity in rectus abdominis were 5.7% and 11.1% for experienced and inexperienced subjects, respectively). The muscle co-contraction significantly affected the magnitude and variability of the spinal load. To further investigate the potential influence of the EMG-assisted

modeling technique on the variability of the spinal load, Marras et al. (1999) conducted a similar study to test the accuracy of an EMG-assisted biomechanical model predictions in different load, velocity, asymmetric, subjects experience conditions. They found the model attributes are very sensitive to individual differences among subjects (e.g., 53.71% of the variability in gain values was related to the subjects' difference), to which this model was designed to be sensitive. In conclusion, this model correctly predicted the spinal load and revealed the difference of variability in spinal load between eccentric and concentric exertions.

Previous research has shown that lowering (eccentric) exertions generate larger spinal loads than lifting exertions (Davis, Marras et al. 1998). This study indicated that lowering exertions also introduced larger variability in maximum spinal compression and shear forces. Therefore the probability that the spinal load exceeded the limits of spinal structure was larger in lowering exertions. The results of this study provided quantitative information about the risk of low back disorders in lifting/lowering exertions which may help in developing guidelines for the safety of the workers during manual material handling activities.

7.3 Limitations of this study

There are several limitations to this study that should be mentioned. First, only sagittal plane lifting/lowering exertions were tested in this research. Certainly as a person moves out of the mid-sagittal plane, the orientation of the ligaments and the fibers in the disc are fundamentally changed, thereby altering their force generating capabilities. Due to the limitations of the finite element model used, this model could only predict the moment generated by passive moments in sagittal plane. Lateral bending and twisting exertions or combinations of these motions were not addressed. The finite element model is capable of

simulating the behavior of the lumbar tissues in pure lateral bending or twisting exertions. But the combinations of these exertions, e.g. asymmetric lifting/lowering exertions, are beyond this current model and therefore were not considered in this study.

Secondly, there were several restrictions in the lifting/lowering exertions performed by the subjects in this study. In experiment one, the subjects were asked to maintain a certain level of extension torque through the full range of trunk flexion range. In experiment two, the subjects were asked to lift and lower the load without disturbing the water on the load. This limitation might alter the performance of the subjects and might not represent real behavior of the subjects in occupational environments. This however, would not impact the quality of the predictions, just the range of activities used to validate the approach.

Thirdly, this EMG assisted biomechanical model assumed that the performance of the passive components was a discrete time stochastic process so that the moment generated by the passive components was not affected by the previous exertions of the trunk. However, the viscoelastic characteristics of ligaments and discs indicate their force generating capacity is related to previous stretches and the duration of the current stretch (Provenzano 2001). Repeated trunk flexion/relaxation exertions involving full flexion posture would actually stretch the ligaments gradually and the full trunk flexion angle for a specific subject would gradually increase during the experiment. This increase could influence the accuracy of the prediction of the moment from passive components in this model.

8 CONCLUSION

This study presented a new EMG-assisted biomechanical model of the spine that includes passive tissue components. This work fills a void in the literature in that it addresses 1) near full flexion postures, 2) full flexion postures, and 3) both concentric and eccentric motions in these two positions. This model has shown itself to be capable of accurately predicting the internal forces that occur during the lifting/lowering exertions that reach full flexion angles and the results from this study confirmed the necessity of using a model with passive components in these situations. The R square value of the measured and predicted moment demonstrated great improvements by involving passive components (37% to 66% in experiment one, 12% to 75% in experiment two, respectively).

The performance of this model was tested in both controlled and free dynamic lifting/lowering exertions. This model used the trunk flexion angle and lumbar flexion angle to distinguish the difference between these two conditions. This method was also used to evaluate the difference of trunk flexion angle between bent knee and straight knee conditions. The results indicated good performance of this model in all of these conditions. For example, the R square value of the measured and predicted moment was 73.6% in bend knee condition, and 76.2% in straight knee condition respectively, where there was no significant difference. This was another significant advantage of this model as compared to previous EMG assisted biomechanical models.

The data of this study was also used to analyze the effects of eccentric and concentric exertions on the variability of spinal load of the subjects. In both controlled and free dynamic lifting/lowering trials, the eccentric exertions, on average, generated larger maximum compression and shear force as compared to concentric exertions. Furthermore, the median

deviation of the maximum compression and shear forces were also larger in eccentric exertions than concentric ones, performance of lifting tasks is more variable in the eccentric phase than the concentric. These two results indicate that eccentric exertions may pose a greater risk of tissue injury because they are more likely to exceed the limits of the spine components.

This EMG assisted biomechanical model was only used to study the sagittal lifting/lowering exertions. Future research might involve the area of this model to lateral bending, twisting or combination of these exertions. The calculation of the maximum muscle stress value will be more complicated in these asymmetric lifting/lowering exertions. Because there will be two or three static/dynamic equilibrium equations need to be fit. The external moment can be projected into sagittal, coronal and transverse planes, while the maximum muscle stress value will be the only variable adjusted to fit these equations. The criteria to choose the “error minimize” maximum muscle stress value need to be carefully chose. Besides that, the infinite element model used in this study only investigated the creep behavior of the ligaments. The viscoelastic property of the ligaments indicates the force generated by the ligaments at the same length will be different in repeated lengthening/shorting exertions. Further research on the finite element model can be conducted to investigate the force-tension curve of the ligaments in repeated lifting/lowering exertions to more precisely estimate the spinal load from passive components.

REFERENCES

- Aagaard, P., E. B. Simonsen, et al. (2000). "Neural inhibition during maximal eccentric and concentric quadriceps contraction: effects of resistance training." Journal of Applied Physiology **89**(6): 2249-2257.
- Arjmand, N. and A. Shirazi-Adl (2005). "Biomechanics of changes in lumbar posture in static lifting." Spine **30**(23): 2637-2648.
- Arjmand, N. and A. Shirazi-Adl (2006). "Model and in vivo studies on human trunk load partitioning and stability in isometric forward flexions." Journal of Biomechanics **39**(3): 510-521.
- Bazrgari, B., A. Shirazi-Adl, et al. (2007). "Analysis of squat and stoop dynamic liftings: muscle forces and internal spinal loads." European Spine Journal **16**(5): 687-699.
- Berkson, M. H. (1979). "Mechanical properties of human lumbar spine motion segments: Part II: responses in compression and shear; influence of gross morphology." Journal of biomechanical engineering **101**(2): 53.
- Bernard, B. P. (1997). Musculoskeletal disorders and workplace factors : a critical review of epidemiologic evidence for work-related musculoskeletal disorders of the neck, upper extremity, and low back, US Department of Health and Human Services (DHHS) publication no. 97-141 (Cincinnati: National Institute for Occupational Safety and Health).
- Bigland, B. and O. C. J. Lippold (1954). "The Relation between Force, Velocity and Integrated Electrical Activity in Human Muscles." Journal of Physiology-London **123**(1): 214-224.
- BLS (2006). TABLE R6. Incidence rates(1) for nonfatal occupational injuries and illnesses involving days away from work(2) per 10,000 full-time workers by industry and selected parts of body affected by injury or illness, 2006, Bureau of Labor Statistics, U.S. Department of Labor.
- Bogduk, N. N., J. J. E. Macintosh, et al. (1992). "A universal model of the lumbar back muscles in the upright position." Spine **17**(8): 897-913.

- Brown, S. H. M. and J. R. Potvin (2007). "The effect of reducing the number of EMG channel inputs on loading and stiffness estimates from an EMG-driven model of the spine." Ergonomics **50**(5): 743-751.
- Chaffin, D. B. (1969). "A Computerized Biomechanical Model-Development of and Use in Studying Gross Body Actions." Journal of Biomechanics **2**(4): 429-&.
- Chaffin, D. B. and W. Baker (1970). "A Biomechanical Model for Analysis of symmetric Sagittal Plane Lifting." AIIE Transactions **2**(1): 16-27.
- Cheng, C.-K., H.-H. Chen, et al. (2000). "Segment inertial properties of Chinese adults determined from magnetic resonance imaging." Clinical Biomechanics **15**(8): 559-566.
- Cholewicki, J. J. and S. S. M. McGill (1992). "Lumbar posterior ligament involvement during extremely heavy lifts estimated from fluoroscopic measurements." Journal of biomechanics **25**(1): 17-28.
- Christou, E. A. and L. G. Carlton (2002). "Motor output is more variable during eccentric compared with concentric contractions." Medicine and Science in Sports and Exercise **34**(11): 1773-1778.
- Clauser, C. E., J. T. McConville, et al. (1969). Weight Volume and Center of Mass of Segments of the Human Body. Ohio, AMRL-TR-69-70, Wright Patterson Air Force Base.
- Colloca, C. J. and R. N. Hinrichs (2005). "The biomechanical and clinical significance of the lumbar erector spinae flexion-relaxation phenomenon: A review of literature." Journal of Manipulative and Physiological Therapeutics **28**(8): 623-631.
- Davis, K. G., W. S. Marras, et al. (1998). "Evaluation of spinal loading during lowering and lifting." Clinical Biomechanics **13**(3): 141-152.
- DeLuca, C. J. (1997). "The use of surface electromyography in biomechanics." Journal of Applied Biomechanics **13**(2): 135-163.
- Dolan, P. and M. A. Adams (2001). "Recent advances in lumbar spinal mechanics and their significance for modelling." Clinical Biomechanics **16**: S8-S16.

- Enoka, R. M. (1996). "Eccentric contractions require unique activation strategies by the nervous system." Journal of Applied Physiology **81**(6): 2339-2346.
- Fang, Y., V. Siemionow, et al. (2001). "Greater movement-related cortical potential during human eccentric versus concentric muscle contractions." Journal of Neurophysiology **86**(4): 1764-1772.
- Fang, Y., V. Siemionow, et al. (2004). "Distinct brain activation patterns for human maximal voluntary eccentric and concentric muscle actions." Brain Research **1023**(2): 200-212.
- Farfan, H. F. (1973). Mechanical Disorders of the Low Back. Philadelphia, Lea and Febiger.
- Friden, J. and R. L. Lieber (1992). "Structural and Mechanical Basis of Exercise-Induced Muscle Injury." Medicine and Science in Sports and Exercise **24**(5): 521-530.
- Friden, J., M. Sjostrom, et al. (1983). "Myofibrillar Damage Following Intense Eccentric Exercise in Man." International Journal of Sports Medicine **4**(3): 170-176.
- Gilgil, E., C. Kacar, et al. (2005). "Prevalence of low back pain in a developing urban setting." Spine **30**(9): 1093-1098.
- Grabiner, M. D. and T. M. Owings (2002). "EMG differences between concentric and eccentric maximum voluntary contractions are evident prior to movement onset." Experimental Brain Research **145**(4): 505-511.
- Granata, K. P. and W. S. Marras (1993). "An Emg-Assisted Model of Loads on the Lumbar Spine During Asymmetric Trunk Extensions." Journal of Biomechanics **26**(12): 1429-1438.
- Granata, K. P. and W. S. Marras (1995). "An Emg-Assisted Model of Trunk Loading During Free-Dynamic Lifting." Journal of Biomechanics **28**(11): 1309-1317.
- Granata, K. P., W. S. Marras, et al. (1999). "Variation in spinal load and trunk dynamics during repeated lifting exertions." Clinical Biomechanics **14**(6): 367-375.
- Granata, K. P. and E. Rogers (2007). "Torso flexion modulates stiffness and reflex response." Journal of Electromyography and Kinesiology **17**(4): 384-392.

- Hill, A. V. (1938). "The Heat of Shortening and the Dynamic Constants of Muscle." Proceedings of the Royal Society of London **126**(843): 136.
- Hoyt, D. F., S. J. Wickler, et al. (2005). "In vivo muscle function vs speed I. Muscle strain in relation to length change of the muscle-tendon unit." Journal of Experimental Biology **208**(6): 1175-1190.
- Huang, Q. M. and A. Thorstensson (2000). "Trunk muscle strength in eccentric and concentric lateral flexion." European Journal of Applied Physiology **83**(6): 573-577.
- Ikai, M. M. and T. T. Fukunaga (1968). "Calculation of muscle strength per unit cross-sectional area of human muscle by means of ultrasonic measurement." Internationale Zeitschrift für angewandte Physiologie einschliesslich Arbeitsphysiologie **26**(1): 26-32.
- Jorgensen, M. J. M. J., W. S. W. S. Marras, et al. (2003). "Effect of torso flexion on the lumbar torso extensor muscle sagittal plane moment arms." The spine journal **3**(5): 363-369.
- Katz, J. N. (2006). "Lumbar Disc Disorders and Low-Back Pain: Socioeconomic Factors and Consequences." J Bone Joint Surg Am **88**(suppl_2): 21-24.
- Lahiri, S. S., P. P. Markkanen, et al. (2005). "The cost effectiveness of occupational health interventions: preventing occupational back pain." American journal of industrial medicine **48**(6): 515-529.
- Lortie, M. and G. Baril-Gingras (1998). "Box Handling in the Loading and Unloading of Vans." International journal of occupational safety and ergonomics **4**(1): 3-18.
- Mallen, C., G. Peat, et al. (2005). "Severely disabling chronic pain in young adults: prevalence from a population-based postal survey in North Staffordshire." Bmc Musculoskeletal Disorders **6**.
- Marras, W. S. (2000). "Occupational low back disorder causation and control." Ergonomics **43**(7): 880-902.
- Marras, W. S., K. G. Davis, et al. (2001). "A non-MVC EMG normalization technique for the trunk musculature: Part 2. Validation and use to predict spinal loads." Journal of Electromyography and Kinesiology **11**(1): 11-18.

- Marras, W. S. and K. P. Granata (1997). "The development of an EMG-assisted model to assess spine loading during whole-body free-dynamic lifting." Journal of Electromyography and Kinesiology **7**(4): 259-268.
- Marras, W. S., K. P. Granta, et al. (1999). "Variability in spine loading model performance." Clinical Biomechanics **14**(8): 505-514.
- Marras, W. S. and C. M. Sommerich (1991). "A 3-Dimensional Motion Model of Loads on the Lumbar Spine .1. Model Structure." Human Factors **33**(2): 123-137.
- Marras, W. S. and C. M. Sommerich (1991). "A 3-Dimensional Motion Model of Loads on the Lumbar Spine .2. Model Validation." Human Factors **33**(2): 139-149.
- Marras, W. W. S. and K. K. P. Granata (1995). "A biomechanical assessment and model of axial twisting in the thoracolumbar spine." Spine **20**(13): 1440-1451.
- Marras, W. W. S., S. S. A. Lavender, et al. (1993). "The role of dynamic three-dimensional trunk motion in occupationally-related low back disorders. The effects of workplace factors, trunk position, and trunk motion characteristics on risk of injury." Spine **18**(5): 617-628.
- Marras, W. W. S., S. S. A. Lavender, et al. (1993). "The role of dynamic three-dimensional trunk motion in occupationally-related low back disorders. The effects of workplace factors, trunk position, and trunk motion characteristics on risk of injury." Spine **18**(5): 617-28.
- Marras, W. W. S. and C. C. H. Reilly (1988). "Networks of internal trunk-loading activities under controlled trunk-motion conditions." Spine **13**(6): 661-667.
- McGill, S. M. (1992). "A Myoelectrically Based Dynamic 3-Dimensional Model to Predict Loads on Lumbar Spine Tissues During Lateral Bending." Journal of Biomechanics **25**(4): 395-414.
- McGill, S. M. and K. Hoodless (1990). "Measured and Modeled Static and Dynamic Axial Trunk Torsion During Twisting in Males and Females." Journal of Biomedical Engineering **12**(5): 403-409.
- McGill, S. M. and R. W. Norman (1985). "Dynamically and Statically Determined Low-Back Moments During Lifting." Journal of Biomechanics **18**(12): 877-&.

- McGill, S. M. and R. W. Norman (1986). "Partitioning of the L4-L5 Dynamic Moment into Disk, Ligamentous, and Muscular Components During Lifting." Spine **11**(7): 666-678.
- McGill, S. M. and R. W. Norman (1987). "Effects of an Anatomically Detailed Erector Spinae Model on L4/L5 Disk Compression and Shear." Journal of Biomechanics **20**(6): 591-600.
- McGill, S. M., N. Patt, et al. (1988). "Measurement of the Trunk Musculature of Active Males Using Ct Scan Radiography - Implications for Force and Moment Generating Capacity About the L4/L5 Joint." Journal of Biomechanics **21**(4): 329-&.
- McGill, S. M., L. Santaguida, et al. (1993). "Measurement of the Trunk Musculature from T5 to L5 Using Mri Scans of 15 Young Males Corrected for Muscle-Fiber Orientation." Clinical Biomechanics **8**(4): 171-178.
- McGill, S. S. M. (1997). "The biomechanics of low back injury: implications on current practice in industry and the clinic." Journal of Biomechanics **30**(5): 465-75.
- McGill, S. S. M. and V. V. Kippers (1994). "Transfer of loads between lumbar tissues during the flexion-relaxation phenomenon." Spine **19**(19): 2190-6.
- McGill, S. S. M. and R. R. W. Norman (1987). "Effects of an anatomically detailed erector spinae model on L4/L5 disc compression and shear." Journal of biomechanics **20**(6): 591-600.
- Mirka, G., D. Kelaher, et al. (1997). "Selective activation of the external oblique musculature during axial torque production." Clinical Biomechanics **12**(3): 172-180.
- Mirka, G. A. and A. Baker (1996). "An investigation of the variability in human performance during sagittally symmetric lifting tasks." Iie Transactions **28**(9): 745-752.
- Mirka, G. A. and W. S. Marras (1993). "A Stochastic-Model of Trunk Muscle Coactivation During Trunk Bending." Spine **18**(11): 1396-1409.
- Montgomery, D. C. (2001). Design and analysis of experiments, John Wiley & Sons, INC.
- Morris, J. M., D. B. Lucas, et al. (1962). "Electromyographic Study of Intrinsic Muscles of Back in Man." Journal of Anatomy **96**(OCT): 509-&.

- Morris, J. M., D. B. Lucas, et al. (1961). "Role of the Trunk in Stability of the Spine." Journal of Bone and Joint Surgery-American Volume **43**(3): 327-351.
- Newham, D. J. (1988). "The Consequences of Eccentric Contractions and Their Relationship to Delayed Onset Muscle Pain." European Journal of Applied Physiology and Occupational Physiology **57**(3): 353-359.
- Newham, D. J., K. R. Mills, et al. (1983). "Pain and Fatigue after Concentric and Eccentric Muscle Contractions." Clinical Science **64**(1): 55-62.
- Nussbaum, M. S. M. and D. S. M. Chaffin (1996). "Development and evaluation of a scalable and deformable geometric model of the human torso." Clinical biomechanics **11**(1): 25-34.
- Perry-Rana, S. R., T. J. Housh, et al. (2003). "MMG and EMG responses during 25 maximal, eccentric, isokinetic muscle actions." Medicine and Science in Sports and Exercise **35**(12): 2048-2054.
- Proske, U. and D. L. Morgan (2001). "Muscle damage from eccentric exercise: mechanism, mechanical signs, adaptation and clinical applications." Journal of Physiology-London **537**(2): 333-345.
- Provenzano, P. (2001). "Nonlinear Ligament Viscoelasticity." Annals of biomedical engineering **29**(10): 908.
- Raschke, U. U. and D. D. B. Chaffin (1996). "Support for a linear length-tension relation of the torso extensor muscles: an investigation of the length and velocity EMG-force relationships." Journal of Biomechanics **29**(12): 1597-604.
- Reid, J. J. G. and P. P. A. Costigan (1987). "Trunk muscle balance and muscular force." Spine **12**(8): 783-6.
- Reilly, C. C. H. and W. W. S. Marras (1989). "Simulift: a simulation model of human trunk motion." Spine **14**(1): 5-11.
- Sallay, P. I., R. L. Friedman, et al. (1996). "Hamstring Muscle Injuries Among Water Skiers: Functional Outcome and Prevention." Am J Sports Med **24**(2): 130-136.

- Schultz, A. B. and G. B. J. Andersson (1981). "Analysis of Loads on the Lumbar Spine." Spine **6**(1): 76-82.
- Schultz, A. B., G. B. J. Andersson, et al. (1982). "Analysis and Measurement of Lumbar Trunk Loads in Tasks Involving Bends and Twists." Journal of Biomechanics **15**(9): 669-675.
- Shellock, F. G., T. Fukunaga, et al. (1991). "Exertional Muscle Injury - Evaluation of Concentric Versus Eccentric Actions with Serial Mr-Imaging." Radiology **179**(3): 659-664.
- Shin, G. (2005). Viscoelastic responses of the lumbar spine during prolonged stooping. Industrial Engineering. Raleigh, North Carolina State University. **Phd**: 145.
- Shin, G., Y. Shu, et al. (2004). "Influence of knee angle and individual flexibility on the flexion-relaxation response of the low back musculature." Journal of Electromyography and Kinesiology **14**(4): 485-494.
- Sutarno, C. C. G. and S. S. M. McGill (1995). "Isovelocity investigation of the lengthening behaviour of the erector spinae muscles." European journal of applied physiology and occupational physiology **70**(2): 146-153.
- Tesch, P. A., G. A. Dudley, et al. (1990). "Force and Emg Signal Patterns During Repeated Bouts of Concentric or Eccentric Muscle Actions." Acta Physiologica Scandinavica **138**(3): 263-271.
- Tsuang, Y. Y. H., G. G. J. Novak, et al. (1993). "Trunk muscle geometry and centroid location when twisting." Journal of biomechanics **26**(4-5): 537-546.
- Van der Helm, F. F. C. and R. R. Veenbaas (1991). "Modelling the mechanical effect of muscles with large attachment sites: application to the shoulder mechanism." Journal of biomechanics **24**(12): 1151-1163.
- van Dieën, J. J. H., M. M. J. Hoozemans, et al. (1999). "Stoop or squat: a review of biomechanical studies on lifting technique." Clinical Biomechanics **14**(10): 685-96.
- Verhaak, P. F. M., J. J. Kerssens, et al. (1998). "Prevalence of chronic benign pain disorder among adults: a review of the literature." Pain **77**(3): 231-239.

Weis-Fogh, T. and R. M. Alexander (1977). The sustained power output from striated muscle. Scale Effects in Animal Locomotion. T. J. Pedley. New York, Academic Press: 511-525.

Westing, S. H., J. Y. Seger, et al. (1990). "Effects of Electrical-Stimulation on Eccentric and Concentric Torque Velocity Relationships During Knee Extension in Man." Acta Physiologica Scandinavica **140**(1): 17-22.

White, A. and M. Panjabi (1990). Clinical biomechanics of the spine. Philadelphia, Lippincott.

Wilkie, D. D. R. (1949). "The relation between force and velocity in human muscle." The Journal of physiology **110**(3-4): 249-280.

APPENDIX

Appendix A: Matlab code

Main file: proclload.m

```
clear all;
close all;
load('SubjectsData.mat','-mat')
% This file contains anthropometric and experimental data including:
% WeightList - list of the weight of the subjects, kg
% StatureList - list of the height of the subjects, m
% WaistDepthList - list of the waist depth of the subjects, m
% WaistWidthList - list of the waist width of the subjects, m
% FullFlexionAngleList - list of the full flexion angle of the subjects,
% degree
% FullFlexionMomentList - list of the full flexion moment of the
% subjects, Nm
% MaxCompressionList - list of the maximum spinal compression force of
% the subjects, N
% TrialConditionList - a matrix presents the condition of each trial,
% load, posture/speed, motion direction
% TrialSeqList - list of the sequence of the trials
MeanGains=zeros(1,6);
MeanSlopes=zeros(1,6);
for OUTPUTDATA=0:1 % Two round of calculation
    % Gain, Slope, Mean Err using mean Gain, Mean Err using mean Slope, R
    % square Gain, R square Slope
    datalog=zeros(36*6,11);
    datalogn=1;
    for SubjectNumber=1:6;
        %Generate filename list
        FilePath=['D:\My Documents\My Works\Eccentric Lifting\DATA\r0'...
            int2str(SubjectNumber+1) '\r0' int2str(SubjectNumber+1)];
        ExtendFileName='.itd';
        TestName=[
            'd1 '
            'd2 '
            'd3 '
            'd4 '
            'd5 '
            'd6 '
            'd7 '
            'd8 '
            'd9 '
            'd10 '
            'd11 '
            'd12 '
            'd13 '
            'd14 '
            'd15 '
            'd16 '
            'd17 '
            'd18 '
        ];
        FullFlexionAngle=FullFlexionAngleList(SubjectNumber);
```

```

FullFlexionMoment=FullFlexionMomentList(SubjectNumber);
MaxCompression=MaxCompressionList(SubjectNumber);
[TestCount x]=size(TestName);
BestGain=10000;
StepWidth=1;
Gain=zeros(TestCount,1);
Gains=zeros(TestCount,2);
Slope=zeros(TestCount,1);
TotalErr=zeros(TestCount,2);
TotalMax=zeros(TestCount,1);
for t=1:TestCount
    TrialNumber=TrialSeqList(SubjectNumber,t);
    FileName=[FilePath deblank(TestName(TrialNumber,:))...
        ExtendFileName]
    file=load(FileName);
    filelength=length(file);
    file=file(1:StepWidth:filelength,:);
    FlexionAngleList=file(:,1);
    AngleVelocityList=file(:,2);
    MomentByLoadList=file(:,3);
    NEMGList=file(:,5:14);

    Weight=WeightList(SubjectNumber);
    Stature=StatureList(SubjectNumber);
    WaistDepth=WaistDepthList(SubjectNumber);
    WaistWidth=WaistWidthList(SubjectNumber);
    MomentByBodyList=sind(FlexionAngleList)...
        *0.47*0.58*Stature*Weight*0.34*9.8;
    % Muscle coefficients
    MuscleAreaCoe=[
        0.0351
        0.0351
        0.0389
        0.0389
        0.006
        0.006
        0.0207
        0.0207
        0.0215
        0.0215
    ];
    MuscleArea=MuscleAreaCoe*WaistWidth*WaistDepth;
    % Muscle origin, insertion and oringtation
    OriginX=[
        0.25
        -0.25
        0.2
        -0.2
        0.1
        -0.1
        0.1
        -0.1
        0.45
        -0.45
    ];
    OriginY=[
        -0.3

```

```

-0.3
-0.3
-0.3
0.55
0.55
0.55
0.55
-0.3
-0.3
];
OriginZ=zeros(10,1);
MuscleOrigin=[OriginX*WaistWidth OriginY*WaistDepth OriginZ];
InsertionX=[
0.6
-0.6
0.3
-0.3
0.1
-0.1
0.45
-0.45
0.45
-0.45
];
InsertionY=[
0.1
0.1
-0.3
-0.3
0.55
0.55
-0.19
-0.19
0.2
0.2
];
InsertionZ=[ones(10,1)*(.0275*Stature)];
MuscleInsertion=[InsertionX*WaistWidth InsertionY*WaistDepth...
InsertionZ];
[n x]=size(NEMGList);
% Angle, Speed, Acceleration, External moment, Muscle moment
% only, Internal moment(passive+active), passive, muscle with
% correct gain, compression force, shear force
OutputData=zeros(n,10);
TotalMuscleMoment=zeros(n,3);
TotalPassiveMoment=zeros(n,3);
TotalMoment=zeros(n,3);
TotalForce=zeros(n,3);
ExternalLoad=zeros(n,1);
ForceVelocityModule=zeros(n,10);
ForceLengthModule=zeros(n,10);
for i=1:n
NEMG=NEMGList(i,:);
MomentByLoad=MomentByLoadList(i);
FlexionAngle=FlexionAngleList(i);
AngleVelocity=AngleVelocityList(i);
MomentByBody=MomentByBodyList(i);

```

```

ExternalLoad(i)=MomentByLoad+MomentByBody...
    +sind(FlexionAngle)*6*0.45359237*9.8*0.22;
MuscleOrientation=directioncosines(MuscleOrigin,...
    MuscleInsertion, FlexionAngle);
ForceVelocityModule(i,:)=forcevelocity(AngleVelocity)';
ForceLengthModule(i,:)=forcelength(FlexionAngle)';
forcevalue=BestGain*MuscleArea.*NEMG...
    .*ForceLengthModule(i,:)'.*ForceVelocityModule(i,:)'';
force=[forcevalue forcevalue forcevalue].*MuscleOrientation;
TotalForce(i,:)=sum(force);
MomentF=cross(MuscleOrigin,force);
TotalMuscleMoment(i,:)=sum(MomentF);
TotalPassiveMoment(i,:)=PassiveMoment(FlexionAngle,...
    FullFlexionAngle,FullFlexionMoment,TotalForce(i,3),...
    MaxCompression);
end
% Calculate the best gain that minimize sum of squared error
mse=ones(200,1)*10000;
TotalPoints=length(Gain);
for tgain=1:100
    er=ExternalLoad-TotalMuscleMoment(:,1)*tgain...
        -TotalPassiveMoment(:,1);
    mse(tgain)=mean(er.*er);
end
[x,Gain(t)]=min(mse);
Slope(t)=sum(ExternalLoad.*TotalMuscleMoment(:,1))...
    ./sum(TotalMuscleMoment(:,1).*TotalMuscleMoment(:,1));
if OUTPUTDATA
    InternalLoad=TotalMuscleMoment(:,1)...
        *MeanGains(SubjectNumber)+TotalPassiveMoment(:,1);
    MuscleLoad=TotalMuscleMoment(:,1)*MeanSlopes(SubjectNumber);
else
    InternalLoad=TotalMuscleMoment(:,1)*Gain(t)...
        +TotalPassiveMoment(:,1);
    MuscleLoad=TotalMuscleMoment(:,1)*Slope(t);
end
datalogn(datalogn,1)=Gain(t);
datalogn(datalogn,2)=Slope(t);
datalogn(datalogn,3)=mean(abs(InternalLoad-ExternalLoad));
datalogn(datalogn,4)=mean(abs(MuscleLoad-ExternalLoad));
[rxypvalue] = corrcoef([ExternalLoad InternalLoad]);
datalogn(datalogn,5)=rxypvalue(1,2)*rxypvalue(1,2);
[rxypvalue] = corrcoef([ExternalLoad MuscleLoad]);
datalogn(datalogn,6)=rxypvalue(1,2)*rxypvalue(1,2);
datalogn(datalogn,7)=SubjectNumber;
datalogn(datalogn,8:10)=TrialConditionList(TrialNumber,:);
datalogn(datalogn,11)=TrialSeqList(SubjectNumber,t);
datalogn=datalogn+1;
if OUTPUTDATA
    OutputData(:,1:4)=[FlexionAngleList AngleVelocityList ...
        MomentByBodyList MomentByLoadList];
    OutputData(:,5)=ExternalLoad;
    OutputData(:,6)=MuscleLoad;
    OutputData(:,7)=InternalLoad;
    OutputData(:,8)=TotalPassiveMoment(:,1);
    OutputData(:,9)=InternalLoad-TotalPassiveMoment(:,1);
    OutputData(:,10)=TotalForce(:,3)*MeanGains(SubjectNumber)...

```

```

        +TotalPassiveMoment(:,2); % compression force
    OutputData(:,11)=TotalForce(:,2)*MeanGains(SubjectNumber)...
        +TotalPassiveMoment(:,3); % shear force

    SaveFileName=[FilePath deblank(TestName(TrialNumber,:))...
        '.opt'];
    save(SaveFileName, 'OutputData', '-ascii', '-tabs');
    [SaveFileName ' saved']
end
end
MeanGains(SubjectNumber)=mean(Gain);
MeanSlopes(SubjectNumber)=mean(Slope);
end
if OUTPUTDATA
    SaveFileName=['DynamicMeanValues.opt'];
else
    SaveFileName=['DynamicVariedValues.opt'];
end
end
datalog=datalog(1:datalogn-1,:);
save(SaveFileName, 'datalog', '-ascii', '-tabs');
[SaveFileName ' saved']
end
end

```

Function file: forcevelocity.m

```

function f=forcevelocity(angvel)
% force-velocity module
% angvel - flexion velocity as degrees/s
x=[
    3.15
    3.15
    28.75
    28.75
    -10
    -10
    -10
    -10
    -10
    -10
];
% vel - muscle length change rate delta(L)/L0
vel=angvel.*x/2000;
% calculate force-velocity module based on vel from Marras and Granata
t=zeros(10,1);
x=find(vel<=0);
t(x)=1-4*vel(x);
t(vel<-0.05)=1.2;
x=find(vel>0);
t(x)=1-0.99*vel(x)+0.72*vel(x).*vel(x);
f=t;

```

Function file: forcetlength.m

```

function f=forcelength(ang)
% muscle force length module
%ang - sagittal flexion angle as degrees
x=[
    10
    10
    20
    20
    -10
    -10
    -10
    -10
    -10
    -10
];
% len vector as L/L0
len=1+(ang-20)/20*x/100;
%Module from Marras
f=-3.2+10.2*len-10.4*len.*len+4.6*len.*len.*len;

```

Function file: passivemoment.m

```

function f=PassiveMoment(angle, maxangle, maxload,force, maxcompression)
% Calculate the moment generated by passive components
% Input:
%   angle - vector, list of the flexion angles
%   load - vector, list of the external load
%   maxangle - trunk flexion angle in FRP
%   maxload - external load in FRP
% Output:
%   PassiveMoment - n by 3 matrix, the moment, compression, shear
% force generated by passive components
l=length(angle);
PolyMatrix=[
    0.4149 -10.646 158.11 350.53 %Moment
    0.012758 -0.56833 6.7022 -11.599 %Compression
    0.001245 -0.10833 1.9346 -5.9115 %Shear
];
% Reference angle for normal people in FRP, 60 degrees and 61.13 Nm
Reference=[
    60 61.13
    60 1100
    60 -11
];
a=max(0,angle-maxangle+Reference(1));
forcefactor=1-force/maxcompression;
if forcefactor<0
    forcefactor=0;
end
m=max(0,polyval(PolyMatrix(1,:),a)/Reference(1,2)...
    *maxload*forcefactor/1000);
if m>0
    c=max(0,polyval(PolyMatrix(2,:),a)*maxload/m);
    s=polyval(PolyMatrix(3,:),a)*maxload/m;
else

```

```
    c=0;  
    s=0;  
end  
f=[m c s];
```

Appendix B: Adequacy of the statistical model

The following figures (Figure 46, Figure 47, Figure 48 and Figure 49) were the examples of the normal probability plots of the residuals and the plots of residuals versus predicted values for the original maximum shear force data and the log transformed maximum shear force data in the controlled dynamic exertions on the dynamometer. These figures showed normality assumptions of the statistical models became valid by conducting log transformation on the data.

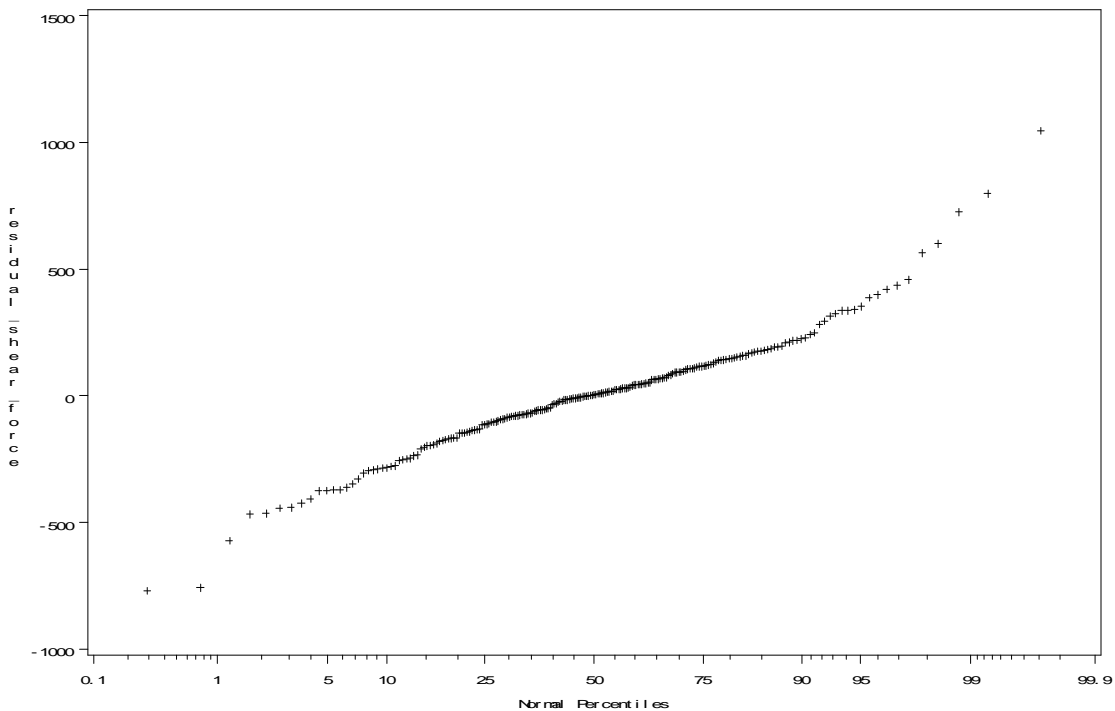


Figure 46. Normal probability plot of the residuals of the original maximum shear force

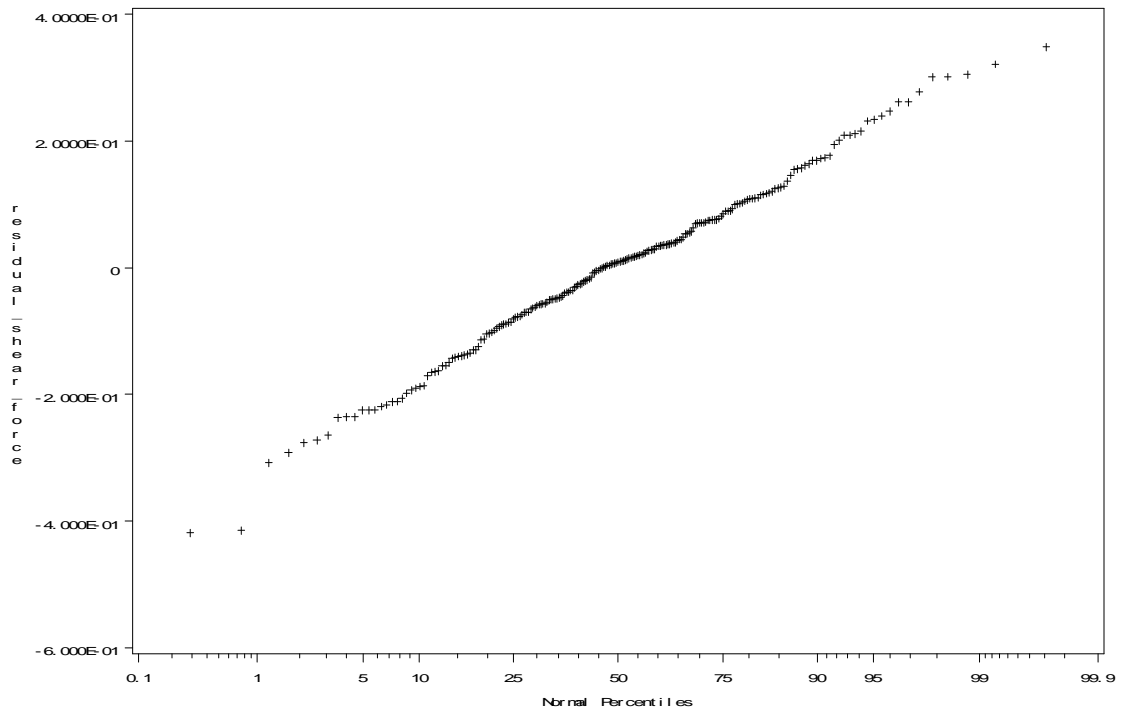


Figure 47. Normal probability plot of the residuals of the log transformed maximum shear force

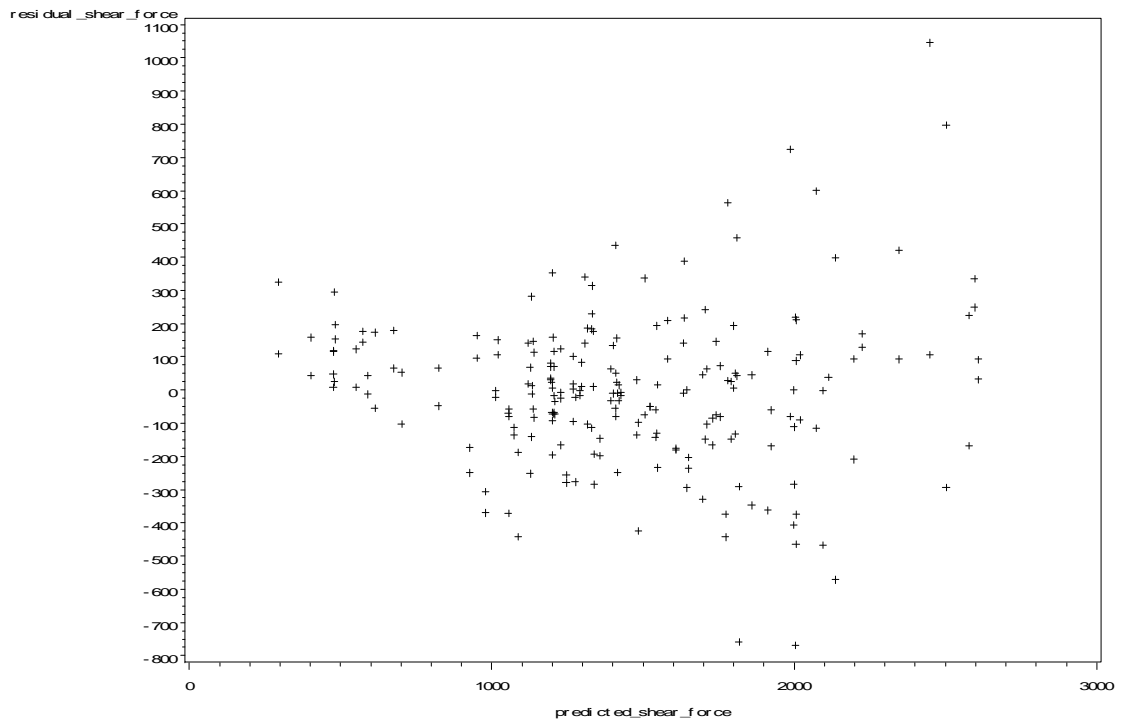


Figure 48. Residuals vs. predicted values of the original maximum shear force data

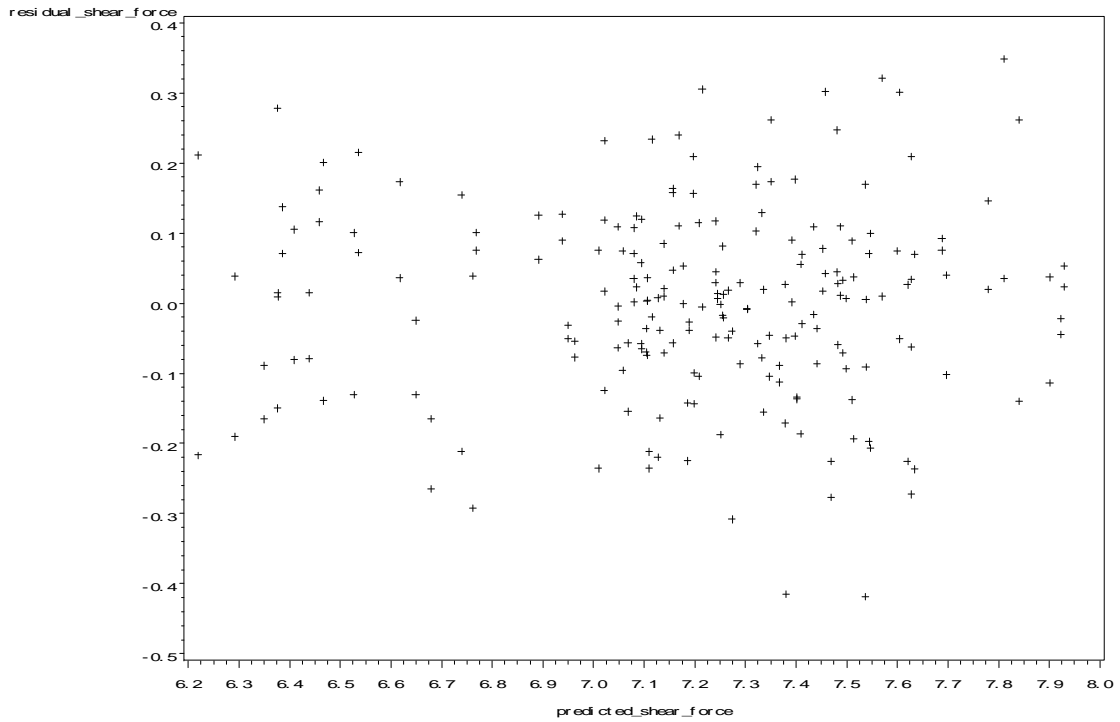


Figure 49. Residuals vs. predicted values of log transformed maximum shear force data

The following figures were the normal probability plots of the residuals and the plots of residuals versus predicted values of the rest dependent variables in experiment one and experiment two. Log transformation of the data was conducted if necessary. Normal probability plots of residuals of the depended variables showed no severe indication of departure from normality and no apparent relationship between the residuals and the predicted values was found in the plots of the residuals versus predicted values.

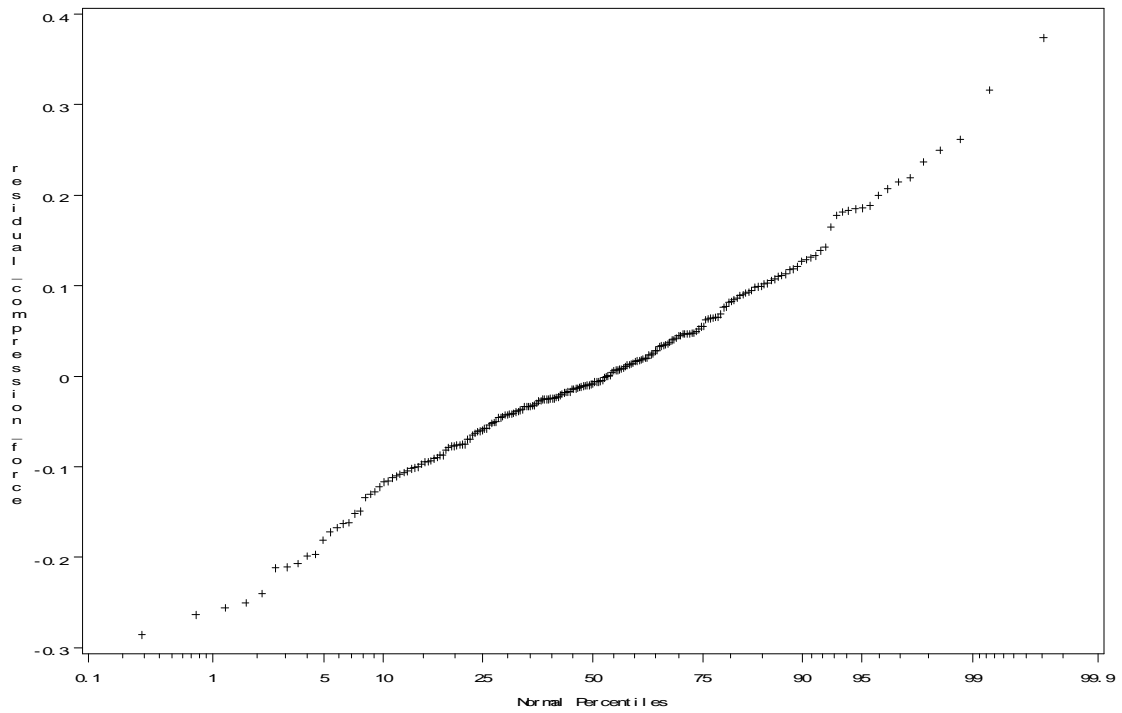


Figure 50. Normal probability plot of the residuals of the maximum compression force

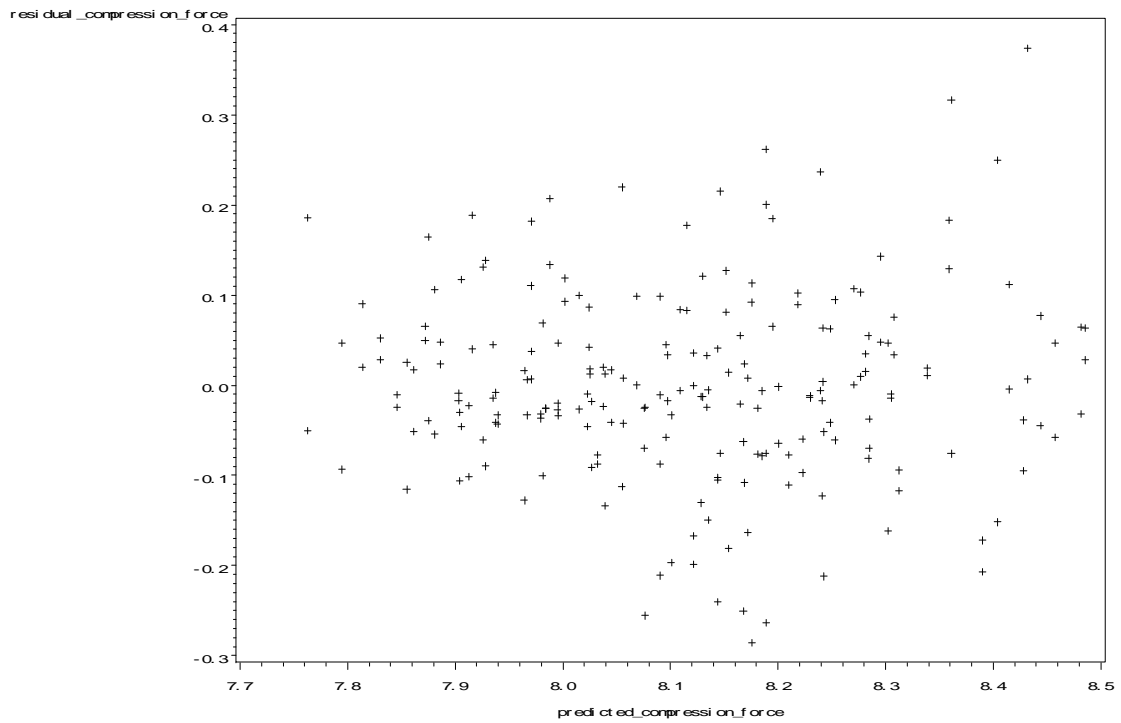


Figure 51. Residuals vs. predicted values of the maximum compression force

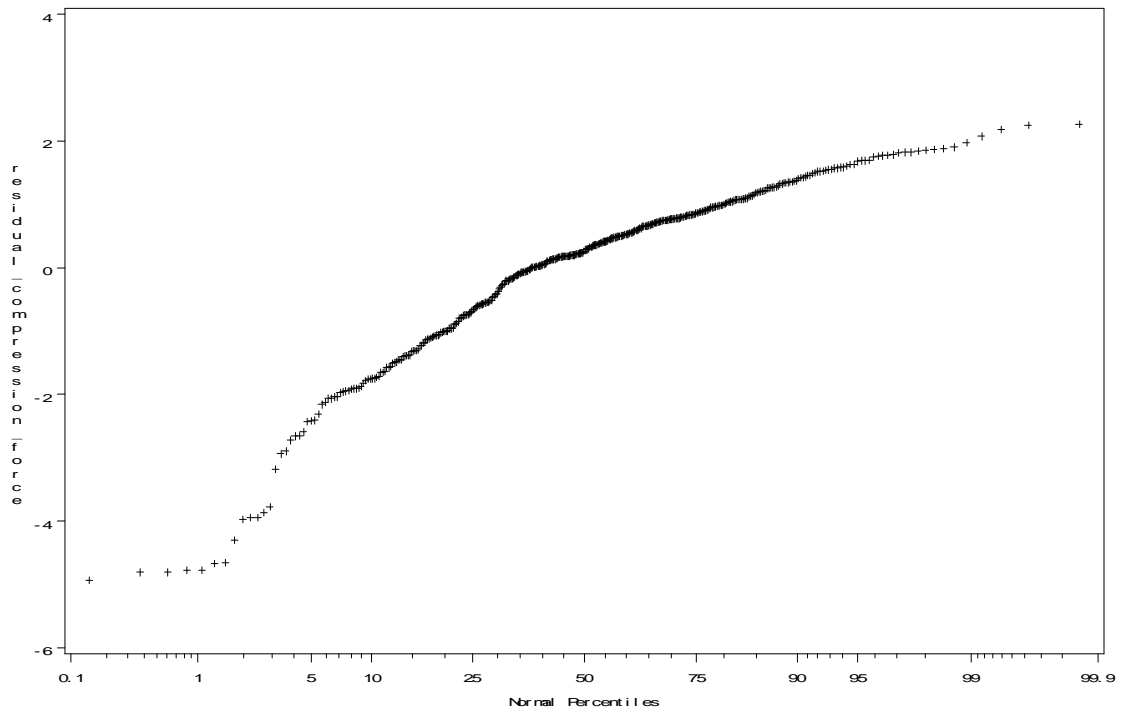


Figure 52. Normal probability plot of the residuals of the median deviation of the peak compression force

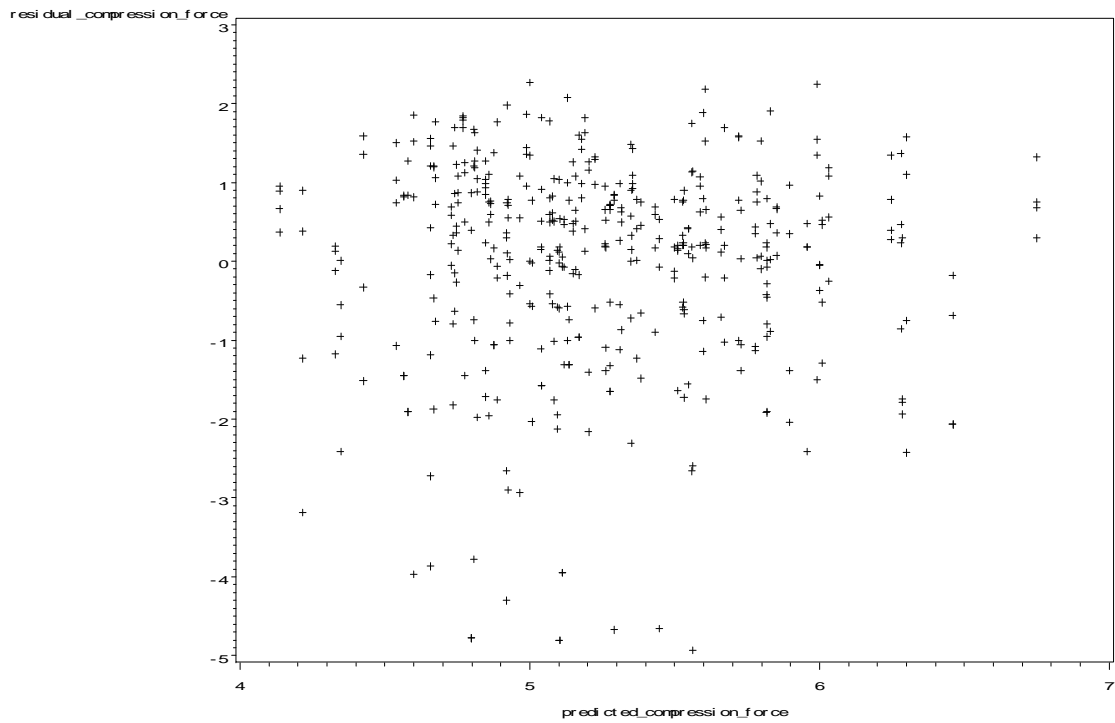


Figure 53. Residuals vs. predicted values of the median deviation of the maximum compression force

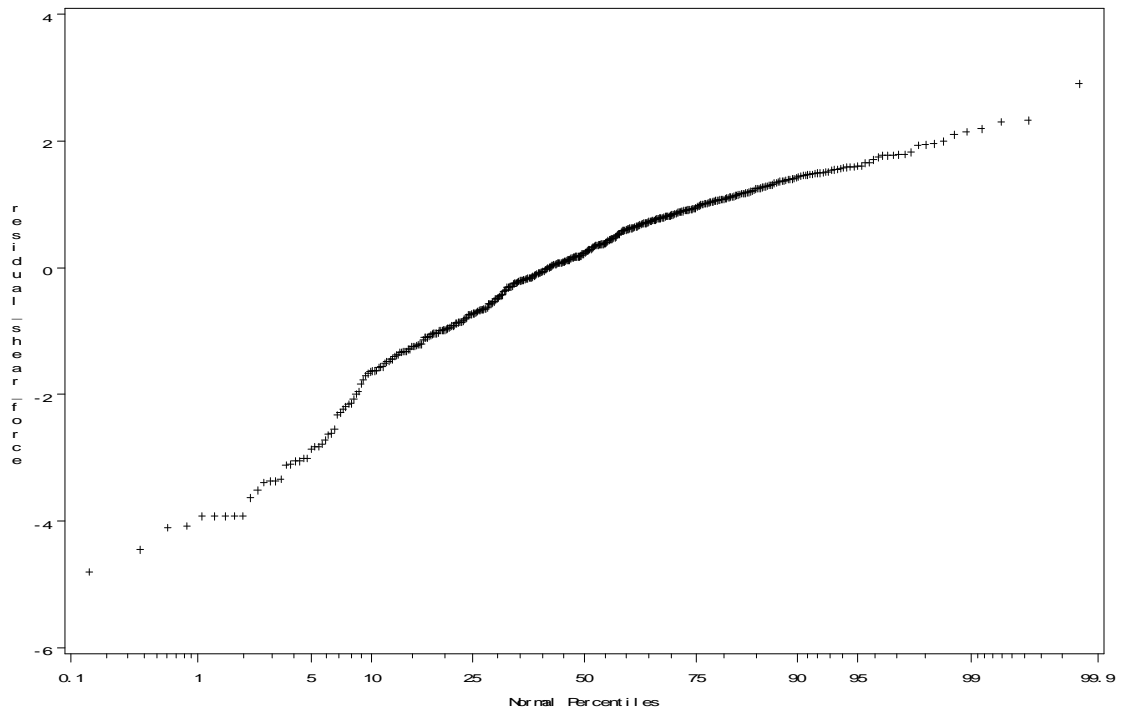


Figure 54. Normal probability plot of the residuals of the median deviation of the peak shear force

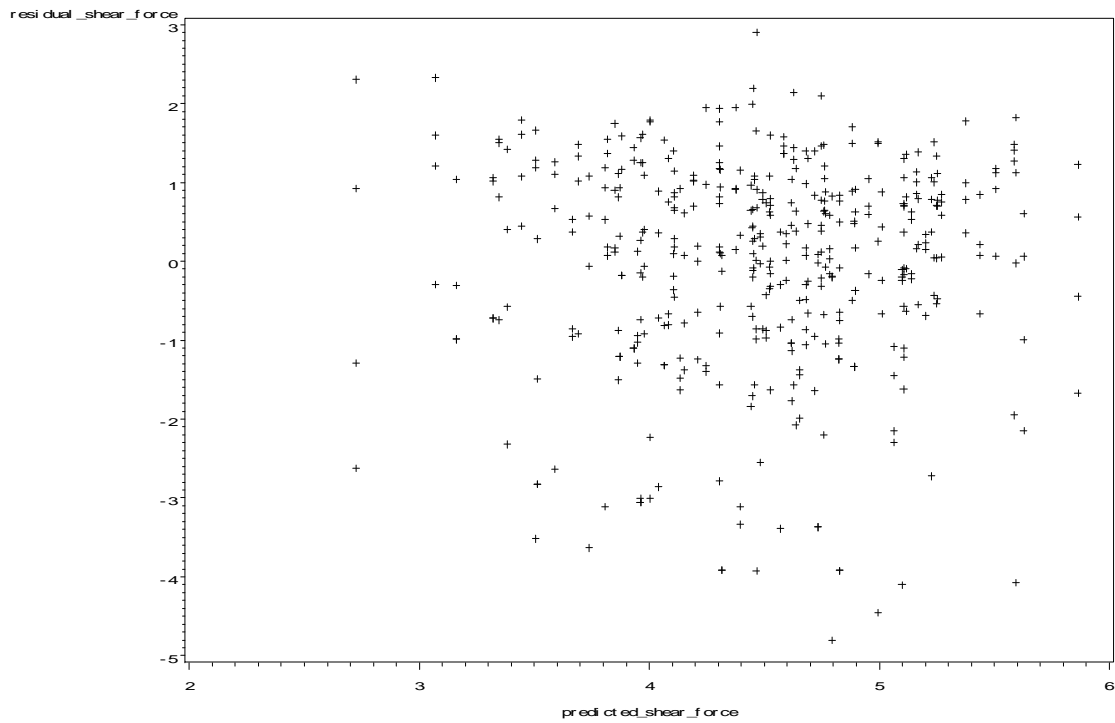


Figure 55. Residuals vs. predicted values of the median deviation of the maximum shear force

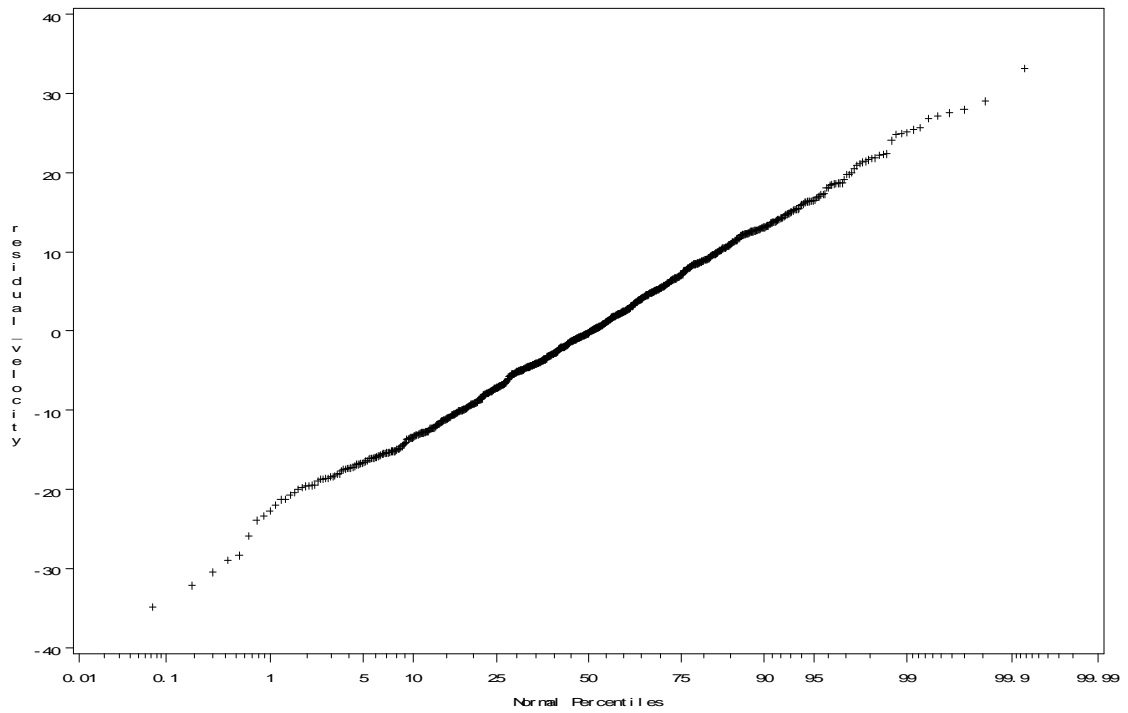


Figure 56. Normal probability plot of the residuals of the maximum flexion/extension velocity

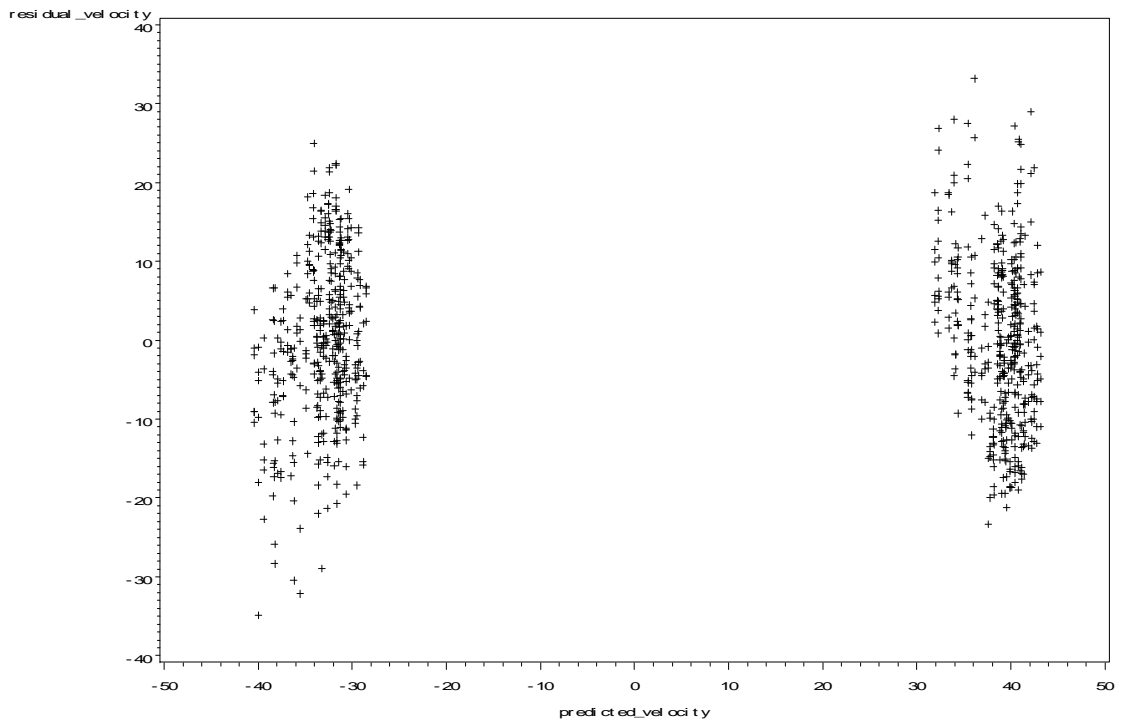


Figure 57. Residuals vs. predicted values of the maximum flexion/extension velocity

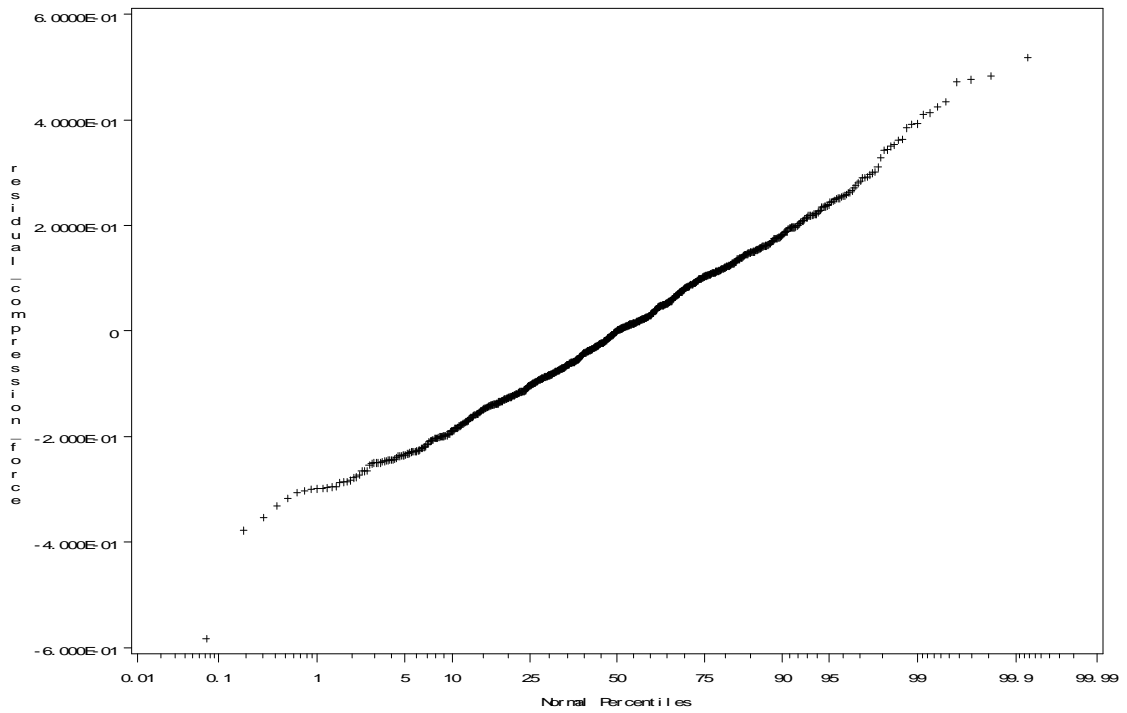


Figure 58. Normal probability plot of the residuals of the maximum compression force

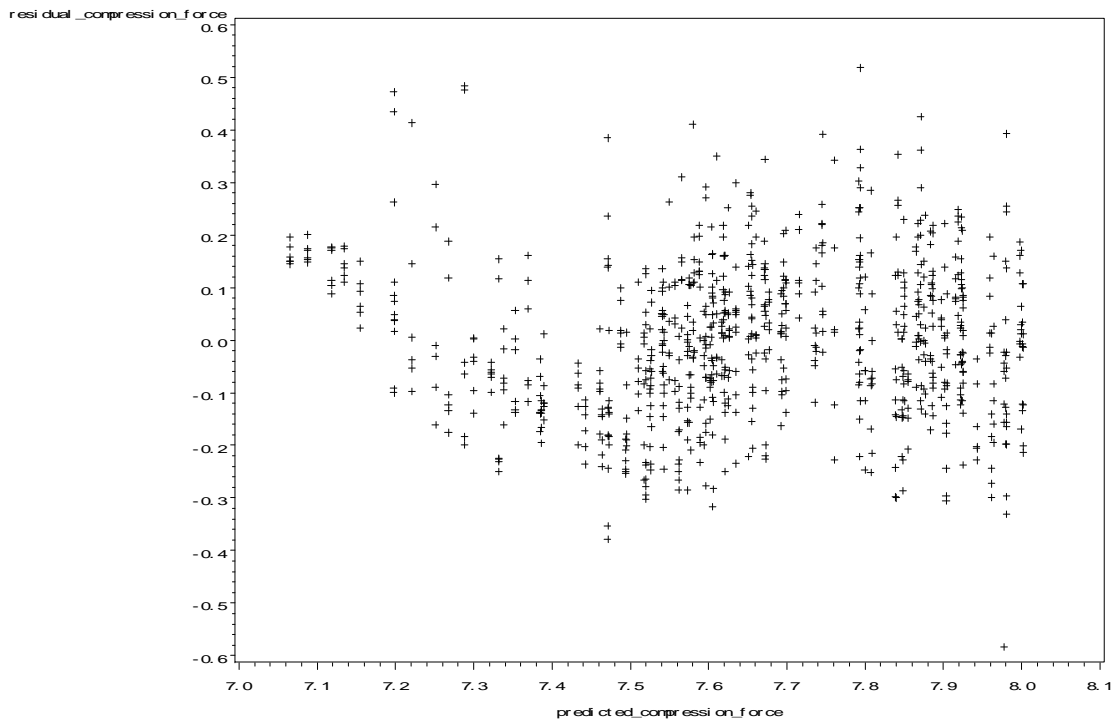


Figure 59. Residuals vs. predicted values of the maximum compression force

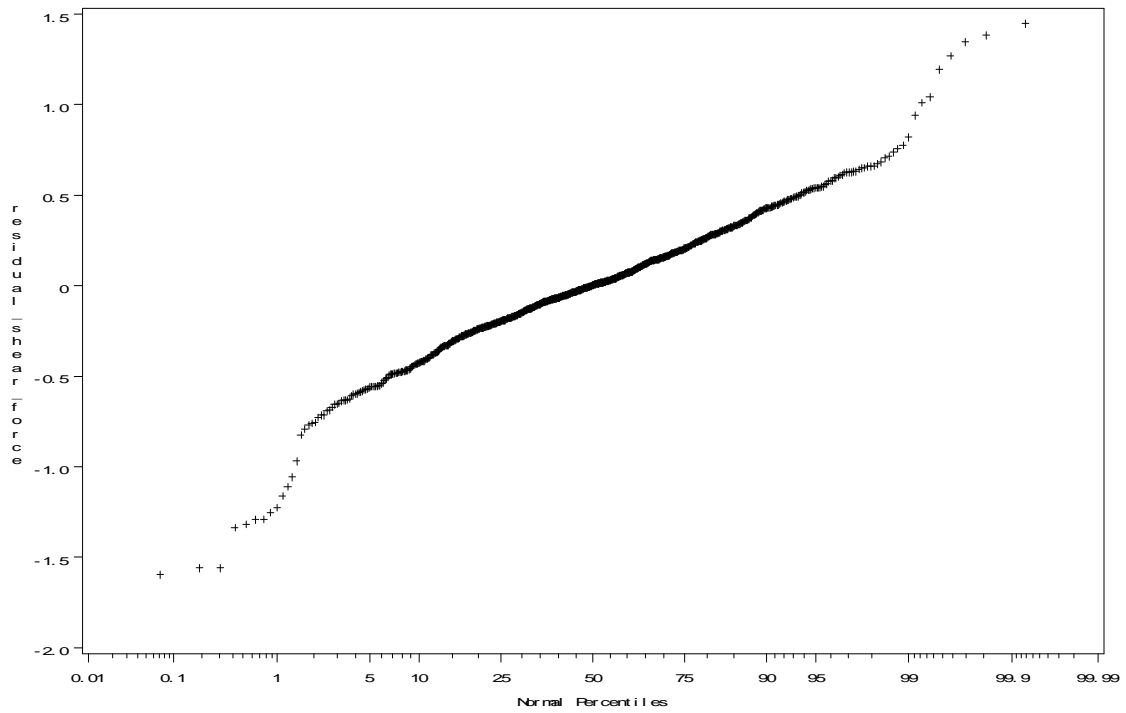


Figure 60. Normal probability plot of the residuals of the maximum shear force

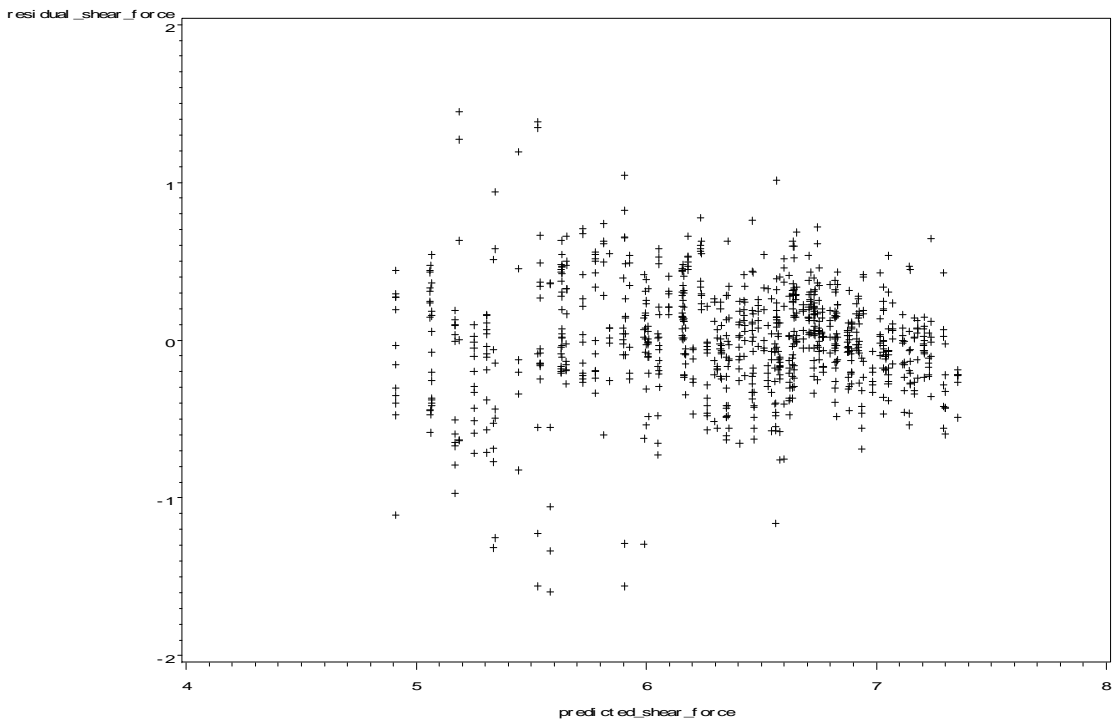


Figure 61. Residuals vs. predicted values of the maximum shear force

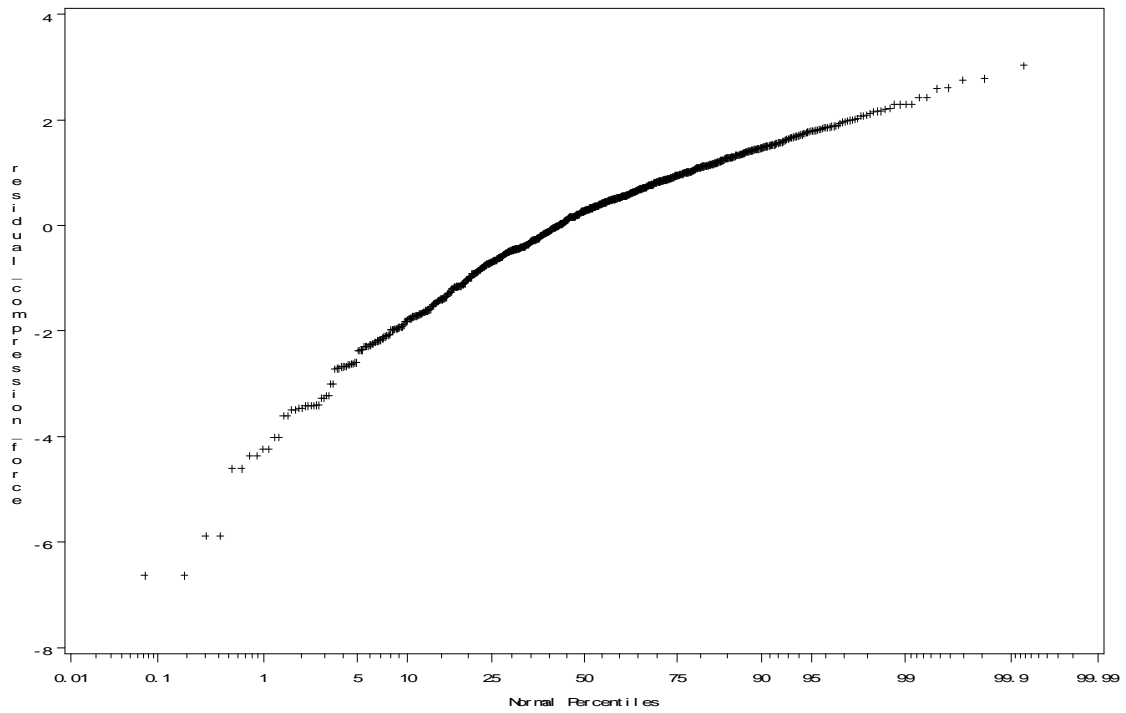


Figure 62. Normal probability plot of the residuals of the median deviation of the peak compression force

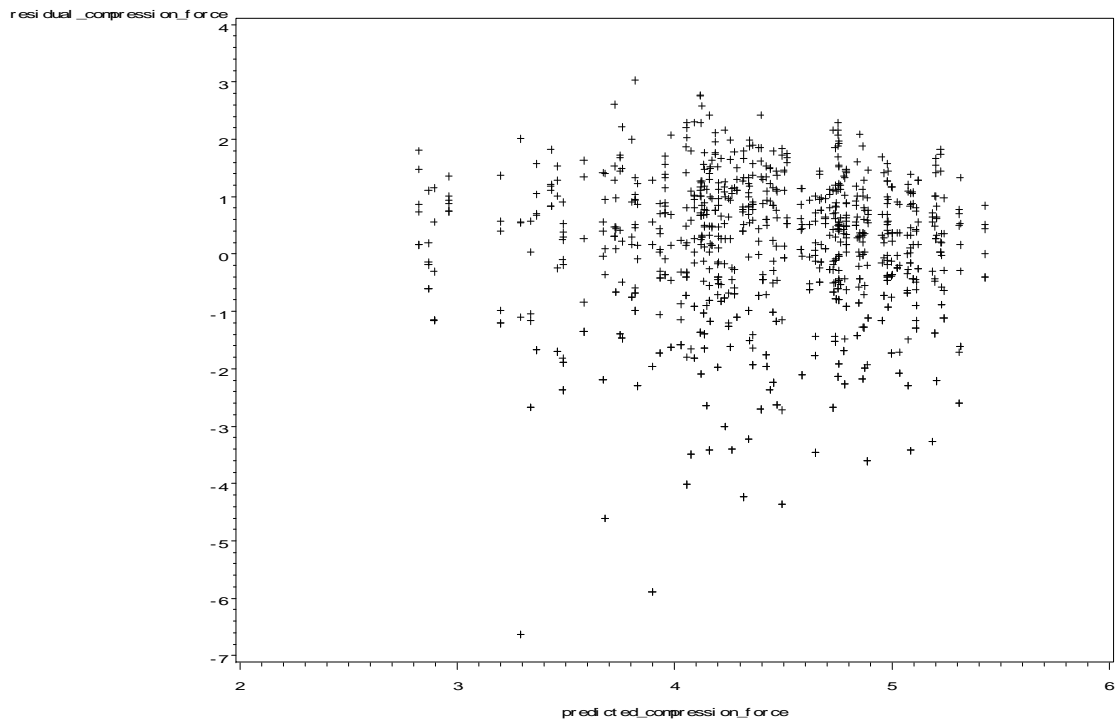


Figure 63. Residuals vs. predicted values of the median deviation of the maximum compression force

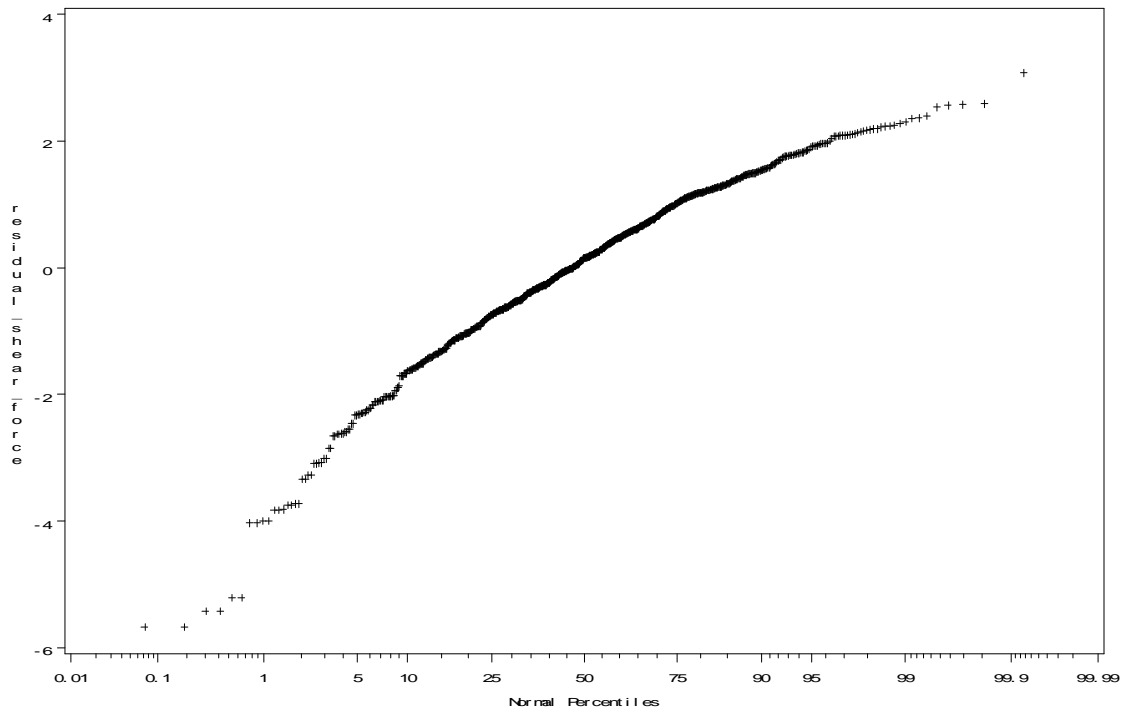


Figure 64. Normal probability plot of the residuals of the median deviation of the maximum shear force

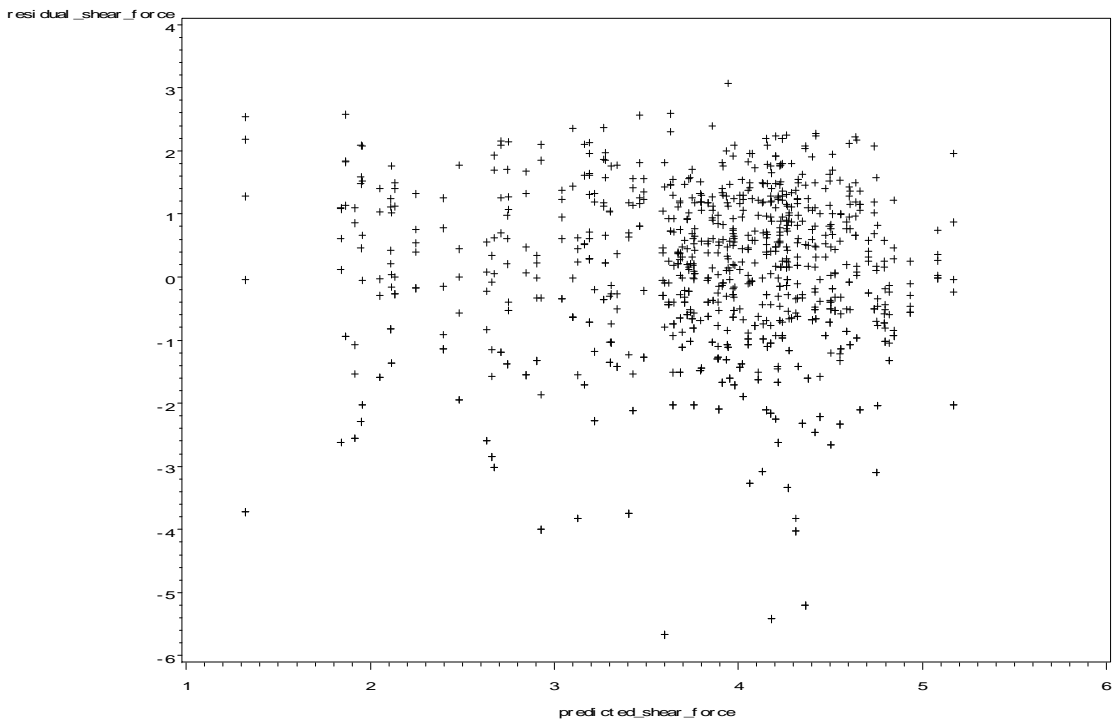


Figure 65. Residuals vs. predicted values of the median deviation of the maximum shear force